The Geology and Mineralisation of the St. Just District, with Particular Reference to Levant Mine.

Jackson, N. J

THE GEOLOGY AND MINERALISATION OF THE St. JUST DISTRICT, ~~WEST CORNWALL~~ WITH PARTICULAR REFERENCE TO LEVANT MINE

A thesis submitted for the degree of Doctor of Philosophy

in the Faculty of Science

The University of London

by

Norman Jeffrey Jackson

Department of Geology

King's College

November, 1976

Now thofe profunder regions they explore,
Where Metals ripen in vaft cakes of Ore.
Here, fullen to the fight, at large is fpread,
The dull unweildy mafs of lumpifh Lead,
There, glimmering in their dawning beds, are feen
The more afpiring feeds of fprightly Tin,
The Copper fparkling next in ruddy freaks,
And in the gloom betrays its glowing cheeks

ACKNOWLEDGEMENTS

I would like to thank,

King's College who financed the majority of this study while I was tutorial student in the Department of Geology.

Professor R.A Howie who supervised the project and all the technical staff in the department who helped me to produce this thesis

The management and staff of Geevor Tin Mines Ltd. and, in particular, Mr. K. Gilbert, the manager, who provided every possible assistance and encouragement, and without whose initial financial support this study would not have been possible.

Mr. J. Trembath (chief sampler), Mr. M Mount (geologist) and Mr. A. Reynolds (geological assistant), all of Geevor Mine, who gave their time and knowledge generously.

Professor G R. Davis and Dr C. Halls for the use of the inclusion facilities in the Mining Geology Division, Royal School of Mines, and Dr. A H. Rankin who supervised the fluid inclusion studies

Mr P. Suddaby of the department of Geology, Imperial College, for help with the microprobe analyses.

Dr. I. Wilson and the management and staff of E C.C L.P. Ltd., for permission to examine the Bostraze Clay Pit and for the use of unpublished mineralogical and chemical data.

Mr. R. Barstow who provided mineral samples from his collection.

Dr. S. Sheppard and Mr. A Halliday for the use of unpublished data.

My friends and colleagues at King's College and the Royal School of Mines for all those valuable discussions.

Mrs. C Trafford who typed the manuscript and my wife who read it, and anyone else who has helped me thank you.

ABSTRACT

An attempt is made to integrate field and laboratory (geochemistry, petrology and fluid inclusion) studies, to produce a model for the development of hydrothermal activity in the St Just district.

The surface geology between Botallack and Levant Mine, and the sub-surface geology at Levant Mine is described The field data are presented on three maps (VOLUME 2)

New chemical and mineralogical data are presented for samples of thermally metamorphosed and metasomatised basalts and pelites, and hydrothermally altered pelites, basalts and granites

The results of a fluid inclusion study of several paragenetically significant ore-gangue samples are also presented.

The last section of the thesis comprises a review of the inclusion data for S.W. England, the presentation of new inclusion data for several specific mineral deposits from the province, and a discussion of the nature of the Cornubian batholithic hydrothermal system

CONTENTS

VOLUME 2

FIGURES

TABLES

PLATES

INTRODUCTION & OBJECTIVES

The expansion of mining activity in south-west England, in the last decade has led to a reapraisal of the mineral potential of the province as a whole and of specific areas in particular The extensive recent research concerned with the association of Sn-W and Cu-Mo mineralisation and 'granite' batholiths elsewhere in the world has also prompted a reinterpretation of the igneous, structural and mineralisation phenomena in the province

In 1972, Geevor Tin Mines Ltd., in co-operation with Union Corporation Ltd., was pursuing an intensive exploration programme in and around the old Levant Mine. I was fortunate to be involved in the final stages of this programme and field investigations during this period form the basis of this thesis.

The objectives of this study are

1) to describe the geology of Levant Mine and the surface area in the vicinity of the mine.
2) to study the mineralisation phenomena in the mine
3) to relate the mineralisation phenomena of Levant Mine with that of Geevor Mine and to construct an overall model for the development of mineralisation in the district.

A further objective, to compare the fluids (as indicated by fluid inclusions) in the St Just district vein systems with other vein systems in the province, was added at a later date.

This study has greatly benefitted from the simultaneous studies of other workers in the province especially Mr. D. Alderton, Mr J. Moore, Mr. A. Halliday and Dr. S Sheppard.

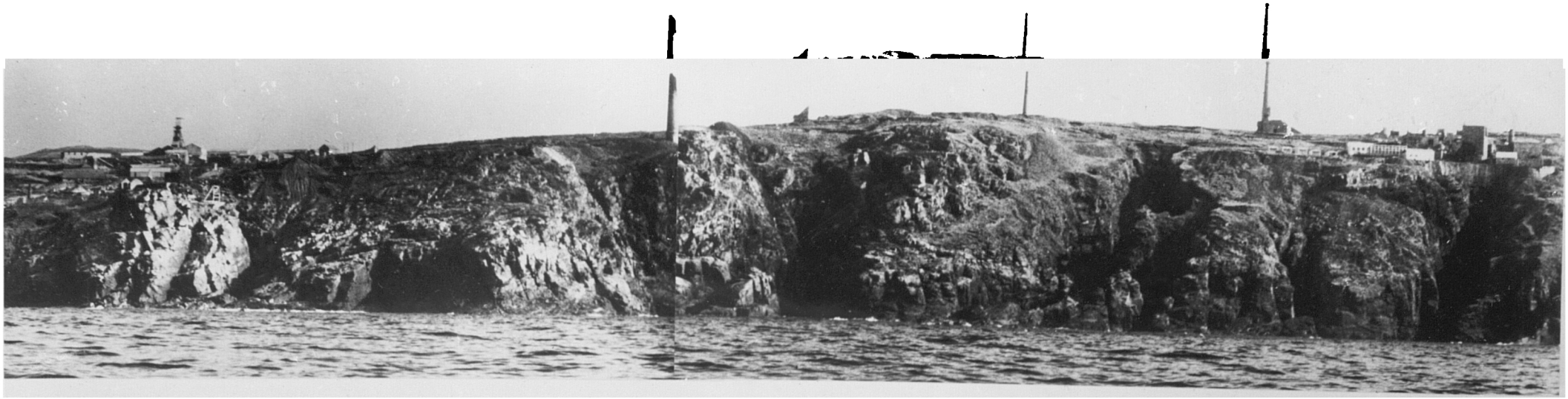

GEEVOR AND LEVANT MINES

PLATE 1

CHAPTER 1
THE GEOLOGY OF CORNUBIA

1 THE GEOLOGY OF CORNUBIA

A Introduction

The Cornubian peninsula, composed of Cornwall, Devon and Somerset, forms the south west extension to the mainland of Britain. It is 200 Km along its NE-SW axis, approximately triangular in shape and reaches a maximum elevation of 420 m.

Geologically, the peninsula is composed of a deformed Upper Palaeozoic, mainly marine sedimentary sequence of predominantly argillaceous rocks with subordinate coarse clastics, cherts and limestones, a contemporaneous suite of basic igneous volcanic and intrusive rocks and a post-kinematic granite batholith. In the south of the peninsula (Lizard and Dodman areas) high grade regional metamorphic complexes with associated basic and ultrabasic intrusions are developed. These complexes are thought to have been formed during an earlier orogenic cycle. Sn-W and Sn-Cu-As-Pb-Zn-Fe mineralisation is spatially and temporally related to the granite batholith.

B Crustal structure

The recent geophysical studies of Bott et. al. (1958), Bott and Scott (1964) and Bott (1970) have produced the following results.

1. A belt of large nagative gravity anomalies of upto 50 mgal amplitude lies along the axis of the postulated buried granite batholith and, in particular, coincides with the belt of Sn-Cu-As-Pb-Zn mineralisation. The continuity of the anomaly is interpreted as indicating the lateral continuity of the batholith.
2. Seismic data suggests a depth of 27 Km to the base of the crust (mohorovicic discontinuity). The granite batholith is probably sheet-like with a vertical thickness of 10-12 Km grading into a residual granitic layer.
3. Gravity data are interpreted as indicating that the shape of the batholith in NW-SE section is inverted shaped (⅂) with the vertical limb in the south and the horizontal limb extending northwards as a sheet upto 10 Km thick.
4. The Bouger anomaly rises south of the batholith by 10-15 mgal, reaching a maximum in the Lizard and Start areas. This positive anomaly coincides with the high-grade metamorphic complexes in these areas and their possible seaward extensions.
5. Seaborne total field magnetic surveys in the western English Channel (Allan 1961) reveal a NW-trending oval shaped magnetic anomaly of over 500 gamma amplitude, located 25 Km south of Eddystone. The data are interpreted as being consistent with a gabbro intrusion. NW-SE trending anomalies are also associated with the Lizard complex.

C Stratigraphy and sedimentation

Reading (1974) distinguished three distinct successions in S.W. England, in south Cornwall, south and north Devon and north Devon. He maintained that all three areas were developed on continental crust. Hendriks (1971) recognised two principal tectonic-sedimentary units, an over-ridding nappe in the south and a more extensive over-ridden unit, representing the pre-orogenic geosyncline in the north. The main stratigraphical units are shown in fig 1a.

In north Devon the succession consists of interbedded continental and shallow marine clastic rocks of Lower to Middle Devonian age. These were deposited on the Old Red Sandstone continental shelf. From late Middle Devonian to Visean times a 'bathyal lull' facies developed in south Devon and north Cornwall. Three sub-facies have been recognised: (a) reef limestones, (b) thin condensed sequences of limestone cherts and muds, (c) thicker beds of mudstones, cherts and limestone turbidites. This sedimentary regime was probably developed in fault bounded basins and on topographic highs (basin and swell structures), and is characterised by a lack of coarse clastic sediments. In south Cornwall, the argillaceous Mylor beds, possibly of Lower Devonian age, are overlain by turbidites of the Middle Devonian Gramscatho Beds. These are followed by Upper Devonian breccia conglomerates of the Gidley Well Beds and the Veryan Series, which contain abundant exotic blocks of Ordovician quartzites and Silurian to Middle

Fig 1

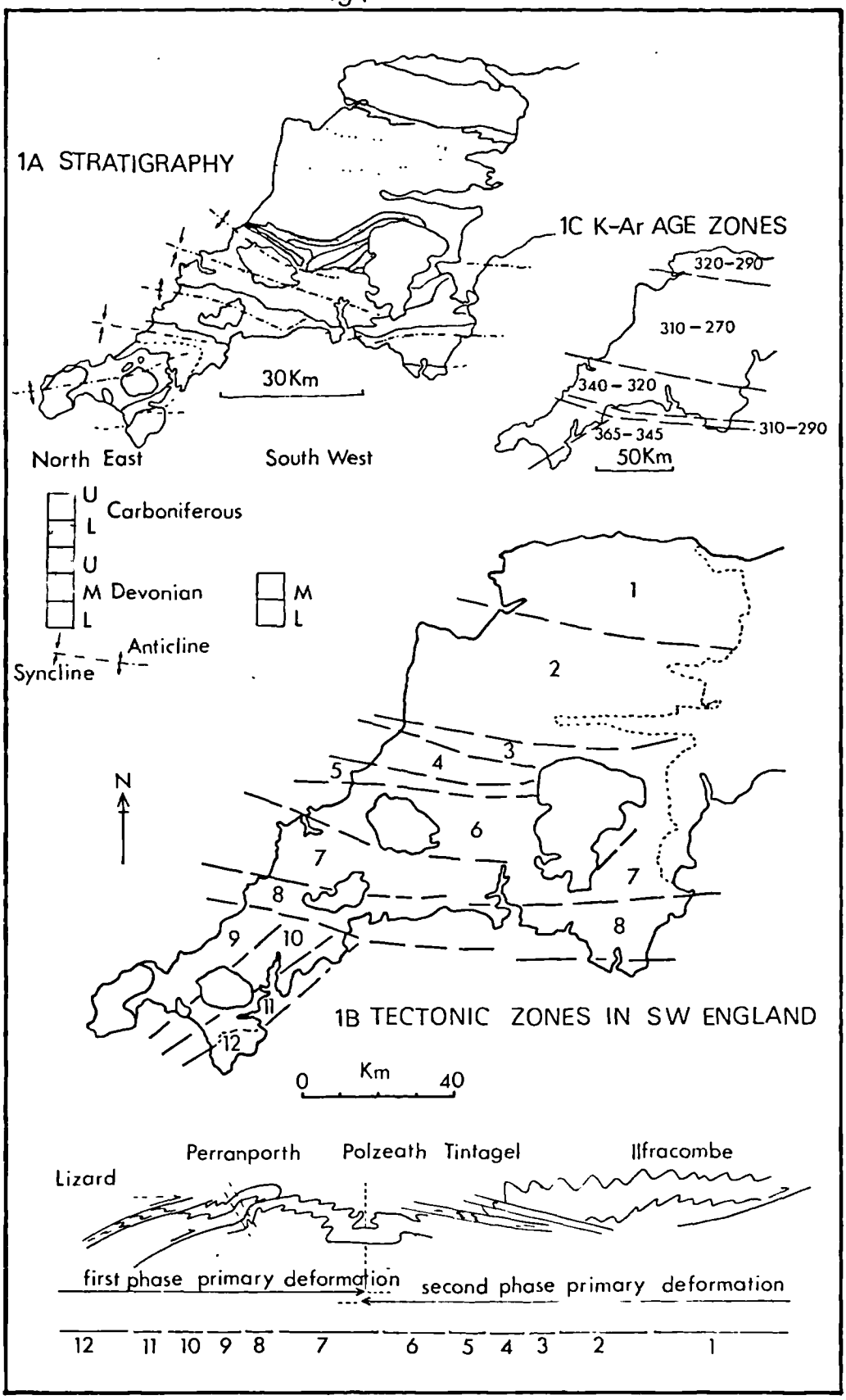
1A STRATIGRAPHY
30Km
North East
South West
U
L
Carboniferous
U
M Devonian
L
M
L
Anticline
Syncline
1C K-Ar AGE ZONES
320-290
310 - 270
340 - 320
310-290
365-345
50Km
N
1
2
3
4
5
6
7
7
8
8
9
10
11
12
1B TECTONIC ZONES IN SW ENGLAND
0
Km
40
Perranporth
Polzeath
Tintagel
Ilfracombe
Lizard
first phase primary deformation
second phase primary deformation
12
11
10
9
8
7
6
5
4
3
2
1

Devonian limestones and cherts, within Upper Devonian black shales and pillow lavas. This regime is therefore a combination of Middle Devonian flysch and Upper Devonian wildflysch and it is probably indicative of tectonic activity at this time in this area.

Carboniferous sediments are preserved in the culm basin. In north Devon paralic sedimentation continued from the Middle Devonian to the Upper Carboniferous. To the south in Devon and north Cornwall, thick sequences of Middle Carboniferous turbidites of the Crackington formation are overlain by non-marine clastics of the Bude formation. This flysch-molasse relationship is indicative of the final silting up and closure of the Upper Palaeozoic Cornubian geosyncline.

D Devonian and Carboniferous magmatism

Volcanic and intrusive igneous rocks are present throughout the Upper Palaeozoic successions of Cornubia. The magmatic activity was predominantly basaltic in character, the basic rocks being known locally as 'greenstones'. In addition to the basic igneous rocks there are also minor acid lavas and pyroclastics.

The distribution of the main igneous masses is shown in fig 2a. Two main zones can be distinguished: a south western NE-SW trending belt and a northern E-W belt.

The basaltic members form massive flows, pillow flows, tuff beds and intrusive sheets and small stocks. The minor acid members are predominantly pyroclastic in

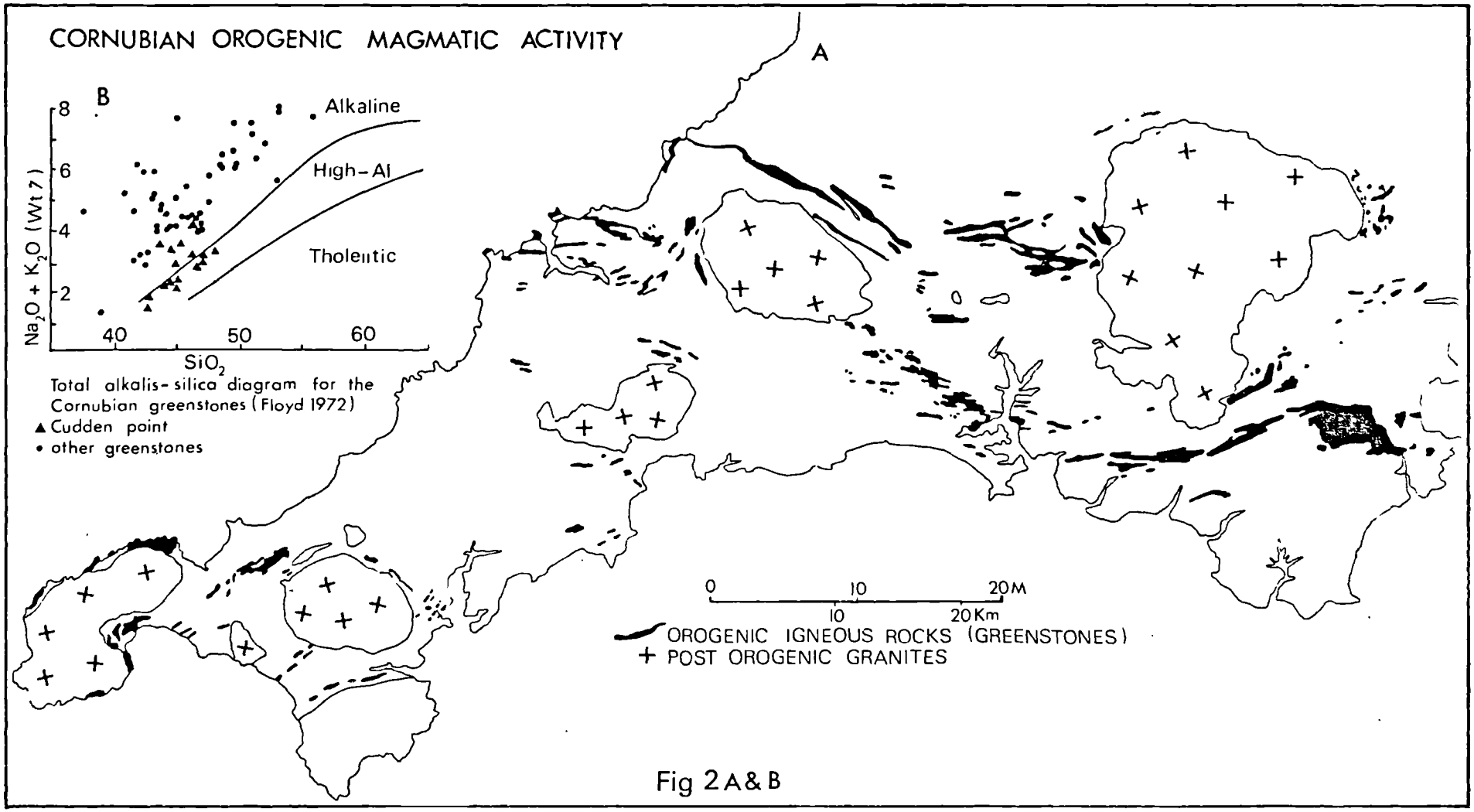
CORNUBIAN OROGENIC MAGMATIC ACTIVITY
A
B
Alkaline
High-Al
Tholeiitic
8
6
4
2
40
50
60
$Na_2O + K_2O$ (Wt %)
SiO_2
Total alkalis-silica diagram for the Cornubian greenstones (Floyd 1972)
▲ Cudden point
• other greenstones
0
10
20M
10
20Km
OROGENIC IGNEOUS ROCKS (GREENSTONES)
+ POST OROGENIC GRANITES

Fig 2A&B

nature, forming local agglomerate, ash and tuff beds.

Within the extrusive sequences two distinct chemical groups have been recognised, a spilitic group developed throughout the whole magmatic province, and a potassic group (K-trachytes and keratophyres) mainly developed in the Lower Carboniferous of the northern outcrop. Intrusive members are usually spilitic in character.

Mineralogically the spilites are composed of albite-amphibole-chlorite-epidote ± calcite and magnetite, replacing an original plagioclase clinopyroxene ± olivine assemblage. Their present mineralogy was developed in response to low grade regional metamorphism.

The position of the greenstones in the CIPW normative classification (Floyd, 1972 a) and on the silica-alkalis diagram (fig 2b) shows the predominantly alkaline nature of the province. Other chemical characteristics (Floyd, 1972 b) are 2 - 8% total alkalis, K/Rb ratios of 300-450 (average 335), K, Rb, Ba, Sr, Ti, Zr, and P values, and Sr/Rb, Na/K, K/Ba ratios, similar to those of other alkali basalts.

E Structure

The broad structural elements have been known for a long time; De La Beche in 1839 appreciated the synclinal nature of mid-Devon and north Cornwall. Additional stratigraphical and structural detail has confirmed the synclinal nature of the Carboniferous but

it has also revealed a complex interplay of Upper and Lower Carboniferous and Lower Carboniferous and Upper Devonian rocks along the southern boundary. The Devonian outcrop is divided by the Carboniferous. In the southern outcrop there are two major anticlines involving the lowest Devonian rocks exposed in the peninsula. Structures in this outcrop are limited in the south by the fault boundary with the Lizard - Start - Dodman metamorphic complexes. The northern outcrop of Devonian rocks consists of a regular descending sequence of strata from the Carboniferous boundary.

Dearman (1969) defined four distinct tectonic zones in the peninsula (excluding the Lizard, Dodman and Start areas). This tectonic zonation was revised by Sanderson and Dearman in 1973, when they defined twelve structural zones based on the attitude of fold axes and axial planes, the facing direction of the axial plane and the relative ages of the fold event. With reference to fig 1b, the main characteristics of the twelve zones are summarised below.

1. East-west subhorizontal fold axes, facing upwards and overturned to the north.
2. East-west trending upright folds with subhorizontal axes. The F_1 folds are overturned in the north as Zone 1 is approached.
3. East-west folds overturned to the south. This zone is transitional into the zone of recumbent folding further south.
4. Recumbent F_1 folds with east-west axes.

5. A narrow zone of intense deformation, resulting in strong stretching within the slaty cleavage and rotation of the fold axes to form oblique folds, with axial directions roughly north-south. Dearman (1969 b) defined this as a zone of tergiversation.
6. South facing recumbent folds, with ENE-WSW trending axes. Zones 4 and 6 form a recumbent fold zone, within which Zone 5 is developed.
7. North facing recumbent folds, with ENE-WSW trending axes.
8. From north to south there is an increase in the development and intensity of F_2 folding and associated crenulation cleavage, folds are overturned to the north.
9. Folds developed in Gramscatho and Mylor Beds. Primary folds are recumbent, with ENE-WSW trending axes, which face north or north west. These folds are affected by mesoscopic upright folds with an intense crenulation cleavage.
10. and 11. Primary folds with SE to SSE gently to moderately dipping axial planes. Zone 10 has NE-SW trending fold axes, whereas oblique folds, plunging to the SE are developed in Zone 11. These zones correspond to the zone of tergiversation in the north (Zone 5). Zones 5, 10 and 11 are thought to mark the transition between an overriding supracrustal region, from a more passive, recumbently folded infrastructural region beneath.
12. Higher grade regional metamorphic complexes of the Lizard and Dodman.

Radiometric age determinations on the slates of S.W. England by Dodson & Rex (1971) has revealed three groups of ages (fig 1c).

1. 365-345 my. in the Dodman and Gramscatho slates, interpreted as an Upper Devonian or Lower Carboniferous phase of folding or a phase of uplift.
2. 340-320 my. in the Devonian slate belt of the Newquay to Padstow area attributed to an end Lower Carboniferous tectonic event.
3. 310-270 my. in north Cornwall and north Devon, indicating late Carboniferous folding.

F The granite batholith

The Cornubian batholith is composed of six major and several minor plutonic masses and their associated hypabyssal sheets and dykes (fig 3a). The major masses display features typical of post kinematic high-level plutons. Each pluton is roughly circular or elliptical in plan, contacts are sharp and usually discordant and the grade of contact metamorphism never exceeds that of the hornblende hornfels facies.

1. The main plutons: Hosking (1962) suggested that the major plutonic masses were connected at depth so forming a continuous batholith. This has been confirmed by geophysical studies (part A). The total length of the batholith is unknown, the recovery of granitic rocks at Haig Fras in the Western Approaches (Smith, Stride,

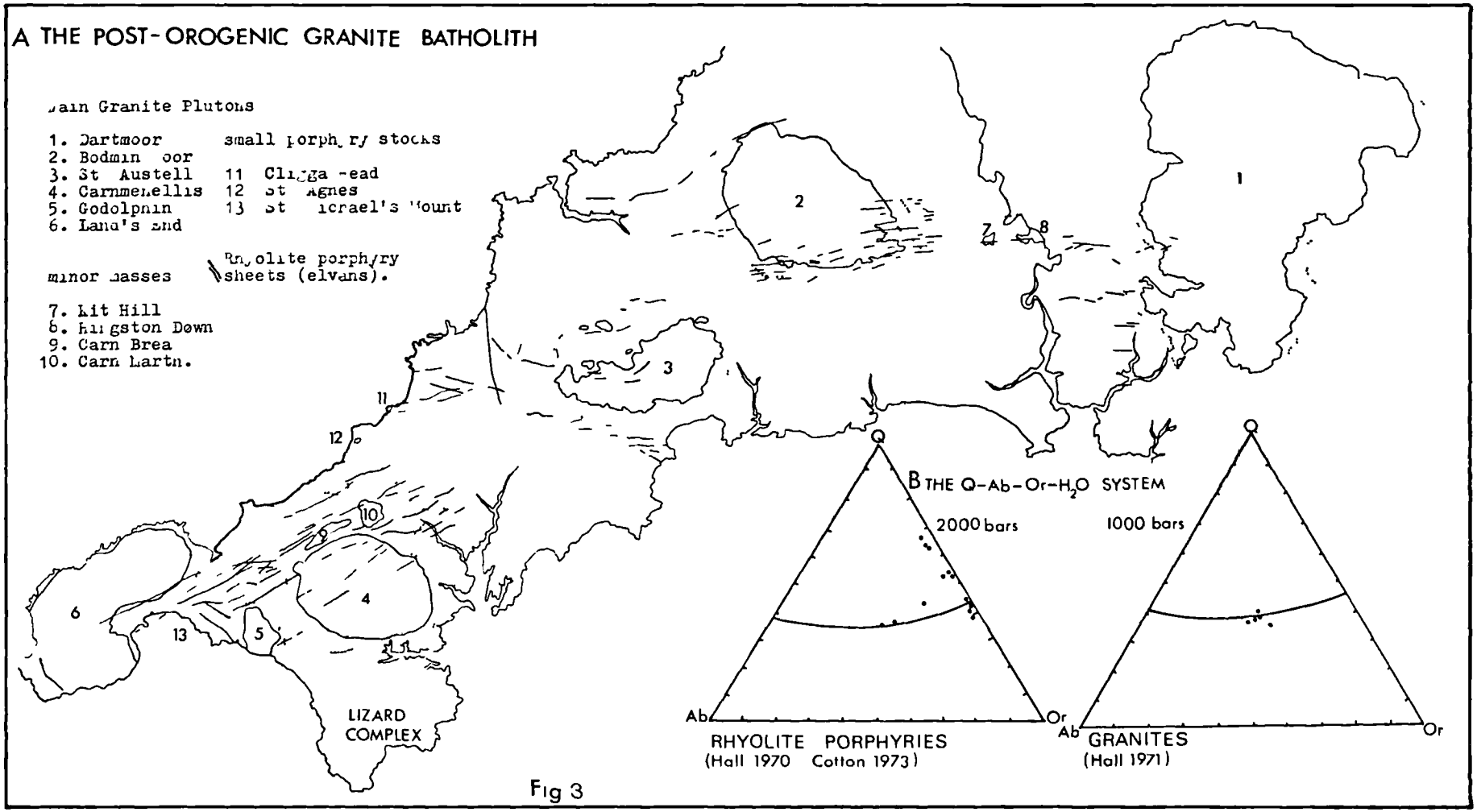
A THE POST-OROGENIC GRANITE BATHOLITH
Main Granite Plutons
1. Dartmoor
2. Bodmin Moor
3. St Austell
4. Carnmenellis
5. Godolphin
6. Land's End
small porphyry stocks
11 Clicga-head
12 St Agnes
13 St Michael's Mount
minor masses
Rhyolite porphyry sheets (elvans).
7. Kit Hill
8. Hingston Down
9. Carn Brea
10. Carn Marth.
LIZARD COMPLEX
B THE Q-Ab-Or-H2O SYSTEM
2000 bars
1000 bars
Q
Ab
Or
RHYOLITE PORPHYRIES
(Hall 1970 Cotton 1973)
GRANITES
(Hall 1971)

Fig 3

Whittard & Sabine, 1965) suggests the total axial length may be in excess of 300 Km. The width is probably less than 50 Km.

Geophysical investigations suggest that the batholith is inverted ⅂ shaped in cross-section with a steep southern limb and a horizontal limb extending northwards as a sheet upto 12 Km thick. The granite is considered to pass into a residual granitic layer below this depth.

The main plutons vary in composition and texture from basic microgranites to coarse porphyritic biotite granites, adamellites and medium grained quartz-feldspar porphyries. The sheets are often banded aplite-pegmatites and the dykes are predominantly quartz-feldspar rhyolite porphyries. Locally, in the roof and marginal zones of the main pluton aplite-pegmatite and leucogranite become dominant.

Mineralogically the granites are composed of quartz, plagioclase (less than An_{40} usually An_{10-20}), perthitic orthoclase ± microcline often as large megacrysts, biotite, muscovite and sometimes a lithium mica. Accessories include tourmaline, apatite, topaz, fluorite, zircon, sphene, rutile, anatase, brookite, magnetite, andalusite, cordierite, garnet, sulphides and cassiterite.

Modal data for some of the coarse porphyritic biotite granites (Exley and Stone, 1964) give ranges for quartz 30-40%, orthoclase 25-35%, plagioclase 15-25%, biotite 2-10%, muscovite 0.5-7%, accessories 0.5-2%.

Chemically the granites are enriched in B, Li, F, As, Cu, Pb, Zn, Sn, U, Cl, Rb, Cs, Nb, and Th (Hall, 1971; Wilson, 1972; Floyd, 1972) compared to published average values for low-calcium granites (Turekian and Wedepohl, 1961). Ba and Sr values and K/Rb ratios are relatively low, a feature which suggests that the granites are well fractionated. The total chemistry is considered to reflect some degree of magmatic differentiation and the superimposed effects of contamination and internal metasomatism. An important chemical feature of the granites is the negative correlation between Na and K. This has been attributed to large-scale metasomatism caused by the migration of K-rich aqueous fluids (Exley and Stone, 1964).

The normative compositions of the unaltered granites, when plotted on a Q-Or-Ab triangular diagram (fig 3b) fall near the 'ternary' minimum for a water pressure of approximately 1000 bars (Tuttle and Bowen, 1958).

Isotopic age determinations indicate that the batholith was emplaced 280 ± 10 my. (Miller and Mohr, 1974).

2. Rhyolite porphyry sheets: the distribution of rhyolite porphyry sheets locally known as elvans is shown in fig 3a. They have a variable trend and commonly occupy dilated extensional fissures probably created by intrusive stresses (Moore, 1975). They are usually steeply inclined

and have strike lengths of upto 15 Km. They vary in thickness from a few metres to 150 m. (Cotton, 1973).

Mineralogically they are composed of phenocrysts of quartz and orthoclase with accessory tourmaline, biotite, zircon, apatite and cassiterite. Phenocrysts form upto 30% and matrix upto 90%. The matrix usually consists of graphically intergrown quartz and alkali feldspar.

The sheets display fine grained chilled aphanitic margins and coarser porphyritic interiors. This has been interpreted by Henley (1974) as due to crystal settling in the original reservoir followed by injection of aphanitic magma and later by porphyritic magma. Another feature, the change from flow-laminated to massive structure is probably due to a change in either viscocity or velocity leading from laminar flow to turbulent flow. The flow folding and flow brecciation structures of Goode (1973) possibly represent instability of the laminar flow before complete turbulence could set in. In many cases however the changes in texture and structure are coincident suggesting a viscocity contrast between the rhyolitic and porphyritic magmas.

The porphyries are usually rich in Si and K and depleted in Na, Mg and Ca. Cl, Cu, Zn, Pb, As, Sn, Rb, Cs, Th, and U are enriched and Ba and K/Rb ratios are low compared to published values for low Ca granites (Turekian and Wedepohl, 1961).

The majority of porphyry analyses are grouped on the quartz-orthoclase line in the system quartz-

orthoclase-albite (fig 3b). However, some analyses e.g. Mellanear elvan (Phillips, 1875) and the Hingston Down elvan (Hall, 1970) plot near the ternary minima for a water pressure of 2000 bars. Hall (1970) reasoned that these rhyolite porphyries had been directly derived from a 'normal' granite magma and that the others could not have been derived from a similar source. Stone (1968) suggested that the K-rich Praa Sands elvan had been derived from a biotite granite magma by alkali exchange. Cotton (1973) suggested that the elvans of the United Mines Gwennap were kaolinised during their emplacement therefore offering an explanation for the low Na/K ratios. If however the emplacement scheme of Henley (1974) is considered ie. crystal settling followed by multiphase intrusion, then this mechanism alone could account for the K-rich nature of the porphyry.

In general the porphyries post date the plutons but pre date the main phase of mineralisation.

G Mineralisation

The Cornubian metallogenic province is characterised by major vein and minor replacement deposits of W-Sn-Cu-As-Fe-Pb-Zn-Sb-Ag-Au-U-Co-Ni. These deposits are spatially and temporally associated with the granite batholith. Compositionally and morphologically the deposits can be divided into:

1. mineralised pegmatites (W-Sn-Zn-As-Be-P-Li)

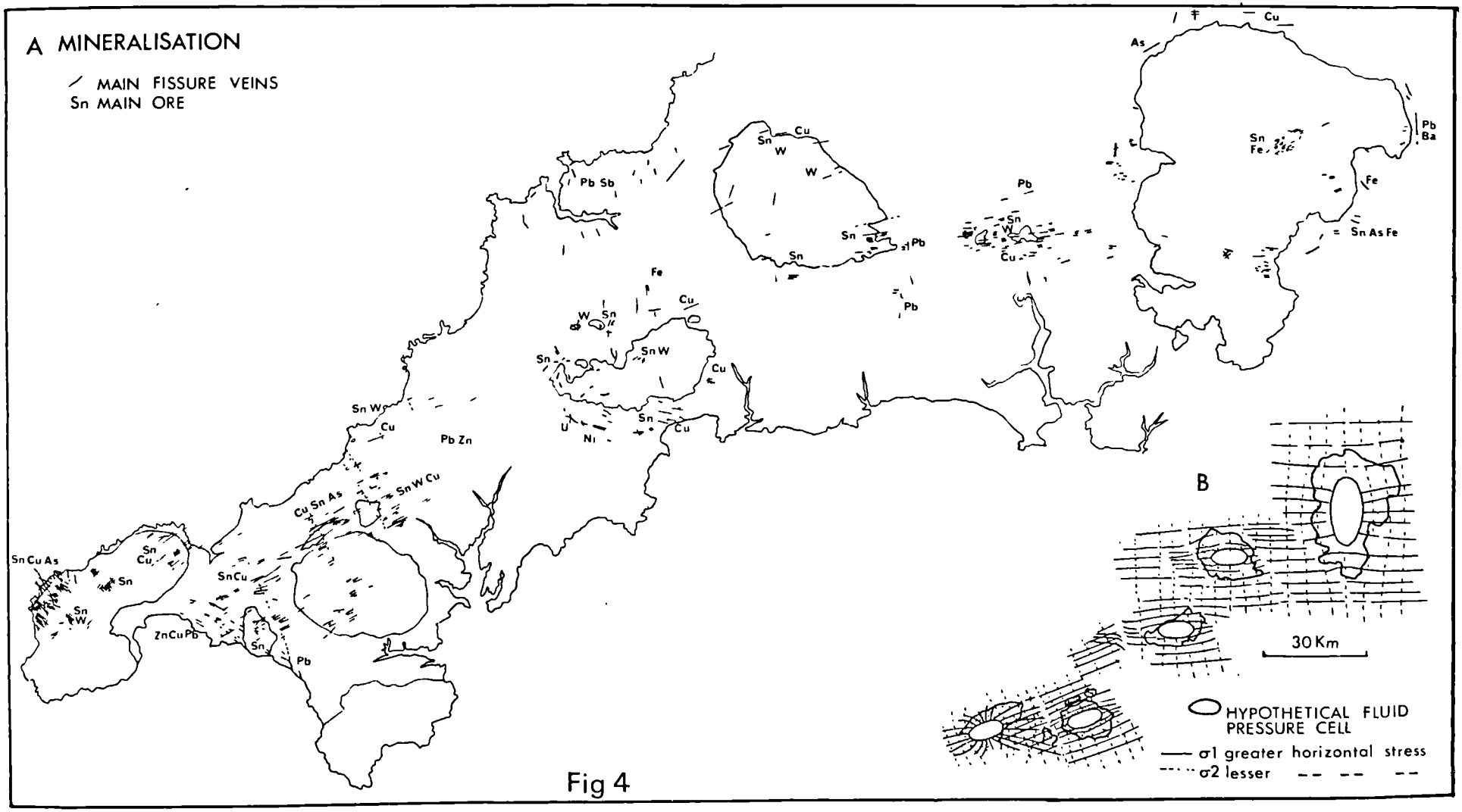
A MINERALISATION
MAIN FISSURE VEINS
Sn MAIN ORE
Cu
As
Pb
Ba
Sn
Fe
Fe
= Sn As Fe
Pb Sb
Sn
W
Cu
W
Sn
Pb
Pb
Sn
W
Cu
Pb
Fe
W
Sn
Cu
Sn
Sn W
Cu
Sn
Cu
Sn
Cu
Pb Zn
U
Ni
Sn
Cu
Cu Sn As
Sn W Cu
Sn Cu As
Sn
Cu
Sn
Sn
W
Sn Cu
Zn Cu Pb
Sn
Pb
B
30 Km
HYPOTHETICAL FLUID PRESSURE CELL
σ1 greater horizontal stress
σ2 lesser

Fig 4

2. single fissure veins, hypo and mesothermal lodes (W-Sn-Cu-As-Fe-Bi-Zn), epithermal cross-courses and caunter veins (Pb-Zn-Ag-Sb-Au-Fe-Co-U)
3. multiple fissure veins both uni and multi-directional (W-Sn-Cu-As-Zn)
4. replacement deposits (carbonas),pipes, floors, sheets or irregular disseminations of Sn-Cu-As-Fe in granite, metasediments or metaigneous rocks.

1. Mineralised pegmatites form sheets and small pods, usually in the roof or border zones of the plutons. They are usually barren but rarely they may contain combinations of wolfram, cassiterite, sphalerite, arsenopyrite, beryl, apatite and tourmaline.

2. Single fissures are usually between 5 cm and 5 m wide, and they are economically mineralised for a strike length of upto 2 Km and a dip length of 1 Km. The fissure is usually a simple subvertical tensional or shear-fracture, with a fairly constant trend. Alteration envelopes surrounding these ore-bodies are variable and depend on; the vein infill, the spatial position within the fissure system and the composition of the host rock. In well developed single fissures the visible alteration may be upto 5 m in width, but is usually less than 1 m. Sericite, tourmaline, feldspar and chlorite are the dominant alteration phases in the envelopes.

Compositionally three types of vein can be distinguished:

a) 'Early', high temperature, complex wolfram ± arsenopyrite and cassiterite veins. These are developed in granite and aureole rocks and they often contain younger phases of mineralisation. A good example of this type is the complex wolfram lode of South Crofty Mine.

b) 'Normal' Sn-Cu-Fe-As minor Pb-Zn-U veins. These are the commonest type of vein in the province and they also show evidence of polyphase mineralisation.

c) 'Late', low temperature Fe-Pb-Zn-Sb-Ag-U-Co veins. These occur in metamorphosed host rocks in fissures trending obliquely to the main hypothermal vein system.

3. Multiple fissure systems are composed of many (several hundred) structurally discontinuous, narrow veins with either a sub-parallel orientation (sheet complex) or multidirectional orientation (stockwork). Individual veins are between 1 and 20 cm wide and they are sporadically mineralised for a strike and dip length of usually less than 100 m.

In granite there are two types of multiple fissure veins:

a) quartz ± tourmaline wolfram-cassiterite-arsenopyrite-chalcopyrite bornite topaz beryl bordered by intense phyllic (greisen) wall rock.

b) quartz orthoclase cassiterite ± arsenopyrite bordered by feldspathised (orthoclase) wall rock.

Type (a) veins are developed in small porphyry stocks (Cligga Head, St Michael's Mount), and cupolas (Kit Hill, Hingston Down, Hemerdon), or internally in the roof zones of some of the larger plutons (Bostraze - Land's End pluton). Type (b) veins are rarer, the only example known to the author occurs at South Crofty Mine.

Multiple fissure veins (stockworks) also occur in metasediments. They usually occur near porphyry stocks and cupolas which contain sheet complexes e.g. Cligga Head and Hemerdon, but they also occur at considerable distances away from known granite outcrops e.g. Mulberry. They commonly contain either cassiterite ± wolfram or tin, copper, iron and arsenic sulphides.

4. Replacement deposits are rare in the Cornubian metallogenic province and unfortunately there are very few examples still available for study. Locally these deposits are known as 'Carbonas' and they can be morphologically divided into pipes and sheets. Pipes are cylindroidal bodies of intensely altered rock with a maximum diameter of 20 m and length of 200 m. They may be vertical, inclined or horizontal and are usually associated with a minor mineralised fissure. Sheets are much more lode-like in character; they are planar bodies of intensely altered rock occurring on the foot-wall of a fault, below the intersection of two fissures, or bordering a normal lode. They are usually subvertical, upto 200 m in strike and dip length, and 20 m in thickness. The ore assemblage is dominantly cassiterite

in association with pyrite, chalcopyrite and arsenopyrite. Fluorite, tourmaline, chlorite and quartz are the main gangue minerals. The associated wall-rock alteration is usually intense but variable, reflecting local fluid compositions, e.g. greisenisation (East Lovell), tourmalinisation (St. Ives Consols), chloritisation and albitisation (Geevor and Levant).

Geographically most of the documented replacement deposits occur in the extreme S.W. of the province, in the Land's End and Carmenellis plutons. Favourable sites for the development of these deposits occur:

a) In the roof of the pluton within a vertical ore-shoot (East Lovell),
b) At the margins of the pluton near the intersection of the ore-shoot with the contact (Geevor),
c) Outside the pluton within the ore-shoot at the intersection of a 'favourable' horizon with a mineralised vein system (Levant, Botallack).

As well as the high-grade (1-2% SnO_2) replacement deposits there are also low-grade (0.1-0.5% SnO_2), subeconomic, disseminated cassiterite deposits. These deposits are usually composed of numerous, small, discontinuous vein and disseminations of pyrite and cassiterite with rare wolfram, arsenopyrite, sphalerite and chalcopyrite.

In granite these deposits are associated with pervasive alteration envelopes of kaolinised, greisenised

silicified or tourmalinised host. They mainly occur in the St Austell district (Rocks, Bunny and Carclaze), In metabasite they are associated with pervasive borosilicate (tourmaline, axinite), biotite and chlorite assemblages and in metapelite with chlorite and sericite.

H Fracture systems

The regional fracture pattern was of fundamental importance in localising the fissure vein ore deposits and the porphyry dykes. Moore (1975) constructed diagrams representing the trajectories of the minimum and intermediate principal stress axes as they were at the time of sheet porphyry intrusion and fissure vein formation (fig 4b).

The trajectory diagrams indicate that the mapped configuration of veins and porphyry dykes results from fluid pressures exerted by the mobile cores of the granite plutons situated within a regional stress field. The stress models also indicate that fugitive dyke magma or hydrothermal fluids, emmanating from a cupola, will make the mechanically easiest exit through the flanks of the intrusion. So explaining the assymetrical disposition of belts of mineralisation which border the granite cupolas of S.W. England.

Throughout most of Cornubia fractures parallel to $\sigma 1$ trajectories are preferentially mineralised with Sn-Cu-W-As ores and fractures parallel to $\sigma 3$ (cross-courses) are barren or contain low temperature

Fe-Pb-Zn-Sb ores. However, deviations and complications occur where two plutonic fracture systems interact.

I Cornubian and Hercynian plate tectonic models

Many plate tectonic models have been proposed to explain the overall geological features of Cornubia and its relation to the rest of the Hercynian orogenic belt. The following text is a synopsis of recent plate tectonic models.

Nicholas (1972) compared the Hercynian orogenic belt with the Andean Cordilleran type. He maintained that the Hercynides were developed on continental crust on the southern margin of the Eurasian Upper Palaeozoic continent above a north dipping subduction zone originating in the present mediterranean region.

Burret (1972) postulated a mid-European Upper Palaeozoic ocean separating northern Europe (RHENO-HERCYNIAN ZONE) from a southern European (ARMORICAN ZONE). This ocean was totally consumed during continental collision at the end of the Carboniferous.

Burne (1973) proposed a similar model to Burret's with a mid-Devonian Island arc system developed above a north dipping subduction zone in south Devon and a south dipping subduction zone below south Cornwall. The central ocean was consumed in Wesphalian times when south and north Cornwall were fused.

Floyd (1972) considered the petrochemistry of the 'greenstone' belt and the granite batholith and

proposed a model similar to that of Nicholas.

Reading (1974) modified the Floyd model by adding an Upper Middle Devonian extending marginal basin situated above a north dipping subduction zone.

Mitchell (1974) suggested that a primary Devonian, Rheic, ocean between mid Devon and south Cornwall was consumed by south dipping subduction in the Middle Carboniferous.

All these models are based on either north and or south dipping subduction zones. However, Bromley (1975) suggested that certain magmatic features of the Hercynian belt might be explained by plate movements over mantle hot spots.

Badham and Halls (1975) proposed a complex model involving microplate tectonics and oblique plate collisions.

None of these models adequately explains all the features of all parts of the Hercynian orogenic belt. However, the model proposed by Badham and Halls shows how many geological features, such as, the irregular distributions in time and space of ophiolite complexes and island arc sequences, major strike slip faults and metallogenic belts within the Hercynian orogen can at least be partly reconciled.

CHAPTER 2

THE GEOLOGY OF THE St. JUST DISTRICT WITH PARTICULAR REFERENCE TO THE BOTALLACK–LEVANT AREA

2. The Geology of the St. Just District with particular reference to the Botallack and Levant area.

A Introduction

The St. Just District can be divided into two units (Map 1): an eastern inland unit, formed by the roof and northern margin of the Land's End granite pluton and a western unit 0.5 Km wide and 5.5 Km long, formed by the contact aureole of the Land's End pluton, comprising an interbedded sequence of thermally metamorphosed and metasomatised basalts and pelites.

B Previous work

The St. Just District has attracted the attention of numerous geologists, petrologists and mineralogists for over 150 years. The first account of the local geology was provided by Davy (1818), who described the coastal exposures around Cape Cornwall. The district has been the subject of two thesis studies. Garnett (1962) described the geology and mineralisation of Geevor Mine and included some fairly detailed geological descriptions of the district. He also included a detailed review of the work completed at that time. Barklay (1959) described the geology of the area between Priests Cove and Pendeen.

In addition to the more general geological descriptions the area has formed the basis for more localised projects. The 'greenstones' have received considerable mineralogical and geochemical attention -

Tilley & Flett (1930), Tilley (1935), Floyd (1965, 1968a & 1967), Khan (1972), Cotton (1973) and Chinner & Fox (1974), while the metasediments were described and analysed by Khan (1972). The marginal facies of the plutonic granite were analysed by Wilson (1972) and Khan (1972). The large volume of varied and detailed work which the area has supported clearly indicates its geological importance.

The Botallack - Levant area.

In view of the many specific and general geological investigations which the St. Just aureole has received, and faced with the need for a surface geological comparison for the subsurface geology of Levant Mine, attention was focused on the area between Botallack (SW 363 334) and Levant Mine (SW 368 345). The area was mapped in detail on a 1 : 1000 scale (Map 5, volume 2). The outcrop is composed of metabasalts and metasediments which form approximately 75 & 25% of the exposure, respectively.

C Metasediments

The sedimentary sequence consists of dominant pelites with subsidiary carbonate - pelite and chert horizons.

The pelites grade from fine grained, poorly laminated, mica rich rocks to strongly laminated pelites with siliceous, detrital laminae (plate 3). The particle size of the least metamorphosed pelites is silt to fine

sand grade (~0.01 - 0.1 mm), although the quartz rich laminae often contain coarser particles. The thermally metamorphosed pelites contain an assemblage of biotite, muscovite, chlorite, quartz and opaque phases. Equigranular polygonal textures are common in the more siliceous pelites but spotted structures and relict oriented fabrics are more common in the micaceous pelites.

Geochemistry - Khan (1972) found, after extensive geochemical (23 major & trace elements of many metasediments) and statistical studies (Q-mode cluster analysis), that he could distinguish distinct groups of metasediments:

1. Q-mode cluster analysis of mafic & felsic elements);
   a) most of the metasediments from Priests Cove, Portheras Cove, Pendeen and the Avarack correlate with each other at 0.75 correlation coefficient.
   b) most of the Cape Cornwall metasediments form a separate group.
   c) the biotite rich metasediments form a separate group.
2. Further groupings were derived by Q-mode clustering (using mainly the mafic elements) correlated with distance from the granite contact:
   a) sediments lying within 600' of the contact. This group is enriched in Al, K, Rb, Zr, Ba, Pb and Th, and depleted in Si, Ca, Na and Sr.
   b) sediments lying between 30' and 1200' of the contact. These rocks are rich in Si, Mg, Ca, Na, P,

PLATE 2 METABASALTS

A Undeformed pillow lavas, Kenidjack

B Amygdaloidal texture (thin section)

C Banded amphibolite (above), vesicular basalt (below)

D Banded texture (thin section)

E Flow banding (thin section)

F Dolerite sheet, Botallack Head

G Two lava flows, The Crowns

H Folding in banded amphibolites, N. face Carn Vellan

I Fold in banded amphibolites, Botallack Head quarry

PLATE 3 METASOMITES AND METASEDIMENTS

A Massive Ca metasomite, Crowns Rock

B Amygdaloidal basalt being converted to Ca metasomite

C Iso-anisotropic garnet in massive Ca metasomite, Crowns Rock (thin section)

D Discordant Ca-B vein metasomite, Botallack Head

E Euhedral, zoned garnet in vein metasomite, Crowns Rock (thin section)

F Zoned axinite in vein metasomite, Botallack Head (thin section)

G Laminated pelite showing alternating bands of biotite-muscovite and quartz (thin section)

H Fold in pelite, Botallack Cliff

I Fold in pelite, S. face Carn Vellan

J Discordant fold in pelite below lava flow, The Crowns

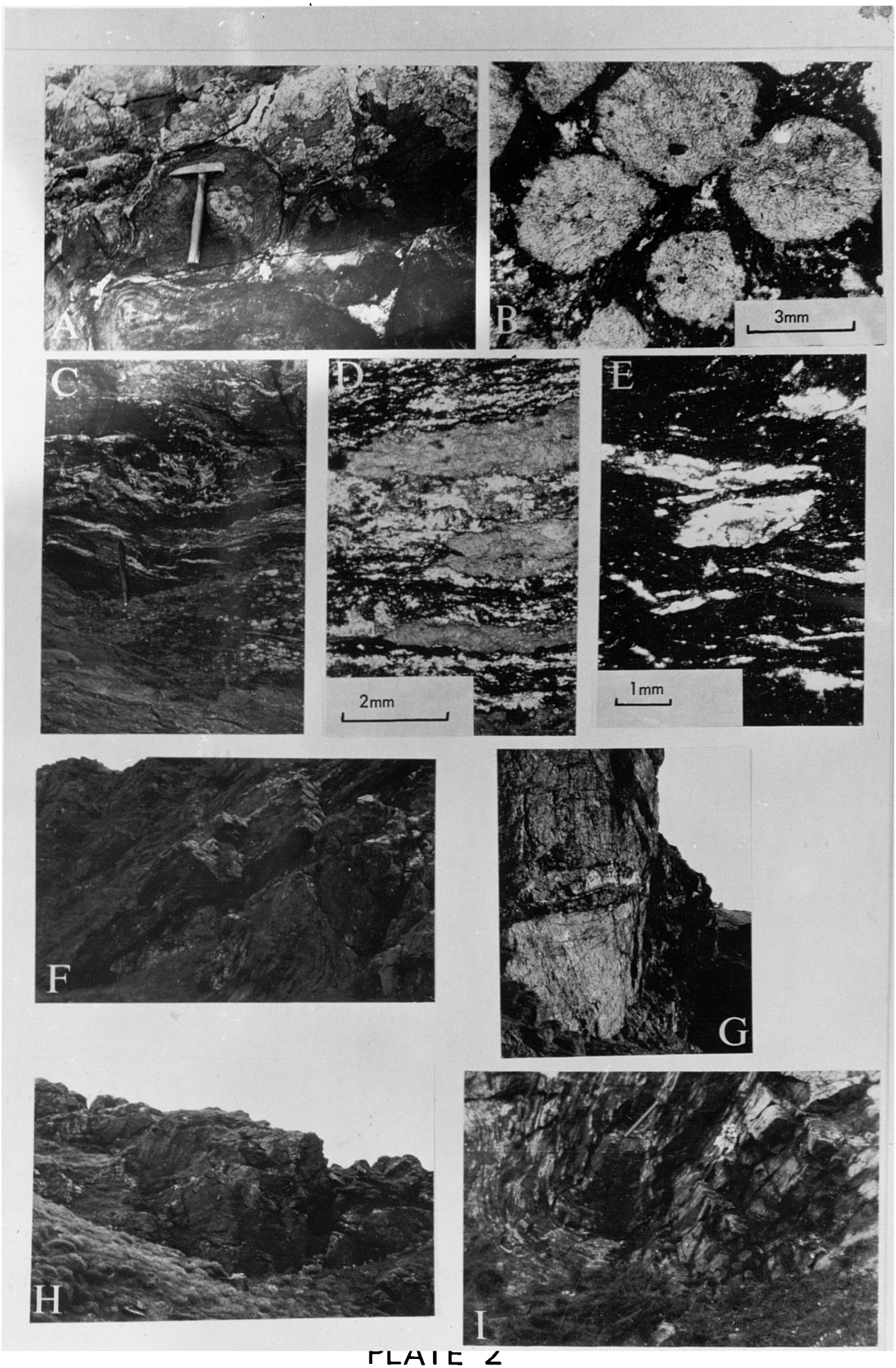

PLATE 2

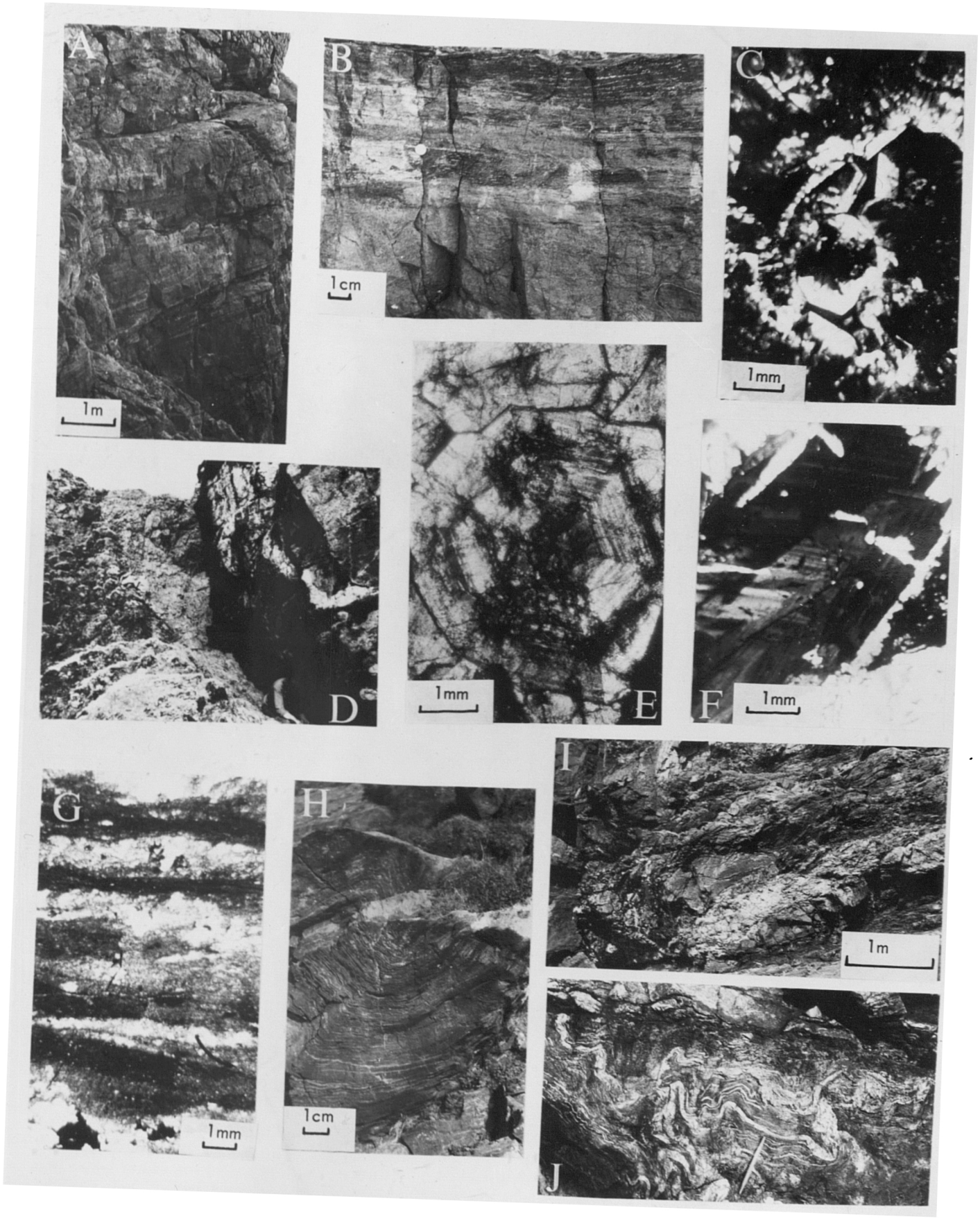

PLATE 3

H_2O, CO_2, S and Sr, and depleted in Ti, Al, Fe^{3+}, Mn, K, Rb, Zr, Ba and Pb.

c) metasomatic biotite rich rocks lying within 20' of the contact. These rocks are rich in Ti, Fe^{3+}, Fe^{2+}, Mn, Mg, K, S, Cl, Nb and Cu, and low in Si, Al, Na, Cr, Ni, Ba, La, Pb and Th.

D Metabasalts

Taylor and Wilson (1975) recognised 4 main groups of rocks within the metabasite sequences of West Cornwall.

1. fine grained pillow lavas.
2. a medium to coarse grained, intrusive, intravolcanic suite, intruded concordantly with the volcanic and sedimentary rocks.
3. agglomerates and tuffs of restricted occurrence.
4. medium to coarse grained intrusive sills which post-date the extrusive rocks but which have been deformed during the later phases of folding.

The basaltic rocks of this part of the St. Just aureole form the following groups:

1. Pillow structured basalts.
2. Massive non-pillowed basalts.
3. Medium grained, intra-volcanic , sheets.
4. Massive, structureless or banded amphibolites of unknown parentage (often intensely metasomatised).

1. Pillow structured basalt flows form approximately 60% of the metabasite outcrop. They occur on the

promontary north of Zawn a Bal, at the base of the cliffs in De Narrow Zawn, at the base of the cliffs between the Crowns and Botallack, at the base of the Carn Vellan cliffs, between Unity Shaft and Carn Du and in Trewellard South Cliff.

Individual pillows are ellipsoidal in shape and are usually between 0.25 - 0.75 m x 0.1 - 0.25 m in size. They occasionally display radiating or polygonal cooling joints and sometimes contain interstitial chert or ferruginous material. Where the lavas are extruded onto soft sediment (plate 3), the sedimentary material is often incorporated in the base of the flow.

The pillow lavas are characterised by amygdaloidal and hyalopilitic textures (plate 2). Amygdaloidal texture, typified by a majority of the pillow lavas, consists of approximately spherical amygdales (0.5 cm diameter), containing a mixture of chlorite, quartz, calcite and alkali feldspar, set in a fine grained (<0.1 mm) devitrified glassy matrix of opaque oxides (magnetite and ilmenite), quartz and feldspar. The matrix may or may not display flow banding (defined by streams of opaque oxides). Hyalopilitic texture, typified by the pillowed basalts at the base of the Carn Vellan cliff, consists of distorted amygdales, elongated parallel to the flow banding, set in a matrix of opaque oxides, plagioclase and biotite. Plagioclase occurs in small (0.1 mm) laths, oriented parallel to the flow banding.

2. Non-pillowed basalt flows form approximately 10% of the metabasite outcrop. They occur on the promontary north of Zawn a Bal, at the base of the cliffs in De Narrow Zawn, Crowns Rock, above the pillow lavas between the Crowns and Botallack Head and in the north face of Carn Vellan. The massive flows are mineralogically and texturally similar to the pillowed flows.

   The essential textural features of the basalt flows are the widespread development of amygdales, a devitrified glassy matrix and flow foliation.

3. The only intrusive sheet to be positively identified, outcrops between Botallack Head and Carn Vellan. The sheet is approximately 10 m thick, dips NW at 25° and could be lenticular in shape, thinning to the NE. Only the lower contact is exposed (plate 2), where it can be seen to be structurally discordant with the underlying, deformed, interbedded pelitic and basaltic volcanic sequence.

   The base of the sheet, which overlies 10 cm of silicified pelites, is foliated and contains ragged, 0.3 mm long, subparallel plagioclase crystals $\sim An_{40}$ and irregularly shaped lenses of actinolite, chlorite and epidote. The upper 5 m of the sheet is a massive structureless, medium grained (0.5 - 0.7 mm), micro-gabbro, composed of altered plagioclase ($\sim An_{50}$) relict clinopyroxene, replaced by fibrous actinolite chlorite and epidote and skeletal ilmenite crystals, partially

altered to leucoxene. The internal fabric of the sheet displays evidence of intense shearing.

4. Banded amphibolites form approximately 30% of the metabasite outcrop. They occur on top of the promontary north of Zawn a Bal, in De Narrow Zawn, at the top of Botallack Cliff, above the pillow lavas between the Crowns and Botallack Head, on the NW face of Carn Vellan, above the pillow lavas between Carn Vellan and Levant Mine and in Trewellard South Cliff.

Many of the horizons are interbedded with, or pass laterally into, basaltic lavas, suggesting that they may be genetically related. The origin of other horizons is, however, more obscure.

The banded appearance of the amphibolite is the result of variations in both texture and composition. Texturally, the amphibolites are uneven grained and xenoblastic. They are characterised by a reticulate fabric of subparallel bands and clots of fibrous amphibole (pale green actinolite or hornblende), with accessory epidote and opaque ores, alternating with bands and lenses of granular plagioclase An_{40-60}, with minor sphene, calcite, opaque ores, epidote and quartz (plate 2).

The banded structure may have been produced: during the extrusion of the lava, during the orogenic activity, during contact metamorphism, or any combination of these events. Most of the banded structure occurs within recognisable basaltic volcanic

horizons, such as occur in the cliffs of Botallack Head. The lateral and vertical gradation into non-banded rocks suggests that this structure is not a primary feature. The frequent occurrence of stripping in areas of intense deformation, such as tight fold closures e.g. Botallack Head Quarry (plate 2), suggests that severe deformation, probably involving shearing or stretching parallel to the original bedding surface, was an important factor in the development of the structure. The structure, however, appears to be confined to a thermal metamorphic environment and so it is probable that it was produced as a result of the thermal metamorphism and partial metasomatism of sheared basalts.

E Metamorphism of the metabasites

The basaltic rocks have been subjected to a great variety of geological processes over a protracted period of time. The present composition and fabric of the metabasites is the result of at least 5, and possibly 6, distinct stages of physical disequilibrium with their environment. These metamorphic stages are listed below:

1. Extrusion of basalt and local submarine degradation.
2. Low grade regional metamorphism and tectonism during the Hercynian orogeny.
3. Thermal metamorphism and minor tectonism during the emplacement of the Land's End pluton (producing

basaltic hornfelses and amphibolites).

4. Internal metasomatism - migration and redistribution of material within the metabasites during contact metamorphism (producing calcium and iron metasomites).
5. External metasomatism - introduction of material, during contact metamorphism, from an outside source (producing boron and potassium metasomites).
6. Hydrothermal alteration bordering fissures and also pervasive hydrothermal activity often associated with (5).

The extreme structural, textural and compositional heterogeneity within the basaltic sequence is due to the interaction of some, or all, of these processes.

The metabasites can be divided into several groups, each containing a distinct mineral assemblage:

1. amphibole (hornblende-actinolite), plagioclase ± sphene, ilmenite, calcite, biotite, pyroxene, apatite.
2. cordierite, cummingtonite, anthophyllite, plagioclase ± ilmenite, spinel, biotite, diaspore, quartz, magnetite, apatite.
3. garnet, magnetite ± hornblende, diopside, clinozoisite, idocrase, calcite, chlorite, biotite sphene danalite, helvine, epidote.
4. axinite, tourmaline ± garnet, epidote, diopside, apatite, calcite, amphibole, chlorite, fluorite, sphene stokesite, danalite, helvine.
5. biotite ± cordierite, quartz, calcite, ilmenite, sphene, chlorite, alkali feldspar, plagioclase feldspar.

6. chlorite, epidote ± quartz, calcite.

These assemblages represent an approach to equilibrium during a combination of contact metamorphic, metasomatic or hydrothermal processes.

Chemistry and origin

1. Basaltic amphibolites containing an assemblage dominated by hornblende-actinolite and plagioclase predominate in this part of the aureole. They undoubtedly formed the parental material, from which the K, Ca, Fe and B metasomites and chloritic hydrothermally altered rocks were derived, as they are intimately related with, and are replaced by, all these lithologies.

Analysed samples of basalt lavas, sheets and banded amphibolites are presented in table 1 . Plots of alkalis/SiO_2 and Al_2O_3/SiO_2 (fig 5) suggest that the basalts and amphibolites may have origianally been alkali basalt in character (although it must be assumed that isochemical metamorphism was very unlikely). Computed niggli values (fig 5) show that the major elements increase in al, alk & c, and decrease in mg & fm as si increases. These trends are almost coincident with the trends displayed by the Karroo dolerites (Walker & Poldervaart, 1949) and the Connemara amphibolites (Evans & Leake, 1960).

The close grouping of niggli values for all rock types probably indicates that the basalts are

TABLE 1 METABASITES. ST. JUST AUREOLE.

	GST 1	2	3	4	5	6	7	8	9	10	11	12	13	14	15	16	17	18	19	20	21
SiO_2	43.40	44.31	42.39	45.21	44.25	43.23	45.1	45.5	46.4	44.4	42.5	47.1	48.7	47.8	47.7	46.4	47.7	45.4	50.0	48.4	48.9
TiO_2	3.63	3.02	2.88	4.27	1.25	0.96	2.70	2.50	2.27	2.67	2.25	2.02	1.40	2.64	1.83	0.98	1.15	2.55	2.63	1.32	1.26
Al_2O_3	16.68	18.48	21.16	19.00	15.51	13.67	18.65	17.62	16.92	18.58	20.28	14.14	17.83	23.14	16.70	12.40	16.00	18.75	17.29	18.00	14.33
Fe_2O_3	1.14	1.22	2.02	0.99	2.67	3.54	1.58	1.03	1.04	1.50	1.42	1.74	1.58	0.39	1.45	1.42	1.73	0.22	0.46	1.48	1.03
FeO	10.78	10.44	16.15	13.87	11.95	13.90	11.60	10.49	10.90	12.80	13.14	9.69	7.61	6.85	8.40	10.34	8.64	10.79	6.50	6.86	8.01
MnO	0.23	0.27	0.22	0.07	0.25	0.38	0.27	0.25	0.34	0.25	0.10	0.25	0.23	0.19	0.20	0.29	0.29	0.21	0.18	0.16	0.24
MgO	7.18	7.41	6.82	7.12	5.47	7.66	10.10	8.26	6.49	5.33	6.49	7.91	6.06	4.38	6.90	14.12	6.69	4.82	2.58	8.28	9.22
CaO	10.05	6.29	0.56	1.54	13.51	10.60	0.25	6.78	8.86	5.86	3.79	12.75	12.87	7.11	13.36	7.74	13.58	10.50	13.85	9.49	12.74
Na_2O	2.01	3.14	2.42	2.89	2.01	0.82	1.06	1.97	2.47	1.26	3.59	1.61	2.21	3.70	1.66	0.65	1.75	1.78	4.52	2.74	1.78
K_2O	1.68	1.63	2.88	1.84	1.15	3.00	4.77	2.93	1.76	5.43	2.46	1.18	0.70	2.92	0.55	3.84	0.28	2.14	0.35	1.78	0.70
P_2O_5	0.03	0.31	0.16	0.31	0.19	0.19	0.26	0.36	0.22	0.38	0.40	0.33	0.16	0.31	0.22	0.45	0.14	0.89	0.21	0.26	0.71
H_2O^+	1.71	2.57	2.02	2.24	1.15	1.53	2.92	1.57	1.54	1.44	3.48	1.06	0.53	0.43	1.15	1.19	0.92	1.10	1.23	1.33	1.25
H_2O^-	0.76	0.47	0.21	0.22	0.23	0.25	0.50	0.31	0.32	0.17	0.18	0.16	0.07	0.17	0.10	0.19	0.21	0.10	0.16	0.15	0.15
Total	99.55	99.56	99.89	99.56	99.59	99.73	99.76	99.57	99.53	99.67	100.08	99.94	99.95	100.03	100.22	100.01	99.08	99.25	99.96	100.25	100.32
Co	45	42	38	35	47	53	67	42	49	60	45	28	26	46	36	45	36	42	29	34	37
Cr	138	140	163	155	34	38	34	32	100	118	74	186	470	415	409	588	298	130	143	243	180
Cu	25	10	37	72	54	43	45	88	15	46	10	16	14	10	8	4	11	17	10	88	10
Li	135	157	15	26	127	93	241	106	67	163	111	79	93	24	118	43	36	115	17	86	24
Ni	42	35	46	33	34	36	30	24	33	63	113	46	142	140	130	489	157	66	59	46	152
Pb	31	36	15	10	9	9	8	9	9	8	11	4	31	18	17	20	8	15	54	10	15
Rb	45	40	68	75	135	95	284	84	58	220	160	60	116	125	25	180	24	188	54	88	54
Sn	<10	<10	<10	<10	12	<10	12	<10	16	15	12	12	14	<10	12	<10	12	<10	12	<10	<10
Sr	164	152	123	136	96	111	125	133	110	153	172	242	196	113	142	162	196	155	111	212	85
Y	22	26	28	35	19	16	25	10	27	29	23	26	15	26	15	27	14	17	19	15	20
Zn	90	60	85	95	73	76	61	68	52	70	79	33	72	7	50	72	79	116	129	11	29
Zr	152	164	196	174	160	152	143	159	166	172	193	143	233	224	173	312	153	211	162	173	146

TABLE 1

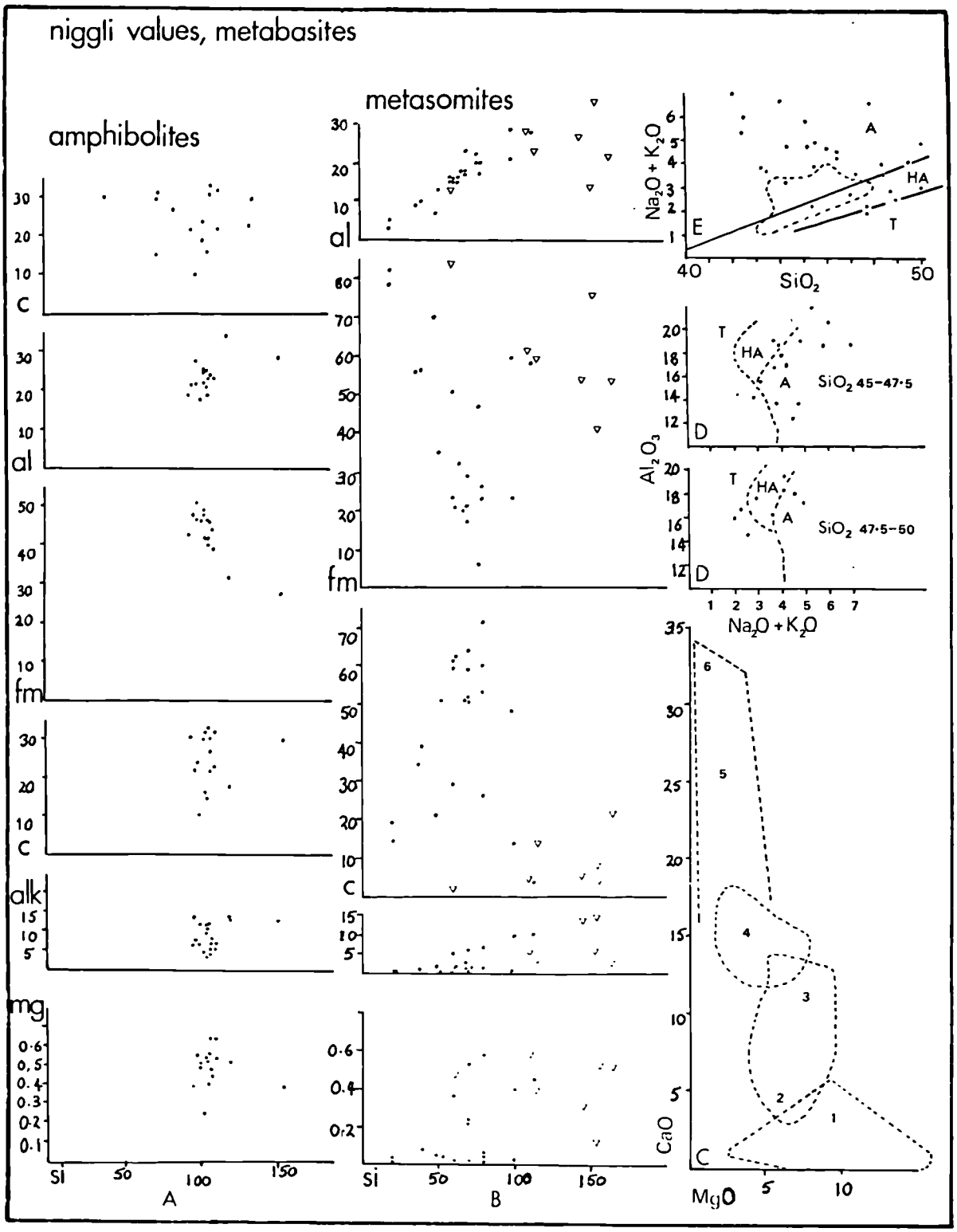

A niggli variation diagrams, metabasalts

B niggli variation diagrams, metasomites and cordierite-anthophyllite hornfelses
Ca+Fe metasomites, cordierite-anthophyllite hornfelses

C MgO/CaO variation diagram, 1) cordierite-anthophyllite hornfelses
2) actinolite metabasalts / 3) hornblende basalts 4) banded amphibole-plagioclas
hornfelses 5) massive garnet metasomites 6) vein garnet metasomites

D distribution of metabasalts on a total alkalis/Al_2O_3 diagram (after Kuno 196)

E distribution of metabasalts on a SiO_2/total alkalis diagram (after Kuno 1966)
field of Cornubian greenstones (Floyd, 1972)

cogenetic and that very little magmatic differentiation has taken place within the lava pile.

The close chemical similarity between the basalts and banded amphibolites suggests that the amphibolites were derived from the basalts. Compared to the pillow lavas and vesicular basalts the banded amphibolites are enriched in SiO_2, TiO_2, CaO, Na_2O, Cr, Cu, Ni, Pb and Zn, and depleted in Al_2O_3, Fe_2O_3, FeO, MgO, K_2O, P_2O_5, Co and Li. Comparing an average St. Just, basalt, greenstone with an average S.W. England alkali basalt greenstone (Floyd, 1972 b & 1974), the St. Just basaltic greenstones are enriched in Al_2O_3, FeO, MgO, CaO and K_2O, and depleted in SiO_2, TiO_2, Fe_2O_3, Na_2O, P_2O_5 and H_2O^+, although the overall rock chemistry is very similar.

2. Cordierite-anthophyllite rocks outcrop in the Kenidjack area, the Zawn a Bal promontary and in the pillow lavas between De Narrow Zawn and Botallack Head.

Tilley & Flett (1929) originally regarded these rocks as having been produced by the contact metamorphism of weathered basalt. It was envisaged that intense atmospheric weathering had produced an alteration assemblage of calcite, chlorite, serpentine, iron oxides and hydroxides from the original plagioclase-pyroxene assemblage and that these alteration products had reacted during thermal metamorphism to produce the observed assemblages. Following a more detailed laboratory study, Tilley

(1935), noted that the enrichment in MgO and FeO was incompatible with any weathering process known at that time and concluded that internal metasomatism was involved. The metasomatic sequence from amphibolite through cummingtonite amphibolites to cordierite-anthophyllite rocks involved the loss of Ca and the redistribution of Si, alkalis and Mg.

Reynolds (1947) considered the same rocks to have been developed from a group of calcareous sediments which had suffered Fe-Mg metasomatism from an advancing basic front during contact metamorphism. However, no calcareous sediments have been found in the area and the assemblages can be found in recognisable pillow lavas.

Floyd (1965), in discussing the origin of similar rocks from the Tater-du area, reached the same conclusions as Tilley (1935) but also emphasised the complementary redistribution of Ca to form the calcifereous metasomites.

Vallance (1967) suggested that the alteration products of submarine degraded basalts, namely chlorite+quartz, could react during thermal metamorphism to produce the assemblage cordierite-anthophyllite. This suggestion was supported by Chinner & Fox (1974), who argued that the presence of complex multiphase assemblages and small scale compositional domains within the cordierite-anthophyllite hornfelses, suggests that they were derived isochemically from previous, heterogeneous,

degraded basaltic material. Floyd (1976) also accepted this mode of formation.

These heterogeneous hornfelses form a sheet-like horizon which constitutes the greater part of the surface and cliffs of the area between Kenidjack and Zawn a Bal. Similar assemblages also occur in the pillow lavas at the base of the cliffs in De Narrow Zawn and in the pillow lavas immediately north of the Crowns. Examples of this rock type can also be found on the Wheal Cock mine dump. It is, therefore, possible that these hornfelses form an extensive, unique horizon which is conformable within the basalt pile. Such a distribution also supports the hypothesis that they were derived from a single, submarine degraded, basaltic horizon.

3. Ca ± Fe metasomites outcrop at two localities: Botallack cliff and the south face of Carn Vellan. The metasomites occur as irregularly shaped, sheet-like horizons, ~15 m thick and dipping ~20° NW (plate 3). The Ca rich metasomites are composed of garnet (grossularite), idocrase, diopside, clinozoisite, zoisite, axinite, calcite, amphibole and sphene. Fe rich metasomites contain an assemblage of magnetite, epidote, chlorite, amphibole, garnet, calcite and sphene. Both assemblages replace earlier basaltic hornfelses and amphibolites.

Analysed samples of Ca-Fe metasomites are presented in tables 2 & 4 .

TABLE 2 METASOMATISED BASALTS (AUREOLE)

GST	30	31	32	33	34	35	36	37	38	39	40	41	42	43	44	45	46	47
SiO_2	31.85	34.07	37.70	33.75	39.52	36.69	35.49	42.50	48.67	37.59	49.41	35.92	35.11	34.99	33.32	21.39	28.92	32.94
TiO_2	1.42	4.00	1.34	0.38	3.58	0.72	0.42	5.03	1.71	2.35	2.38	2.07	2.49	1.93	1.69	1.24	0.52	2.98
Al_2O_3	13.47	15.26	16.09	15.06	14.25	17.59	16.68	15.77	19.00	19.17	19.08	14.93	20.00	16.36	15.23	9.95	7.14	14.69
Fe_2O_3	4.42	8.68	7.39	13.98	9.66	7.02	6.27	7.26	1.99	6.80	2.58	5.05	3.99	5.80	11.82	34.48	42.01	23.12
FeO	3.64	3.27	3.46	1.11	1.62	2.54	2.72	4.85	8.71	3.04	3.92	2.42	1.97	1.29	2.69	9.41	-	-
MnO	2.76	1.94	2.68	1.30	0.93	1.40	1.30	0.22	0.19	0.07	0.46	0.28	0.34	0.39	0.60	0.57	0.23	0.29
MgO	1.18	2.22	1.16	0.20	0.94	0.62	0.84	5.46	6.64	5.45	2.19	3.63	3.71	3.43	0.60	0.55	7.00	6.64
CaO	27.04	23.97	23.30	32.38	27.00	31.36	33.76	16.29	4.93	16.01	9.42	32.15	23.31	30.19	30.13	19.89	11.52	14.83
Na_2O	0.16	0.39	0.24	0.10	0.13	0.13	0.42	0.66	4.29	0.59	0.78	0.60	0.32	0.36	0.56	0.44	0.96	1.62
K_2O	0.12	0.28	0.12	0.13	0.16	0.16	0.34	0.33	1.91	3.94	7.19	0.69	4.29	1.97	0.17	0.16	0.84	1.89
P_2O_5	10.77	3.68	0.24	0.38	0.69	0.54	0.45	0.39	0.33	0.87	0.23	0.17	0.27	0.09	2.30	1.41	0.40	0.16
B_2O_3	2.11	1.03	4.42															
F	0.52	0.42	0.10															
H_2O^+	1.06	0.75	1.18	0.69	0.81	0.27	0.32	0.87	0.92	3.45	2.03	0.79	2.78	1.69	0.44	0.39	0.80	1.10
H_2O^-	0.33	0.22	0.38	0.20	0.25	0.18	0.24	0.14	0.20	0.48	0.18	0.54	1.05	1.23	0.47	0.25	0.38	0.26
O F	0.23	0.19	0.04															
Total	100.62	99.99	99.76	99.66	99.54	99.22	99.25	99.77	99.49	99.81	99.85	99.34	99.63	99.72	100.02	100.13	100.72	100.52
Be	68	32	43	10	10	10	10											
Co	1,500	50	35	45	35	30	30	50	45	34	29	46	29	35	6	19	35	48
Cr	70	35	35	38	35	35	35	35	48	55	49	45	55	51	42	28	19	5
Cu	24	30	187	57	45	12	15	19	86	30	8	26	165	175	40	33	31	22
Li	25	46	41	18	53	45	35	101	128	284	139	23	139	91	20	20	28	114
Ni	580	30	30	30	50	20	25	60	41	25	26	19	21	35	14	31	52	50
Pb	118	36	36	63	42	50	65	42	5	19	41	16	20	15	21	17	20	17
Sn	900	860	945	160	631	1,500	2,050	10	10	15	10	350	280	560	430	240	12	10
Zn	217	214	188	65	143	65	70	125	112	256	166	177	206	226	171	430	330	270

Compared to the basaltic hornfelses Ca metasomites are enriched in Al_2O_3, Fe_2O_3, CaO, MnO, P_2O_5, Sn, Pb & Zn and depleted in SiO_2, TiO_2, FeO, MgO, Na_2O, K_2O, Co, Cr, Li & Ni.

Compared to the basaltic hornfelses Fe metasomites are enriched in Fe_2O_3, FeO, Co, Cu, Pb, Sn, Zn and depleted in SiO_2, TiO_2, Al_2O_3, Cr, Ni, Li.

The Ca and Fe material from which the metasomites were formed could have been derived from two different sources: the metasediments, and the basalts and amphibolites. Although the pelites only contain small amounts of Ca (between 2.5 - 6%, Khan, 1973), it occurs in calcite and is, therefore, in an easily removable form. It is possible that at least some Ca could have been derived from this source. A more likely source, however, is from within the basalt pile. Floyd (1974) discussed the formation of the Ca-metasomites and concluded that they were formed by the replacement of earlier basaltic hornfelses, the Ca being derived from partially degraded, sheared basalts. Field and laboratory investigations in this study support this hypothesis for the following reasons:

1) There is a continuum of Ca (Fe) values from basalt hornfelses through actinolite and hornblende hornfelses to Ca-Fe metasomites (fig 5).
2) Ca-Fe metasomites replace rocks which are clearly

of basaltic origin and they are often spatially related to banded amphibolites.

Two structural-lithological features appear to be associated with the Ca-Fe metasomatic horizons: the close proximity of highly deformed (folded and sheared) banded amphibolites and the presence of pelitic sediments (usually forming a structural-lithological cap to the metasomatic horizon). Both of these features are associated with the metasomites at Botallack, Carn Vellan and Levant Mine. The proposed sequence of events needed to generate the Ca-Fe metasomatites is as follows:

1) Deformation (folding and shearing) of unaltered or partially degraded basalt.
2) Lateral migration of Ca-Fe from the deformed amphibolites, during thermal metamorphism.

This migration of material was controlled by a) structure and b) lithology. Primary (bedding) or secondary (tectonic) foliation acted as channelways for the migrating material and the amount of transport was controlled by the presence of impermiable, fine grained, sedimentary barriers.

4. B ± Ca metasomites occur in two forms, either as irregularly shaped, sheet-like horizons e.g. Grylls Bunny Mine, Botallack (plate 9) and the south face of Carn Vellan, or as discordant, subvertical, vein-like bodies e.g. Stamps and Jowl Zawn, Wheal Cock promontary (plate 3), Crowns Rock, Carn Vellan and

Carn Du. Mineralogically, the metasomites range from tourmaline (schorl) > 90%, in Ca poor horizons, to axinite >90%, in Ca rich horizons. Accessory minerals include, garnet (grossularite), epidote, clinozoisite, zoisite, amphibole, chlorite, diopside, apatite, calcite, fluorite, sphene, quartz, danalite, helvine and stokesite.

Sheet-like horizons may be lenticular in shape and confined to a small area e.g. Grylls Bunny Mine, or may be extremely irregular in shape and size e.g. Carn Vellan. Vein metasomites are between 10cm - 2m thick and usually dip steeply south. Individual minerals in both types of metasomite are usually well shaped and display optical and compositional (?) zoning.

Analysed samples of B-Ca vein metasomites are presented in table 2 .

Compared to the basaltic hornfelses, the vein metasomites are:

enriched in Fe_2O_3, MnO, CaO, P_2O_5, B_2O_3, Pb, Sn & Zn,

and depleted in SiO_2, TiO_2, Al_2O_3, FeO, MgO, Na_2O, K_2O, Co, Cr, Li & Ni.

Compared to the massive Ca metasomites, the vein metasomites are:

enriched in Fe_2O_3, MnO, (CaO sometimes), B_2O_3, P_2O_5, Sn, Pb, Zn & Be,

and depleted in SiO_2, TiO_2, Al_2O_3, FeO, MgO, Na_2O, K_2O, Co, Cr, Li & Ni.

Wallrocks, adjacent to the vein metasomites, show no depletion in CaO. This component must, therefore,

have been derived from deeper tectonic levels, either by further leaching of hornblende-actinolite hornfelses or by the remobilisation of Ca from massive Ca metasomites. B was probably derived from a metasedimentary or granitic (hydrothermal) source.

Several reasons suggest that the vein metasomites are a late stage metasomatic or early hydrothermal phenomena. Structurally, they cut all other metamorphic or metasomatic rock types but are themselves cut by NW trending, hypothermal mineral veins. The rocks are rich in Sn, B and Be (elements typical of the hypothermal stage of mineralisation). Mineral parageneses indicate that the later formed species are richer in Sn and Be (Jackson & Alderton, 1974). Phases such as stokesite, danalite and helvine have recently been found in these veins (Barstow, pers. comm.). P and PS, 2 phase (liquid + gas) inclusions in zoned axinite, from the vein metasomite near Wheal Cock, yielded homogenisation temperatures in the range 360 - 380°C (salinity < 26 equiv. wt. % NaCl). These temperatures are similar to those obtained for early hypothermal mineralisation in the district (discussed in later sections).

5. Biotised basalts occur sporadically throughout the aureole. They are associated with all rock types and grade from amphibolites into biotised hornfelses, by a progressive increase in the amount of biotite, usually at the expense of amphibole.

Analysed samples of partially biotised basalt are presented in tables 1, 6 & 12 . Compared to the actinolite-hornblende hornfelses, the biotised hornfelses are:
enriched in SiO_2, Al_2O_3 & K_2O, Cu, Li, Pb, Sn, Zn
and depleted in CaO, Co, Cr, Ni.

The K needed to produce the biotite could have been derived either from within the basaltic sequence or from an external source (metapelite or granite). Wallrock alteration studies of pelites at Levant Mine (chapter 4) suggest that K is frequently removed from pelites in the hydrothermal environment, so it is conceivable that the K could have been derived from the pelites. There is also some evidence that K was introduced into the sediments adjacent to the granite (Khan, 1972). The association of banded amphibolites, depleted in K, and biotised basalts, enriched in K, within a few metres of each other, suggests that K could have been derived locally from within the basalts. As most of the banded amphibolites are depleted in K and are frequently cut by microfractures containing sericite, it could be that these rocks represent the source material for the K. The most likely origin for the K, however, is the pelitic sedimentary sequence.

6. Chloritised amphibolites occur sporadically throughout the aureole but they are particularly well developed in areas which have been mineralised, either adjacent

to fissure veins e.g. near the Hazzard Lode, or in areas of more pervasive mineralisation e.g. at Grylls Bunny Mine. A more detailed discussion of hydrothermal alteration is presented in chapter 4 but the two main features associated with these rocks are the development of an assemblage dominated by chlorite (and hematite) and the spatial association of mineralisation phenomena. The formation of this rock type is considered to be directly attributable to the activity of hydrothermal fluids associated with mineralisation.

Summary

The distribution and origin of the metamorphosed basaltic lithologies can be explained in terms of the following chronological sequence of events:

1. Extrusion of basalt onto the sea floor and local, partial degradation to chlorite-calcite-epidote or chlorite-quartz assemblages.
2. Deformation during the Hercynian orogeny, producing local, intensely deformed (folded and sheared) lava-pelite sequences and realtively undeformed massive lava sequences.
3. Granite emplacement and isochemical metamorphism of the relatively unaltered basalts to actinolite - plagioclase hornfelses, sheared basalts to banded amphibole-plagioclase hornfelses and degraded basalts to cordierite-anthophyllite, and cordierite-cummingtonite-hornblende-plagioclase hornfelses.

4. Internal metasomatism, involving the redistribution of Ca and Fe within the sheared amphibolites to produce Ca-Fe metasomites.
5. Internal and external metasomatism to produce B ± Ca vein and massive metasomites (tourmaline and/or axinite rich assemblages), and K metasomites (biotite rich assemblages). B and K could have originated from a granitic (hydrothermal) or metasedimentary source and Ca was probably derived from the Ca metasomites.
6. Local, hydrothermal degradation of all basaltic hornfelses and metasomites to produce chlorite-hematite rich assemblages.

F Structure

Folding - previous structural studies in the district were performed by Barkley (1959) and Garnett (1962).

Barkley distinguished two groups of folds: a dominant set of fold axes, trending 020° and plunging 25° NNE and a subsidiary set, trending 325° and plunging 17° NW.

Garnett confined his studies to folding in the metapelites and recognised the following fold axis orientations:

1. A dominant set, trending 017° and plunging 18° NNE.
2. Two minor maxima, trending 354° and plunging 12° N, and trending 064° and plunging 33° ENE

3. A minor maxima, trending NW and plunging at low angles to the NW and SE.

The following sequence of folding was recognised in this study:

1. The earliest fold structures are minor warps and disharmonic folds, usually only a few centimetres in wavelength, which were produced either by slumping of partially consolidated sediment or by local disturbances caused by lava extrusion (plate 3).
2. F1 folding produced local (?), small scale, recumbent folds with subhorizontal axial planar cleavage. This stage of folding is recognised by the deformation of the associated cleavage during later stages of folding.
3. F2 folding produced moderate wavelength (>15 m), upright, NE trending, N plunging folds (fold axis maxima 018/20° N, Map 5), with moderate to steep dipping (30 - 70° NW) axial planes. Axial planar cleavage is locally developed but is usually weak or absent. These folds are usually Z (occasionally M) shaped in the south but predominantly S shaped in the north (Pendeen area), (plates 2 & 3).
4. F3 folding produced minor folds coaxial with, and occurring on, the steep dipping limbs of F2 folds (plate 2). These folds have subhorizontal axial planes, sometimes with associated axial planar or shear cleavage.

5. F4 folding in pelites and amphibolites produced minor, NW trending, NW plunging, open flexures (fold axis maxima 310/25° N, Map 5).

The difference in competency between the thick, massive amphibolite and pillow lava units and the pelitic sediments and thinner interbedded volcanic horizons led to the formation of tectonic-lithological horizons, in which zones of intense folding in the pelitic units alternate with zones of minor folding and intense shearing in the massive amphibolite units e.g. the mixed pelite-amphibolite sequence of Botallack Cliff.

The pelites may display one or more cleavages related to one or more phases of deformation. Shear cleavage is locally developed within fault zones e.g. adjacent to the reverse fault of Trewellard South Cliff. A local, shear cleavage is also developed near the base of the intrusive basalt sheet near Wheal Cock.

Jointing - many different generations of joints are developed in the aureole but three main groups can be distinguished: primary igneous joints in the basaltic amphibolites, tectonic joints related to folding and tectonic joints related to the emplacement of the pluton.

Primary igneous cooling joints are developed in the dolerite sheet, north of Wheal Cock (3 sets approximately perpendicular to each other) and in pillow lavas (either radial or polygonal joint systems). Individual folds are characterised by longitudinal and

cross-joints and diagonal, shear joint systems.

Although these two groups of joint systems are locally important, a majority of the joints in the aureole were generated during the emplacement of the granite pluton. These joint systems are uniformly developed over large areas and are often associated with a major fracture or fault, which is known to have been produced or was active during, or soon after, granite emplacement.

A study was made of the distribution of joints between Trewellard Cliff and Botallack. A summary of the main joint sets, based on the sterograms presented in Map 1, is outlined below. The notation describes the strike and dip of the joint sets.

1. Trewellard Cliff to Levant - 050/65°S, 295-310/75°S, 350/80°S, 290-070/30°N.
2. Carn Du to Wheal Cock - 315/80°S, 330/80°S, 055/30°N, 020-060/85-60°S.
3. Botallack Head to the Crowns - 340/80°SW, 305/80°SW, 275/70°S, 290-080/70-50°S, 065/75°S, 040-090/30-50°N.

The four main joint sets developed in the aureole are WNW/75-80°SW, NW-NNW/80°S, NE-ENE/60-70°SE, E-W/steep south or flat north dipping.

Major fractures - the following groups of major fractures can be distinguished in the area:

1. ENE to NE-trending, south dipping (80-50°) fractures which sometimes contain Ca-B vein metasomites and aplite veins.

2. NNE trending, south dipping (30-40°) low angle, reverse faults associated with extensive hydrothermal alteration (quartz, sericite, tourmaline and albite). e.g. Trewellard South Cliff, or Ca-B vein metasomites e.g. Carn Vellan.
3. NW to WNW trending, steep dipping (65-85° NE or SW), normal, reverse or oblique slip faults and dilatant extensional fractures. These structures are associated with mineralisation (pyrite, chalcopyrite, chalcocite, arsenopyrite and limonite) and hydrothermal alteration (quartz, sericite, tourmaline and chlorite) and they cut and displace group 1 and 2 fractures.
4. N to NE trending fractures with a variable dip (vertical to ~ 55°NW or SE) and a variable sense of movement either normal (reverse ?) or oblique slip. These fractures are often mineralised (quartz, hematite, limonite and minor sulphides) and they cut and displace group 1, 2 and 3 fractures.

A discussion of the generation of these fractures is deferred until chapter 4.

G Distribution of lithological and tectonic units

The geology of the project area, between Zawn a Bal and Levant Mine, will be described with reference to several cross-sections A - F (fig 6).

The promontary north of Zawn a Bal (sketch section A).

The cliff section comprises a vertical sequence (from the base to the top) of hornblende-plagioclase

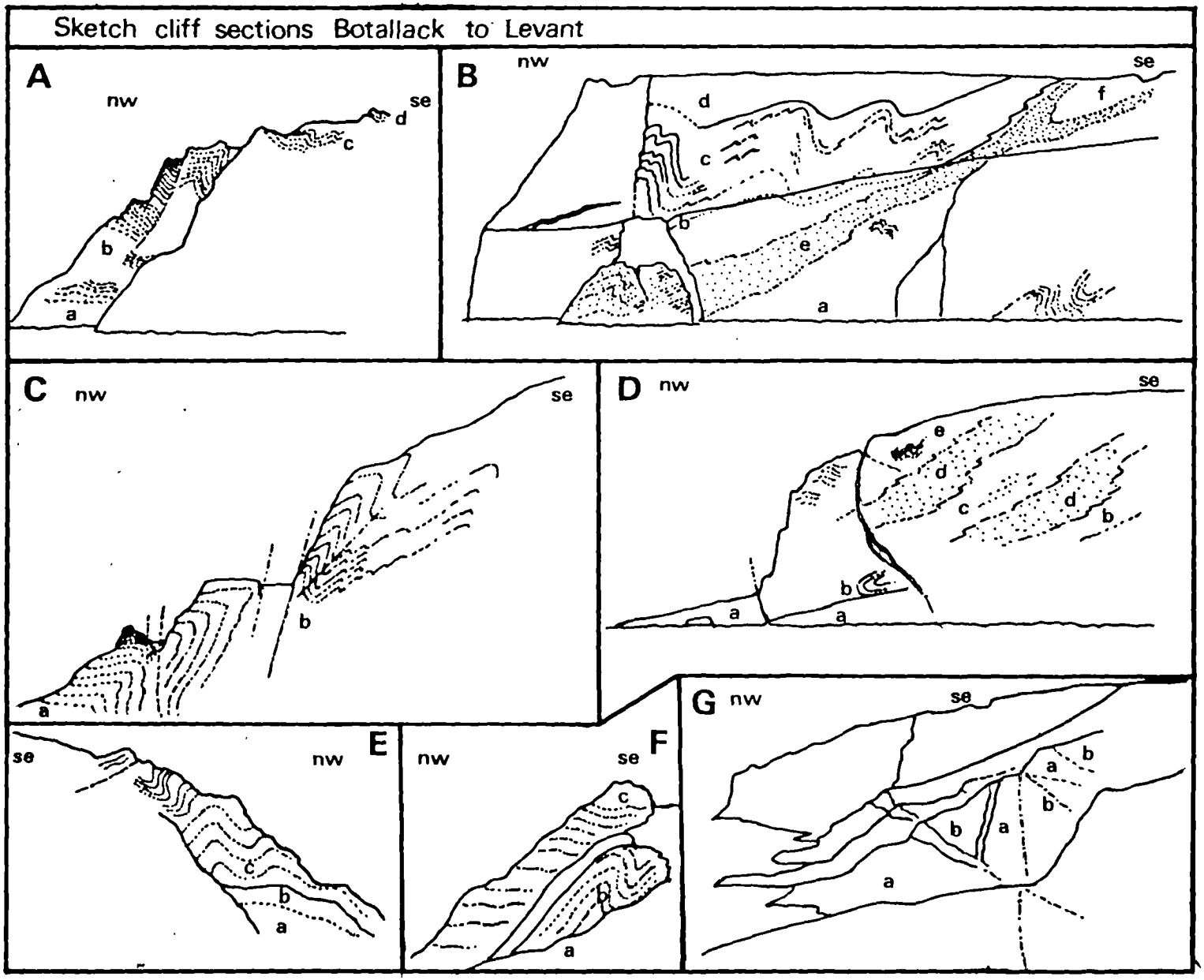
Sketch cliff sections Botallack to Levant
A
nw
se
d
c
b
a
B
nw
se
d
f
c
b
e
a
C
nw
se
b
a
D
nw
se
e
d
c
d
b
b
a
a
E
se
nw
c
b
a
F
nw
se
c
b
a
G
nw
se
a
b
b
a
b
a

FIG 6

amphibolite, probably originally pillow lava (a), overlain by vesicular basalts (b)(cordierite, biotite, cummingtonite, anthophyllite), minor pelite (c) and banded (hornblende-plagioclase) amphibolite (d). The local introduction of potassium along microfractures has led to the formation of biotite rich, K metasomites within horizon (b). A 10 cm wide, NE trending, steep dipping, garnet-epidote-diopside vein metasomite cuts the vesicular basalt horizon.

The promontary is bounded on the south side by the Zawn a Bal, NW trending fracture system and on the north by the N and NW trending fracture systems of De Narrow Zawn.

Deformation has produced a sheared, lower amphibolite unit, grading upwards into a zone of tight, assymetrical, NNE trending, N plunging folds within the vesicular basalt and pelite horizon.

Botallack Cliff (sketch section B).

The cliff section comprises a complex sequence of basaltic lavas and pelitic sediments. The lower unit (a) which is approximately 40 m thick, consists of basaltic pillow lavas and massive vesicular basalts, with minor pelitic sediments. The lavas are composed of cordierite, biotite, cummingtonite, hornblende, actinolite, epidote and plagioclase. Only minor folds are developed in this lower unit, the most notable area of folding occurring on the beach west of the Hazzard Shaft. Above the lavas there is a transitional zone (b) $\sim$ 4 m thick, composed of

alternating pelites, banded cherty pelites and basaltic volcanic rocks. This zone is succeeded by ~ 20 m of pelites (c) which in turn are succeeded by ~ 10 m of banded actinolite-plagioclase amphibolites (d). The difference in competency between the massive basaltic amphibolite horizons (zones a & d) and the pelites and thin interbedded volcanic horizons (zones b & c) has resulted in the production of a tectonic sandwich, in which the amphibolite units are highly sheared but display only minor folding and the central pelite unit is intensely folded (assymetrical NE trending, N plunging folds).

The cliff is traversed by a shallow dipping (~ 20° NW), ~ 10 m thick, sheet-like horizon of Ca, Fe ± B metasomites (garnet-magnetite, axinite-tourmaline) (e). A 20 cm wide, NE trending, steep S dipping, garnet vein cuts massive Ca metasomites at Crowns Rock. Two NE trending, S dipping aplite veins also cut the cliff. In the extreme SE of the area a replacement cassiterite ore-body has been formed (f).

The cliff and zawn are traversed by numerous fractures, many of them containing mineral veins. The zawn itself contains a major, NNW trending, east dipping, fracture belt which hosts veins of quartz, hematite, limonite and jasper. Slickensides on the walls of several of the veins indicate strike slip movement. These fractures cut and displace two other groups of fractures: a NW trending, south dipping ($70 - 85^{\circ}$) family, some of

which contain cassiterite-sulphide bearing veins e.g. the Hazzard Lode, and a minor family of NE trending fractures.

Botallack Head (sketch section C).

The area between the Crowns and Botallack Head comprises a structurally complex sequence of basaltic volcanic rocks and pelitic sediments. The cliff section consists of a lower 10 - 15 m thick, pillow lava unit (a), which is overlain by a 50 m thick zone of interbedded pelites, vesicular basalts (hornblende, actinolite, plagioclase, biotite) and banded (actinolite, hornblende, plagioclase) amphibolites (b). Immediately south of Wheal Cock, an ~ 10 m thick micro-gabbro sheet, dips 30° NW. A 0.5 - 2 m wide, ENE trending, steep dipping, Ca-B vein metasomite cuts the amphibolites immediately south of Wheal Cock Zawn.

The basaltic volcanic and sedimentary sequence is intensely deformed (F2 and F3 folds) and the sheet is highly sheared. At the base of the cliff an overturned anticline in the pillow lava unit has a shallow dipping NW limb and a steep SE limb.

A north-south trending, subvertical fracture zone, which is an extension of the De Narrow Zawn fracture system, separates the lower pillow lava unit from the upper lava-pelite unit. Slickensides in the fault plane indicate strike slip movement. The fracture belt cuts and displaces a family of NW trending, steep dipping, normal faults and several minor, NE trending fractures.

Stamps and Jowl Zawn.

This area consists of a lower, 50 m thick unit of structureless amphibolites, banded amphibolites and pillow lavas with minor siliceous pelites, overlain by an intrusive, sheared, amphibolite sheet. The zawn is traversed by a 1 m wide, NE trending, subvertical, garnet-axinite, vein metasomite.

The area is traversed by numerous NW trending fissures, several of which are mineralised and were exploited in Wheal Cock Mine.

Carn Vellan (south face, sketch section D).

The south face of Carn Vellan (sketch section D) consists of a complex sequence of basaltic volcanic rocks, banded amphibolites, metasomites and pelites. The cliff section comprises a lower, 10 m thick unit of basaltic pillow lavas (a), overlain by 3 m of pelites (b), 40 m of banded amphibolites (c), and garnet-axinite metasomites (d), and capped by 5 m of sediments (e). A garnet-diopside vein metasomite cuts all the horizons.

The lower pillow lavas are only slightly deformed (minor, NE trending warps), but the overlying pelites (b) form a recumbent, NE trending, N plunging, F2 fold (plate 3). NW trending and plunging minor folds (F4) are developed in a continuation of this horizon to the SE. The upper amphibolite unit is folded into an open, NE trending syncline and the metasomatic horizons cut the amphibolite horizon at a low angle ($10-20^{\circ}$ NW).

A majority of the fractures which traverse the

cliff trend between N and NNW and dip steeply east. A low angle, NE trending reverse fault partially controls the distribution of the vein metasomite and also forms the junction between the sedimentary capping and the underlying amphibolite.

The north west face of Carn Vellan (sketch section E) consists of a lower pillow lava unit (a) overlain by ~ 4 metres of buff coloured silicified pelites (b) and ~ 25 m of banded amphibolites (hornblende, plagioclase) (c).

The fold axes of a major anticline and syncline in the amphibolite horizon (plate 2) trend NNE and plunge NE at 15°. The axial plane dips NW at 50 - 70°.

Carn Du (sketch section F).

The cliff section at Carn Du comprises three tectonic-lithological unit, a basal unit of massive structureless amphibolites (hornblende-plagioclase) (a) which may have originally been pillow lava, a central wedge of buff coloured siliceous sediment (b) and an upper pillow lava unit (c).

The basal unit suffered only minor shearing during deformation but the metasediment was folded into a NNE trending, N plunging, upright anticline and syncline with a wavelength of ~ 5 m, and steep dipping (70° NW) axial planes. The upper pillow lava unit displays minor, NE trending open flexures.

The cliffs between Carn Vellan and Carn Du are traversed by two main families of fractures: NW trending,

steep dipping fractures which contain sporadic pyrite and chalcopyrite e.g. the Unity vein, and a family of ENE trending, steep dipping fractures, some of which contain an assemblage of epidote, actinolite, axinite and tourmaline. These latter veins are probably equivalent to the garnet, axinite veins of the Botallack area.

Trewellard South Cliff (sketch section G).

The cliffs between Levant Mine and Trewellard Zawn comprise a complex sequence of sheared pillow lavas, vesicular basalts, banded amphibolites and minor, silicified, pelitic sediments. The base of the cliffs between Boscregan Zawn and Zawn Brinny is composed of light coloured pelite (muscovite-quartz) (a). This sediment is bounded to the east by a normal fault, south of Boscregan Zawn, and by a low angle reverse fault (dipping $30-40^{\circ}$ SE) to the north of the zawn. The fault zone is intensely silicified. Above the fault the succession is dominated by sheared amphibolites (actinolite, plagioclase) (b), with minor interbedded pelites (a). A second, low angle reverse fault intersects the top of the cliff.

Deformation in the pelites has produced small scale (<10 cm wavelength), NE trending F2 folds with a well developed cleavage trending 024° and dipping 50° NW. The amphibolites are intensely sheared.

Three main groups of fractures can be distinguished in the area around Levant Mine:

1. NW trending, steep (70 - 80°), north or south dipping fractures containing a vein assemblage of pyrite, chalcopyrite and chalcocite.
2. North-south trending, west dipping (55 - 60°) normal faults containing a vein assemblage of quartz, limonite, jasper and hematite. These fractures cut and displace the other groups of fractures.
3. NNE trending, SE dipping (30 - 40°), low angle reverse faults. These fractures were formed at an early stage as they are cut and displaced by the NW trending fractures. They are also associated with extensive hydrothermal alteration (pelites adjacent to the fractures are converted to an assemblage of quartz, sericite, tourmaline and albite).

H Chronology of main geological events

The sequence of major geological events in the district is outlined below:

1. Middle Devonian (?) - deposition of sediments and extrusion of alkali basalts in a submarine environment, and the local submarine degradation of a distinct lava horizon.
2. Upper Devonian (?) - low grade regional metamorphism and deformation during the Hercynian orogeny.

3a. Lower Permian - emplacement of the Land's End pluton.

3b. Thermal metamorphism of the aureole rocks upto the hornblende hornfels facies. Crystalisation of the

outer granite shell and formation of joint systems in granite and aureole.

3c. Contact metasomatism - formation of Ca, Fe, B and K metasomites by the redistribution of Ca ± Fe & K within the aureole rocks and the introduction of B and K (?) into the aureole from the granite.

3d. Formation of major fracture systems in and around the periphery of the pluton by the enlargement and dislocation of pre-existing joints.

3e. Mineralisation (Sn, Cu, As).

4. Post-mineralisation fracturing.

CHAPTER 3

MINING AND MINERALISATION IN THE St. JUST DISTRICT

3. Mining and Mineralisation in the St. Just District

A Introduction

The St. Just mining district is located on the north west margin and roof of the Land's End pluton. It covers an area of approximately 20 Km^2 and for the purpose of this study includes:

1. The Hermon and Bellan setts, about 1 Km SW of St. Just.
2. The Balleswidden sett, about 2 Km SE of St. Just.
3. The coastal 5.5 Km section between Cape Cornwall and Pendeen, including the major setts of Bosweeden, Owles, Botallack, Levant, Geevor, Boscaswell Downs and Pendeen Consols.

B History

Although there is very little evidence for very early (Bronze age) mining activity in the district, there are numerous examples of Bronze age occupation on the peninsula and it seems likely that the outcropping mineralised fissure veins must have received a certain amount of attention at this time. One of the earliest historical references to mining activity in the district is provided by Norden (1600) quoted by Noall (1973), who stated that, 'the tin mines then working in St. Just were Boseighan, Ball-u-hall and Carnmeal-Ball'. However, it is probable that these mines were opencast operations, true subsurface mining probably not being developed until later that century. The first steam engine was erected

APPROXIMATE OUTPUT OF THE MAIN PROPERTIES OF THE ST. JUST DISTRICT

MINE OR SETT	OUTPUT (TONS)						
	Sn	Cu	As	Fe	U	Au	Ag
Balleswidden	12,000	-		-			
Boscaswell Downs	6,200	700 (9% Cu)		-			
East Boscaswell	300	100 (10% Cu)		-			
Boscean	2,500	-					
Boswedden	1,400	200 (10% Cu)		75 Fe			
Botallack	15,500	24,300 (12% Cu)	1,600 As				
Bal	440						
Carnyorth	1,000	-					
Cock	-	2,200 (10% Cu)					
Geevor	40,500	-					
Hermon, Bosorne, Bollowal Utd, Letcha	1,500	-					
Levant	26,000	130,000 (10% Cu)	4,000 As minor Au Ag				
North Levant	4,000	60 (12% Cu)					
Owls	9,000	2,000 (9% Cu)			5 cwt U		
Edward							
Pendeen Consols	200	6,400 (5% Cu)					
Spearn Consols	1,500	150 (10% Cu)					
St. Just Amalgamated							
St. Just United	3,500	-					
Cape Cornwall							
Other Minor Properties	1,000	1,000 (10% Cu)					
TOTAL	126,540	167,110					

TABLE 3

at Carnyorth in 1807, so initiating the period of 'deep' mining. Between 1825 - 1875 mining activity was at its zenith but the 'knocking' of Balleswidden in 1873 signalled the end of this phase. The closing years of the century saw the mines fighting a losing battle against falling metal prices and rising costs until, finally, only a couple of mines were left. At the present time only Geevor mine is in production. However, it is hoped that Levant mine, now part of the Geevor sett, will be producing again in the near future. In addition to metaliferous mining, kaolinite is extracted on a small scale from the Bostraze area.

C Previous work

The area has attracted many distinguished mineralogists, petrologists and economic geologists. Consequently, many articles concerned with different aspects of the mineralisation have been published. Garnett (1962) gave a detailed review of this literature, the most important works being produced by; Boarse (1822), Carne (1822a, 1822b), Collins (1912), Hawkins (1818, 1822), Henwood (1843), MacAlister (1907), Pearce (1878), Rowe and Foster (1887) and Trounson (1942).

D Mining statistics

Reid and Flett (1907) listed 74 separate properties in the St. Just district, although Dines (1956)

7a St JUST MININC SETTS 18 7

7b TREND OF THE ORE SHOOTS IN THE C NTACT Z NE

only listed 49. Figure 7a shows the main mining setts in 1857 when mining activity was at its peak. Any estimation of the number of mines is difficult, as there was a progressive trend of amalgamation, whereby two or more mines were combined under a single registered company. For similar reasons there are difficulties in assessing the total output of the individual mines, especially as the records of many mines are incomplete. Bearing these factors in mind, Table 3, based on Dines (1956), Garnett (1962) and Trounson (1942), gives the approximate total production in Sn, Cu and As for the main St. Just setts. The total output for the district is about 127,000 tons of tin concentrates (65% Sn), 167,000 tons of copper concentrates (10% Cu) and about 6,000 tons of crude arsenic. In addition 5 cwt of uranium ore is recorded from Wheal Owles and minor amounts of Ag, Au and Pb have also been reocrded. Dines (1956) calculated that the district has produced 12.7% Sn, 2.2% Cu and 1% As of the total Sn-Cu-As production of the whole metallogenic province.

E Mineralisation

Several distinct types of mineralisation can be distinguished in the district.

I Fissure veins and sheeted vein systems containing quartz, tourmaline, muscovite, cassiterite, wolframite, native bismuth and minor pyrite chalcopyrite and arsenopyrite. These deposits occur in the roof of the granite at Balleswidden Mine.

II Fissure veins containing quartz, tourmaline, fluorite, cassiterite, arsenopyrite, pyrite, chalcopyrite, chalcocite, bornite, hematite and limonite with minor

Zn, Pb, Sb, Ni, Bi, Co, Ag, Au and U phases. These deposits are localised in NW or WNW trending fissures in the granite and aureole, and they are known locally as lodes.

III Fissure veins containing quartz, hematite, limonite, jasper and minor carbonates, pyrite and chalcopyrite. These veins are localised in N and NW trending fissures in the granite and aureole, and they are known locally as guides.

IV Fissure veins containing combinations of quartz, galena, sphalerite, pyrite, limonite-hematite and pitchblende. These veins are rare; Dines (1956) records that two north-south trending veins at Pendeen Mine and Wheal Owles contained galena and pitchblende-limonite respectively.

V Replacements of cassiterite or cassiterite-sulphide (arsenopyrite-pyrite-chalcopyrite) in granite, pelite and metabasalt, at Balleswidden, Geevor Levant and Botallack Mines.

VI Barren podiform pegmatites of quartz, alkali feldspar, muscovite and tourmaline occur near the granite contact at Priests Cove.

Fissure veins (lodes and guides)

Lodes: although individual lodes often have distinct characteristics of their own, it is possible to describe features which are common to most of them. In this study the term lode will refer to any portion of a fissure and its wallrock which contains economic quantities, either past or present, of ore. Fissure veins containing ore phases of unproven viability are termed mineralised fissure veins.

Lodes and mineralised fissure veins can be structurally divided into two components, the fissure infill or vein and the adjacent altered host rock known as the wallrock.

The vein is usually between 0.2 - 2 m wide with an average width of about 1 m. Economic (tin) mineralisation occurs, usually sporadically, over a maximum strike length of 3000 m (average less than 1000 m) and a maximum dip length of 400 m (average 200 - 300 m), although the dimensions of the uneconomically mineralised fissure may be much greater. The vein dips at an angle of between 50-90^{o} but is usually relatively flat (about 65^{o}) or relatively steep (about 80^{o}).

The fissure infill is usually structurally complex with any portion of the vein showing repeated phases of deposition of gangue, quartz, feldspar, tourmaline, fluorite, chlorite and calcite, and metal phases, cassiterite, chalcopyrite, pyrite, arsenopyrite, hematite with minor chalcocite, bornite, tetrahedrite, uraninite, galena, sphalerite and rare supergene phases. The infill typically shows textures and structures which are characteristic of open space filling i.e. vugs and cavities, fine grained margins and coarser interiors, crustification, cockade and comb structure, matching walls and symmetrical internal banding. However, the polyphase nature of the infill has often produced complex replacement relationships which vary spatially within the fissure system.

The lodes of the St. Just district differ from lodes in other parts of the province in the following respects:

1. They are narrower and less continuous.
2. They contain little evidence of lateral zoning, most veins containing both 'high' and minor 'low' temperature ore phases.
3. They strike approximately NW-SE, compared to the regional NE-SW trend.
4. They display a greater variation in strike and, therefore, intersect more frequently.

Guides: a guide or crosscourse is an unmineralised fissure vein, trending approximately normal to the mineralised fissure vein system i.e. NE-SW to N-S. These structures were often utilized by the nineteenth century miners during crosscutting and they were said to guide the miner to the ore.

They are usually more persistent in strike than lodes, with recorded lengths of upto 3 Km and they dip east and west at between $50 - 90^{o}$.

The fissure infill usually consists of quartz (banded, massive and vuggy), chalcedony, calcite, hematite (massive and specular), jasper, limonite and goethite. They are characteristically unmineralised but, near lode intersections, they sometimes contain economic quantities of ore phases (tin and copper). Occasionally the strike of the guide conforms to that of the mineralised vein system. When this occurs, the guide often contains

economic quantities of tin and copper e.g. Guide lode, Levant mine. Unlike other crosscourse veins in the province the St. Just guides rarely contain 'low' temperature metal phases. However, the Pendeen Silver lode (Dines, 1956) and a U-Pb vein in the Wheal Owles mine (Pearce, 1878) may be examples of 'typical' Cornubian crosscourse mineralisation.

Textures and structures within the fissure are characteristic of polyphase open space infill i.e. vugs and cavities, combstructure crustification and symmetrical internal banding. Internal brecciation and cockade structures are also common.

The guides of the St. Just district differ from crosscourses in other parts of the province in the following respects:

1. They usually display only a small amount of movement.
2. They rarely contain the 'low' temperature ore species.
3. They often contain sub-economic quantities of tin and copper.
4. They sometimes conform to a typical lode strike and carry normal hypothermal species.

With reference to map 2 (and also Garnett, 1962 and Dines, 1956), the main distributional characteristics of the fissure veins are outlined below:

1. The lodes are distributed approximately equally in plan along the granite contact.
2. The main axis of mineralisation in the district trends NW-SE through Carnyorth and Spearn Consols mines.

This axis may be extended, though probably not continuously, as far as the Bostraze-Balleswidden area in the SE of the district.

3. The mean lode strike is NW-SE, but there is a wide variation in the strike of economically mineralised fissures between E-W and N-S, with two lode maxima at WNW (280°) and NW (310°).
4. The WNW and N trending mineralised structures are usually confined to the granite. Lodes in the aureole usually strike between NNW and NW.
5. The lodes tend to be curved in plan, generally concave to the south, north of the main axis of mineralisation and concave to the north, south of the main axis.
6. Out of a total of 109 mineralised veins in the district, 38% dip north and 62% dip south. Between Wheal Owles and Pendeen i.e. around the main axis of mineralisation 26% dip north and 74% dip south. Both statistics emphasise the predominance of south dipping mineralised structures.
7. In granite, those lodes striking N of NW generally dip NE and those striking S of NW dip south. In the aureole lodes dip NE or SW, irrespective of trend.
8. Lodes in granite tend to dip steeply NE (greater than 80^{o}) or SW, either at low angles ($60-65^{o}$), or at moderately steep angles ($75-80^{o}$). Lodes in the aureole tend to dip steeply NE or SW.

9. Only the NW striking, steep dipping (80^{o}) lodes are continuous through, and productive on both sides of, the granite contact. WNW trending, shallow dipping lodes usually become unproductive and structurally discontinuous as the contact is approached. If they are structurally continuous and productive on both sides of the contact the economic portions are usually separated by a zone of impoverishment upto 200 m wide on either side of the contact.
10. Economic tin values in the fissure systems in the contact zone are generally terminated in the SE against NE-SW or N-S lines which lie approximately 1200 m inside the granite contact at O.D. In the north of the district (Boscaswell Downs) these limits are extended to about 1700 m inside the contact.
11. WNW striking, SW dipping lodes tend to occur in groups, bounded between the same NE-SW or N-S limits e.g. Spearn Consols, Carnyorth and East Botallack. Adjacent steep dipping, NW striking lodes tend to be confined between similar NE-SW limits e.g. Simms lode and Boscaswell main lode.
12. The lode distribution in plan is complex, but there is a zig-zag pattern formed by the flat dipping WSW trending lodes in granite and the steeper NW trending lodes in granite and host rocks. The pattern is repeated three times between Simms lode, in the north, and the Owles and Edward sett, in the south.
13. Guides occur in granite and the aureole, strike between NW and NE, and dip steeply east and west.

Continuous strike lengths of the order of 2-3 Km are recorded but they are more commonly only a few hundred metres in length. They often have a sigmoidal form in plan. When they junction with mineralised fissure veins, they often assume the lode strike, either indefinitely, or for some considerable distance.

Replacement deposits

These deposits occur in granite, metasediments and metabasites and they are classified according to their morphology. Two types can be distinguished in the district:

1. Sheets - either subvertical or subhorizontal.
2. Irregular disseminations and massive replacements.

All replacement deposits are associated with intense wallrock alteration.

In granite three main replacement deposits are known. At Balleswidden two irregular zones of greisenised granite contain disseminations of cassiterite, pyrite, chalcopyrite, arsenopyrite and wolfram. Near the granite contact at Geevor mine disseminated deposits of cassiterite and Cu-Fe-As sulphides occur in highly altered wallrock (feldspathised and chloritised), bordering the Footwall Branch, Hangingwall Vein and Coronation lodes on levels thirteen, fourteen and fifteen. Also in the contact zone in Levant mine a massive and disseminated cassiterite and Cu-Fe-As sulphide deposit occurs, in a feldspathised

granite sheet, at its junction with the Footwall Branch mineralised, fissure vein system.

In the aureole replacement cassiterite deposits occur at: Wheal Cock mine, near the intersection of two fissure veins, Levant mine, bordering some fissure veins and, also, as replacements in metasomatic basic horizons, Botallack, as replacements within metasomatised amphibolites (Grylls Bunny) and as similar deposits elsewhere in Botallack mine.

Pegmatites

All the pegmatites so far recorded in the district are unmineralised. They occur as sheets and pods in the contact zone and they are mainly confined to Preists Cove and Porthledden Cove. They are composed of various combinations of quartz, muscovite, tourmaline and alkali feldspar.

CHAPTER 4

THE GEOLOGY AND MINERALISATION OF LEVANT MINE

4. The Geology and Mineralisation of Levant Mine

A Introduction

Levant Mine is situated on the cliffs 3 Km north of St. Just (SW 368 346). Its long and eventful history, together with its precarious cliff top position and its submarine workings, have earned it a unique position in Cornish mining lore, where it is known as 'the mine beneath the sea'.

The Levant sett embraces the ancient workings of Wheal Shop, Wheal Unity, Zawn Brinny and Boscregan. It is bounded on the north by the Geevor sett and in the south by the Botallack sett. Tin and copper mineralisation is localised in narrow, steeply dipping, NW striking fissures. The mineralised zone exploited by the mine is approximately 800 m x 2 Km traversing the granite/metasediment contact but mainly confined to the aureole. The ore shoot is between 200 - 300 m thick and plunges north-west at between 10 - 20°.

The earliest known record of production for Levant Mine is 10 tons of copper ore in 1793, but the mine did not come into steady production until 1820, when it was operated by a small local company. By 1820 the mine was already well developed. Hawkins (1820) states that a level 17 fm below H.W.M. extended for 40 fm beneath the sea. Between 1820 and 1840 the mine showed a clear profit of £200,000. This was on an initial investment of £400. The first record of continuous tin

production was for 1835 and by 1848 the mine was an important tin producer. In that year the mine reached a depth of 210 fm below adit.

By 1870 the mine was in decline. This was due to a combination of mismanagement, the lack of investment in a new plant and a depression in the price of tin and copper. In 1872 a new Levant company, on the cost book principle, was formed. After a period of heavy losses in the 70's the mine began to prosper again in the 80's. During this period Spearn Moor mine was added to the Levant sett and Wheal Unity was developed.

Production of tin and copper was maintained at a high level until about 1900. In 1904 the mine reached a depth of 350 fm, its present bottom level. By 1910 the mine was again in financial difficulties but the war brought an increase in metal prices and the mine prospered once again. After a serious strike in 1918-19 the mine was flooded to the 278 fm level. This terminated all work below this level.

On October 20th 1919 the mine suffered a major disaster when the man engine collapsed killing 31 men and injuring many more. As well as the tragic loss of life, the only means of transporting the men to the lower levels was lost. This effectively made the lower levels inaccessible and all the workings below the 190 fm level were abandoned.

In 1920 a limited company was constructed. The mine continued to work, weathering the post-war slump of

1921-22 until its final collapse during the world wide depression in 1930.

The total production and value of metals extracted during the mine's 130 years existence is as follows: 137,000 tons Cu ore (10% Cu), value £0.9 x 10^6, 24,900 tons Sn ore (70% Sn), value £1.92 x 10^6, 4,000 tons As, value £35,000. The total value of metals extracted was £2.85 x 10^6.

Although several companies expressed an interest in restarting Levent after its closure, it wasn't until 1959 that operations were started by Geevor Tin Mines to re-open the mine. Following a preliminary investigation, the mine was found to be flooded with sea water which had entered from a hole in the sea bed, located above an area in the mine workings known as the '40 backs'. The hole was successfully sealed and the mine partially de-watered to the 40 fm level by 1969.

The next phase in the history of the mine was between February 1969 and November 1973. During this period an extensive exploration and development programme was pursued by Union Corporation and Geevor Tin Mines. The exploration programme was based on several intersections recovered from three long, surface diamond drill holes (SJ 3, 4 and 5). It had two main objectives:

1. to evaluate several fissure vein intersections, in particular the Spar and Unity lodes.
2. to evaluate the potential of low grade cassiterite deposits localised in basic igneous rocks and known as 'greenstone ore'.

An initial objective to completely de-water the mine was abandoned at an early stage.

The target area for the two objectives occupied an area ~ 500 m x 800 m SW of the main Levant lodes and north of the Botallack lodes. Exploration of this target area was by three major SW trending cross-cuts at 60 fm (110 m), 130 fm (238 m) and 180 fm (329 m). These levels were redefined as 1, 4 and 6 levels and their respective cross-cuts are 101, 401 and 601. In addition, over 6250 m of diamond drill core was recovered. The exploration programme formed the basis of this study. All the underground development was mapped on a scale of 1 : 240 and the results of this work are presented on maps 3 and 4 volume 2

B Geology (summary)

The subsurface geology of Levant Mine is similar to the geology of the rest of the aureole at outcrop. Three lithologies comprise the rock succession:

1. granite - the contact zone of the Land's End pluton and numerous leucogranite and aplite sheets.
2. metasediments - fine grained pelites with subsidiary calcareous sediments.
3. greenstones - interbedded basaltic volcanic rocks, banded and massive amphibolites and metasomites of basaltic, calcareous metasedimentary and unknown parentage.

Contact metamorphism produced biotite-muscovite-quartz assemblages in the pelites, amphibole-plagioclase (epidote-calcite-diopside) assemblages in the amphibolites, and calcareous metasediments and garnet-magnetite-calcite-epidote-amphibole ± axinite assemblages in the metasomites.

Pre-granite deformation produced NE trending folds and post-granite fracturing formed steep dipping normal, reverse and oblique slip NW and NE trending faults. The main geological features of the Levant Mine are illustrated on Maps 3 and 4 volume 2

C Granite

The main plutonic granite is exposed at two localities in the mine. In the cross-cut, from 14 level Geevor Mine into Levant Mine, the granite contact is intersected at an acute angle (plate 4). The contact is also exposed 5 m SE of Skip Shaft on the Old Bal Lode, 6 level. Diamond drill holes SJ3, SJ5 and UL42 also penetrated the main plutonic granite. The contact is always knife sharp, occasionally with a 1 cm fine grained margin. The outer ~20 cm zone sometimes displays aplitic banding and metasomatic effects, i.e. numerous, subparallel, K feldspar megacrysts and clots of biotite. The exposures and old mine sections indicate that the plutonic contact dips west at between 50 - 80°, although there are many local irregularities.

The plutonic granite is a white or pink, medium

grained (0.5 cm) rock composed of large perthitic orthoclase megacrysts in a matrix of biotite, muscovite, plagioclase An_{18-26}, quartz and tourmaline, with accessory fluorite, apatite, zircon, opaque ores, chlorite and rutile. An average mode for 4 plutonic granites is quartz 30.3%, perthitic orthoclase 38.6%, plagioclase 24.1%, muscovite 2,1%, biotite 3.1%, tourmaline 1.4%, accessories 0.4%. The granite is similar in texture and composition to that of the Geevor granite which forms the west and central portions of Geevor Mine.

In common with plutonic granites from the rest of the batholith, the Levant Mine granites (table 4) are enriched in B, Li, Rb, As, Sn, and F, and depleted in Ba and Sr compared to a published value for low Ca granites (Turekian and Wedepohl, 1961). There is no apparent difference in the major and trace elements between these granites and the Geevor granite (table 13).

In addition to the plutonic granite, numerous discordant leucogranite sheets and aplite veins are exposed in the mine workings, particularly on the 6th level. Four leucogranite sheets, including one composite body, were examined in the 601 cross-cut.

Sheet 1 intersects the cross-cut ~45 m NW of Skip Shaft. It is 1 m wide, dips 20° SE and is composite in nature. Three facies comprise the sheet:

a) Coarse (1 cm), equigranular leucogranite, consisting of quartz 35%, perthitic orthoclase 40%, plagioclase An_{12}, 24%, muscovite 0.3%, biotite 0.5% and accessory

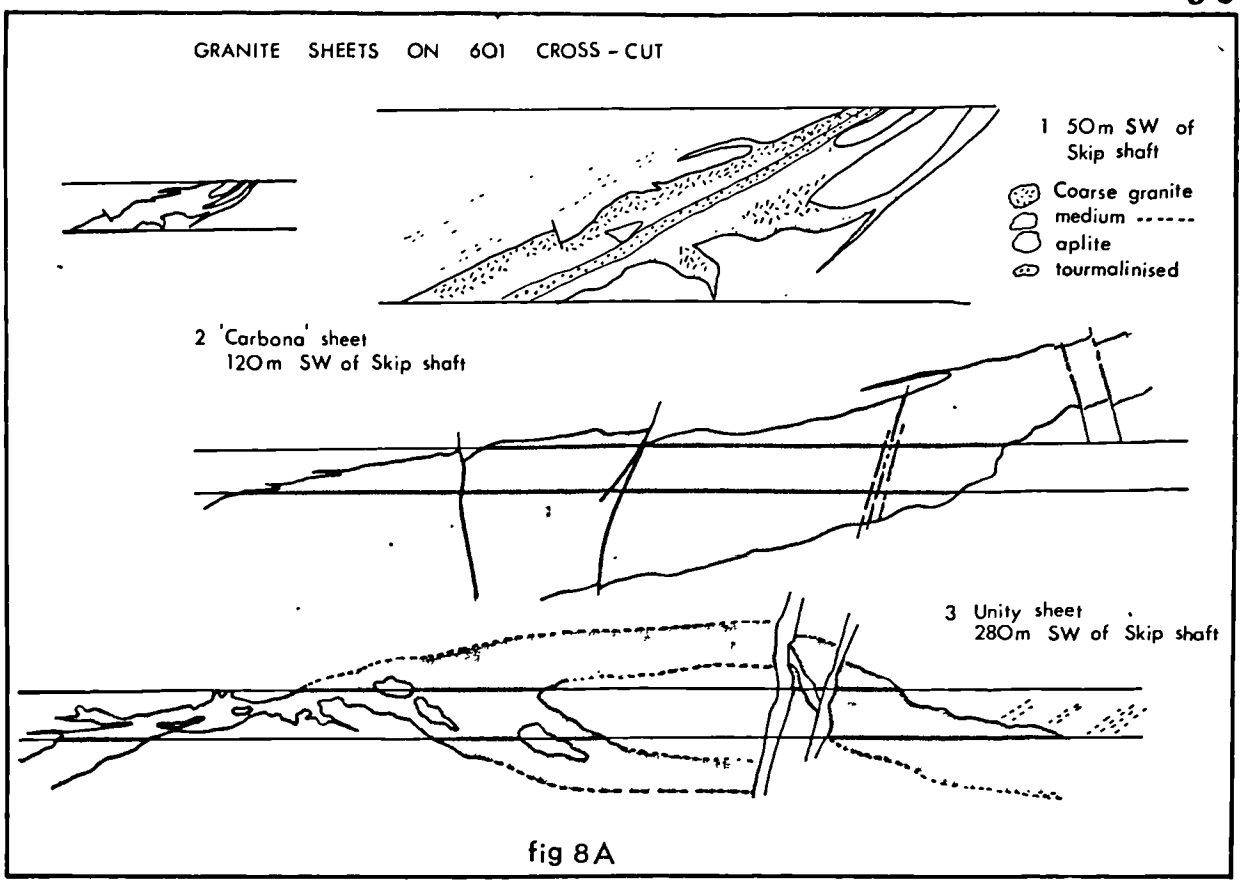

fig 8A

fig 8B

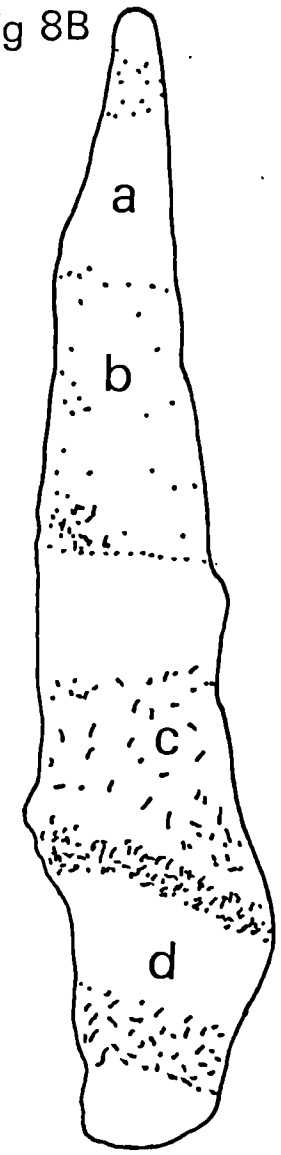

Petrographic section sheet 3. (UNITY GRANITE)

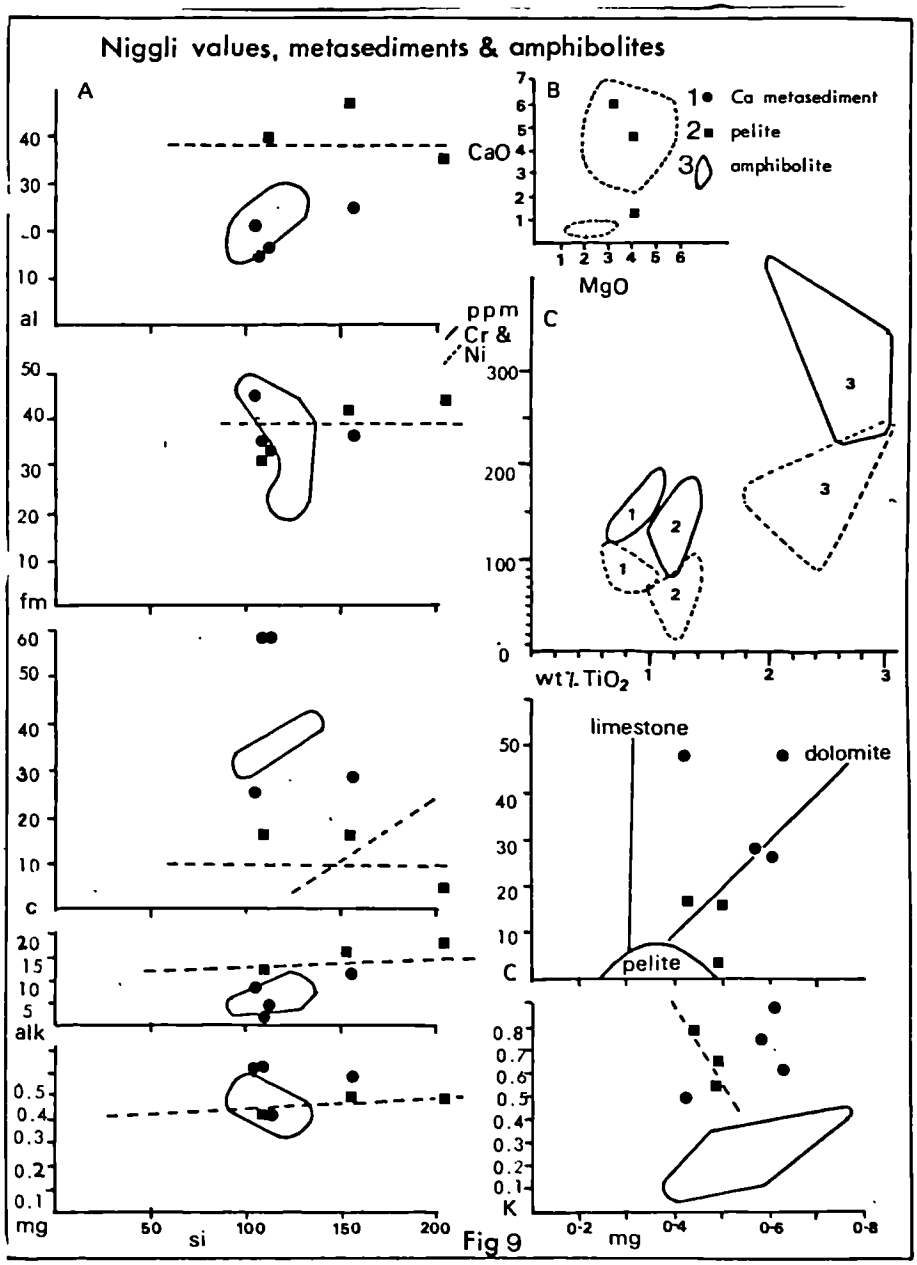

Fig 9

tourmaline and apatite 0.2%. This facies forms most of the upper part of the sheet.

b) A fine grained (1 mm) equigranular aplite consisting of quartz 35%, perthitic orthoclase 35%, plagioclase An_5, 30%, muscovite 0.5% and accessory tourmaline and apatite forms the base of the sheet.

c) A medium grained equigranular rock, consisting of quartz 35%, orthoclase 22%, plagioclase An_{10}, 35% and tourmaline 8% forms the centre of the sheet.

Sheet 2 intersects the cross-cut between 91 - 128 m SW of Skip Shaft. The sheet is 5 - 8 m thick and dips SE at 20 - 25°. The granite is a white, moderately coarse (0.5 cm), equigranular rock composed of quartz 35%, perthitic orthoclase 33%, plagioclase 27%, muscovite 2%, biotite 2.5% and tourmaline 0.5%.

Sheet 3 intersects the cross-cut 250 m SW of Skip Shaft. The sheet is between 1 - 3 m thick and dips SE at 10 - 15°. The sheet is characterised by well developed banding (plate 4), due to variations in mineralogy and texture. A petrographic traverse through a banded zone (FIG 8b) revealed the following mineralogical and textural variations:

Zone a) is a 3 cm wide, coarse grained (½ - 1 cm) band containing quartz 37%, perthitic orthoclase 15%, plagioclase An_{5-10}, 45%, and pale brown (Li?) mica 2%.

Zone b) is a medium grained (2 mm), equigranular band containing quartz 33%, perthitic orthoclase 38%,

plagioclase An_{5-8}, 22%, muscovite 1% and tourmaline 6%. This band is separated from the next by a layer similar in texture and composition to zone a.

Zone c) is a medium grained equigranular band containing quartz 44%, perthitic orthoclase 38%, plagioclase An_{5-7}, 9% and tourmaline 16%. This zone terminates abruptly ie. tourmaline decreases to ~1% and passes into zone d) which consists of alternating fine (1 mm) and medium (2 - 4 mm) grained, equigranular bands, with a bulk modal composition of quartz 26%, orthoclase 38%, plagioclase 34% and tourmaline 2%.

The only common accessory mineral in the sheet is andalusite which locally forms upto 5% of the rock.

Sheet 4 intersects the cross-cut 24 m NE of the Hen vein. The granite sheet is 30 cm wide, dips steeply SE and consists of relatively large (0.5 - 2 mm) subhedral quartz, alkali feldspar and mica crystals in a fine grained (0.1 - 0.2 mm) quartz and alkali feldspar matrix. The modal composition of the rock is quartz 31%, albite 49%, orthoclase 15%, mica (Li?) 3%, tourmaline and topaz <1%. The early perthitic orthoclase crystals are surrounded by a core of albite suggesting late stage Na metasomatism.

In common with the plutonic granites the leucogranite sheets are enriched in B, Li, Rb, As, Sn and F, and depleted in Ba and Sr (tables 4 & 8), compared to a published value for low Ca granites (Turekian and

Wedepohl, 1961). They are also depleted in Ti, Mg, Ca, Li, Sr and Zr, and enriched in alkalis and Pb, compared to the Levant Mine plutonic granites.

D Metasediments

The sedimentary sequence consists of dominant pelites with subsidiary carbonate-pelite and tuffaceous horizons.

Pelites - This group of sedimentary rocks grade from homogeneous poorly laminated mica rich pelites to strongly laminated pelites with quartz laminae and lenses. Grain sizes within the pelites are between 0.01 - 0.1 mm i.e. mainly silt to fine sand grade. Quartz rich laminae and lenses often contain coarser particles (0.1 - 0.3 mm). The present mineralogy of the pelites is quartz, biotite, muscovite, chlorite and opaque ores with occasional calcite and epidote.

Locally, some pelitic horizons contain an assemblage of chlorite, biotite and occasionally cummingtonite or actinolite. These horizons are often spatially associated with amphibolite horizons of probable basaltic origin and it is possible that they are either the degraded surface of submarine basalt flows or mixed tuff-pelite horizons. An example of this type of rock occurs in 601 cross-cut adjacent to a major emphibolite horizon 430 m SW of Skip Shaft.

Contact metamorphism of the pelites has produced the dominant assemblage quartz, biotite,

muscovite and opaque ores. Pelites actually in contact with the main plutonic granite are converted to an equigranular, polygonal (0.1 - 0.2 mm grains) mosaic, consisting of quartz, biotite and K feldspar. This inner contact zone, which is usually <2 mm wide, grades into finer grained (<0.1 mm) pelite, containing an assemblage of quartz, biotite, muscovite and opaque ores, in which the original sedimentary banding, i.e. the orientation of micas and the presence of siliceous laminae, is preserved. Another common feature within the pelites in the intermediate contact zone i.e. between $\sim 20 - 100$ m outside the granite contact, is the presence of numerous irregularly shaped quartz-chlorite masses which are probably the result of Si migration from the inner contact zone.

Partially digested pelitic xenoliths in the plutonic granite consist of a relatively coarse (0.2 mm) interlocking equigranular matrix of quartz, alkali feldspar, biotite and muscovite, and subhedral porphyroblasts of quartz, perthitic orthoclase and partially degraded garnet.

In addition to the quartz and mica rich pelites several horizons contain considerable amounts of carbonate (calcite and dolomite). These metasediments are usually well laminated, consisting of light bands (0.1 - 5 mm thick) of calcite, dolomite, quartz, muscovite and Ca-plagioclase, and dark bands of quartz, muscovite, biotite chlorite and minor carbonate. One such horizon is situated near the South Lode approximately 750 m

outside the granite contact.

Several very finely laminated horizons occur on 4 and 6 level, their gradual transition into pelites, limited thickness, fine scale textural and compositional banding and mineralogy i.e. alternating bands of calcite, quartz and calcic plagioclase, and epidote, amphibole and diopside, suggests that these horizons may be thermally metamorphosed marls.

Geochemistry - three samples of pelite and two each of calcareous - pelite and finely laminated calcareous metasediment (?) were analysed for major and a limited number of trace elements (table 4).

Compared to the data of Khan (1973), the Levant Mine pelites are similar in composition to the pelites in the aureole at outcrop. Calculated niggli values (fig 9) show that the Levant Mine pelites plot close to the trends of the aureole pelites i.e. increasing mg and alk, and relatively constant c, fm and al with increasing si, and decreasing K with increasing mg. They also plot outside the pelitic field of Leake (1965) on an mg/c diagram indicating that they are higher in Mg and Ca than most other pelites. Although only three pelites were analysed they appear to be enriched in MgO, CaO, Na_2O, K_2O and Cu and depleted in Fe_2O_3, SiO_2, Ni, Zn, Pb and Sn compared to another group of analysed Devonian pelites (Henley, 1974).

Compared to the pelites the mixed pelite-carbonate sediments are enriched in MnO, MgO, CaO, P_2O_5, Li, Pb and Zn, and depleted in Al_2O_3, Fe_2O_3, Na_2O, K_2O,

PLATE 4, GRANITES & METASEDIMENTS

A Plutonic granite/pelite contact, 601 cross-cut Geevor Mine

B Plutonic granite, quartz, perthitic orthoclase, oligoclase, muscovite and biotite

C Banded leucogranite sheet, 601 cross-cut near the Unity vein

D Leucogranite sheet, 601 cross-cut near the Hen vein. Phenocrysts of quartz and albite in a matrix of quartz and alkali feldspar.

E1 Banded pelite (drill core), alternating micaceous and siliceous layers

E2 Banded calcareous metasediment, 601 cross-cut, alternating layers of Ca plagioclase and epidote.

E3 Banded calcareous metasediment, 101 cross-cut, alternating layers of calcite, quartz and epidote, and mica

F Pelite (thin section), alternating lenses of quartz and layers of mica

G Banded calcareous metasediment, 601 cross-cut

H Calcareous metasediment (thin section), alternating layers of mica and epidote

I Calcareous metasediment, old mine workings, South Lode

PLATE 5 METABASALTS & METASOMITES

A&B Banded amphibolite (thin section), alternating bands and lenses of plagioclase feldspar $\sim An_{50}$ and actinolite or hornblende

C&D Banded amphibolite, macroscopic banding

E Axinite, biotite, sphene and calcite assemblage, (B-K metasomite)

F Magnetite, calcite, epidote, axinite assemblage, (Fe-Ca-B metasomite)

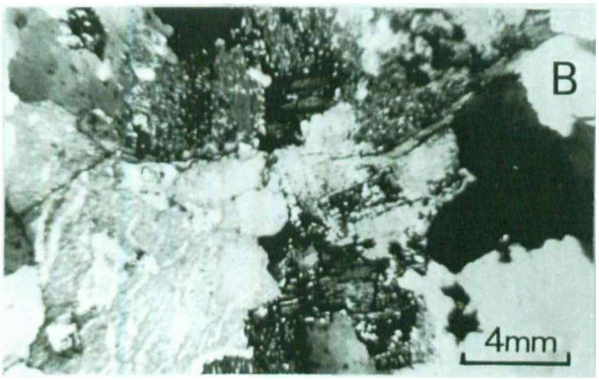

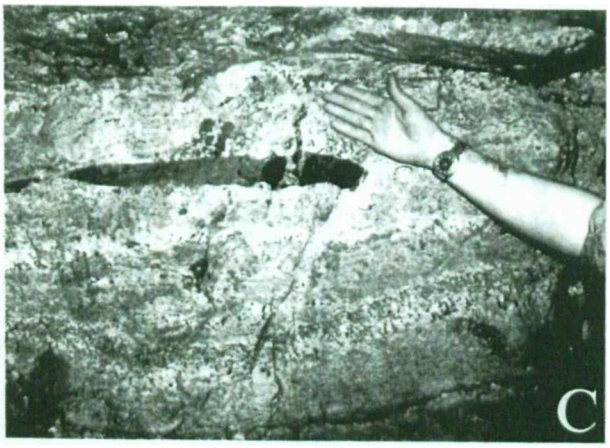

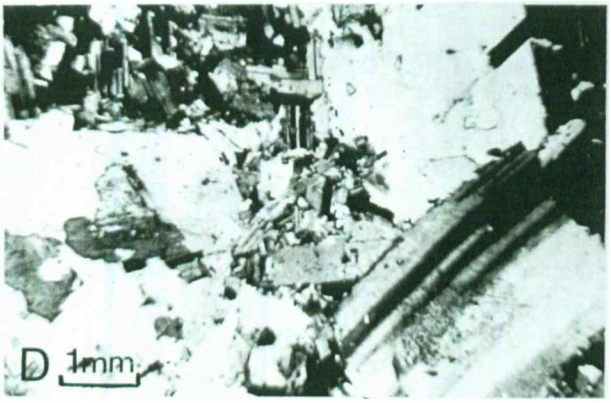

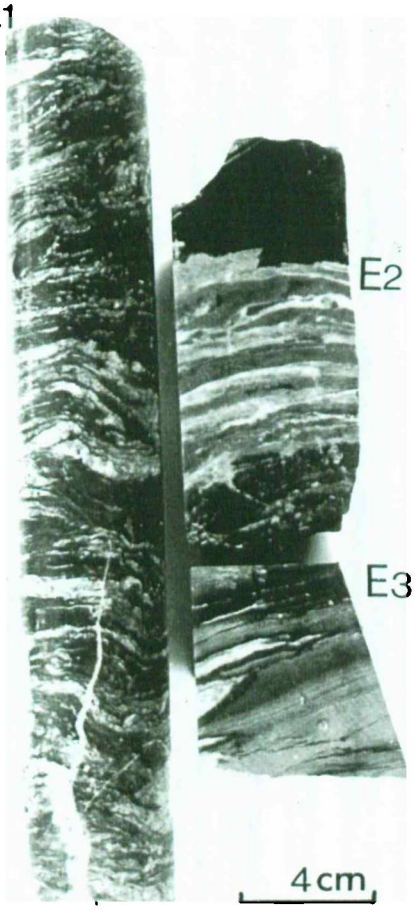

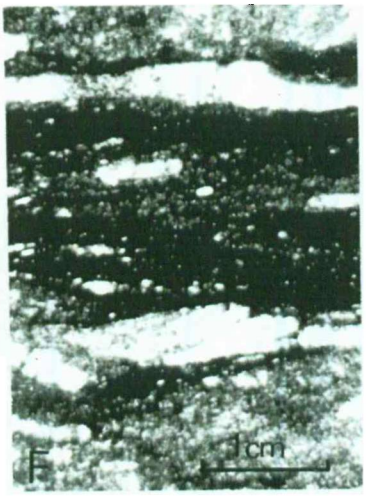

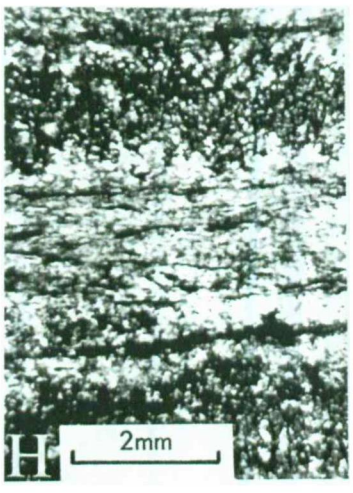

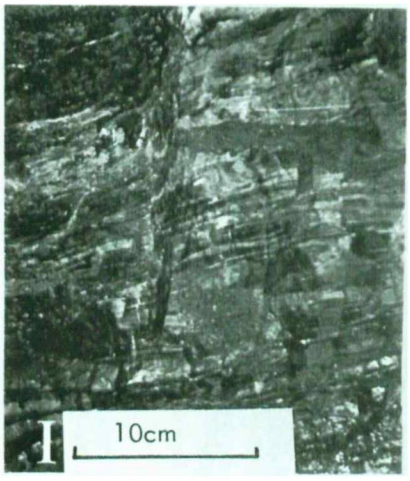

PLATE 4

METABASALTS AND METASOMITES

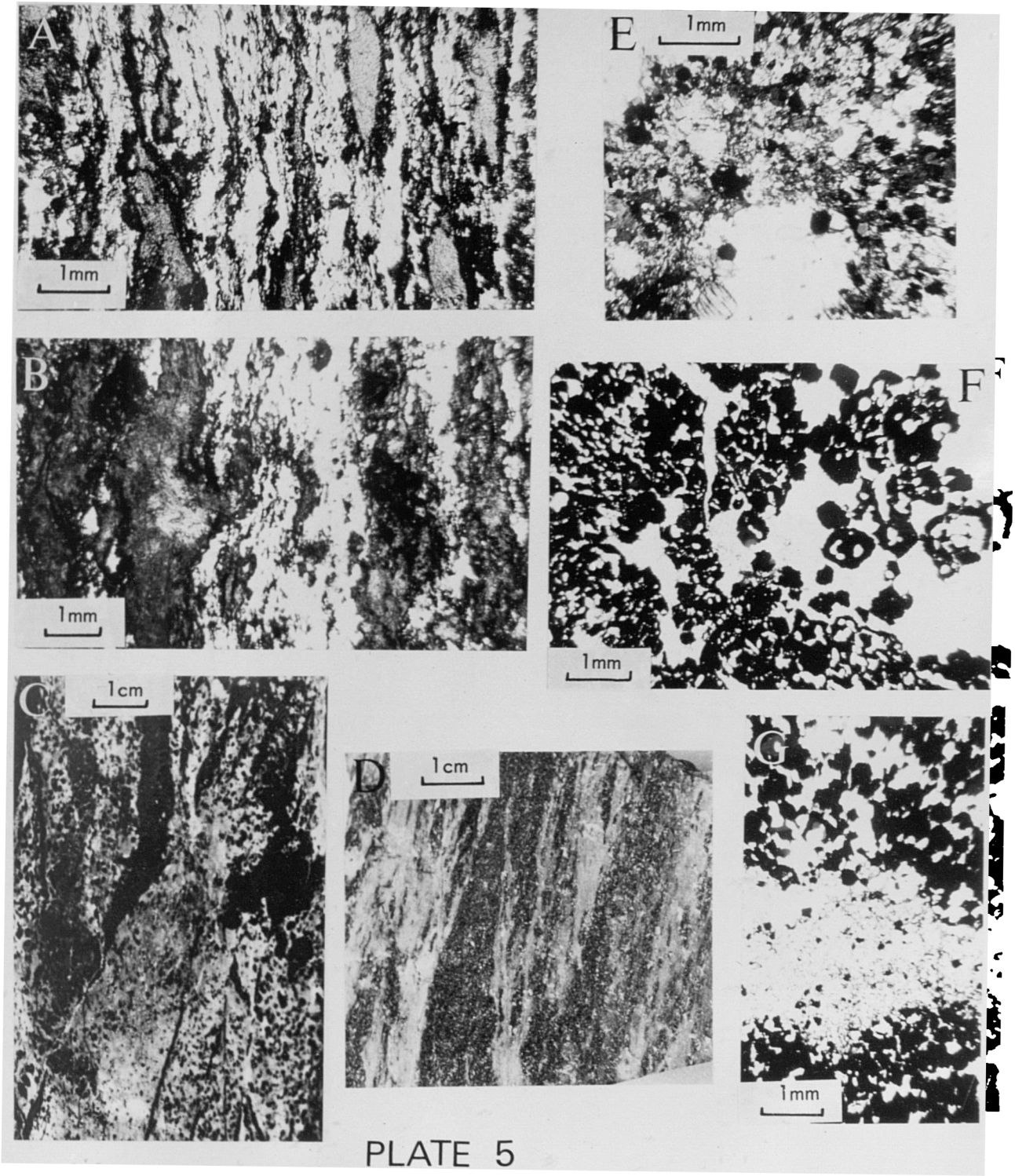

PLATE 5

TABLE 4 LEVANT MINE

	Le 1	2	3	4	5	6	7	8	9	10	11	12	13	15	16	17	18	19	20	21	22	23	24	25	26
SiO_2	71.7	72.3	72.1	72.1	75.3	74.1	71.4	73.4	72.3	72.5	73.8	72.5	74.8	47.2	49.5	45.3	48.3	46.0	46.2	24.3	13.8	12.4	29.9	36.0	43.3
TiO_2	0.34	0.41	0.33	0.39	0.14	0.14	0.14	0.14	0.08	0.17	0.14	0.16	0.01	2.30	1.82	2.02	2.95	2.44	2.99	1.63	1.83	0.96	1.38	1.97	0.11
Al_2O_3	13.98	14.62	14.38	14.31	13.46	13.66	14.50	14.72	14.00	13.94	14.40	13.87	12.94	16.25	18.24	14.20	19.57	13.66	17.00	9.75	5.10	3.20	12.97	14.37	15.37
Fe_2O_3	0.18	0.26	0.30	0.69	0.27	0.17	1.63	0.51	0.60	1.59	1.42	1.20	0.10	1.33	1.09	2.14	0.89	0.80	0.21	26.37	46.87	49.52	20.53	6.79	10.36
FeO	2.09	1.41	1.29	1.54	0.05	0.70	0.88	0.22	0.10	0.18	0.19	1.45	0.88	8.76	6.22	10.69	4.40	10.05	10.15	11.26	17.97	16.41	3 82	6.14	0.04
MnO	0.03	0.03	0.02	0.05	0.01	0.02	0.02	0.01	0.01	0.03	0.02	0.05	0.01	0 16	0.15	0.28	0.19	0.41	0 23	0.98	1.01	0.29	0.78	0.47	2.77
MgO	0.53	0 40	0.35	0.57	0.09	0.09	0.28	0.09	0.06	0.03	0 16	0.08	0.18	4.47	2.66	6.84	3.25	6.54	4.44	1.22	1.38	0.66	0.69	4 03	2 33
CaO	1.11	1.50	0.75	0.71	0.67	0.54	0.67	0.70	0.56	0.53	0.45	0.72	0.49	14.40	14.24	14.75	14.80	12.81	12.52	20.88	8.19	11.63	27.79	24.34	19.34
Na_2O	2.62	4.46	3.10	1.69	3.30	2.69	2.75	2.61	3.14	3.24	3.53	5.01	3.42	2.74	3.24	1.25	3.57	2.17	2 00	0.12	0.10	0.16	0.16	0.15	0.14
K_2O	5.09	3.52	6.03	6.44	5.70	6.47	4.02	6.34	7.46	6.70	4.58	3.41	5.53	0.83	0.81	0.95	0.52	2.50	0.64	0.06	0.07	0.12	0.25	0.77	0.04
P_2O_5	0.30	0.32	0.37	0.32	0.25	0.14	0.33	0.37	0.23	0.21	0.22	0.28	0.18	0.25	0.18	0.16	0.23	0.31	0.52	0.24	0.90	0.62	0.39	0.45	0.33
B_2O_3	0.44	0.25	0.16	0.31	-	-	1.61	0.43	0.37	0.36	0.28	0.31	0.10	-	-	-	-	-	-	1.00	1.35	0.10	-	-	4.09
F	0.23	0.36	0.32	0.26	-	-	0.50	0.03	0.37	0.03	0.22	0.42	0.53	-	-	-	-	-	-	0.49	0.26	0.26	-	-	0.26
H_2O^+	0.45	0.36	0.78	0.68	0.20	0.44	0.46	0.48	0.22	0.23	0.33	0.35	0.37	1.02	1.21	1.46	0.56	1.47	1 46	0.90	1.08	0.52	0.55	2.65	1.43
H_2O^-	0.38	0.15	0.13	0.27	0.21	0.28	0.14	0.24	0.18	0.14	0.18	0.29	0.17	0.22	0.34	0.13	0.16	0.14	0.19	0.14	0.20	0.27	0.22	0.73	0.12
CO_2	-	-	-	-	-	-	-	-	-	-	-	-	-	-	-	-	-	-	-	1 29	0.48	3.38	-	-	-
O ≡ F	0.16	0.13	0.13	0.12	-	-	0.21	0.01	0.16	0.01	0.09	0.18	0 22	-	-	-	-	-	-	0.21	0.11	0.11	-	-	0.12
Total	99.30	100.22	100.28	100.19	99.65	99.44	99.12	100.28	99.52	99.87	99.83	99.92	99.71	99.93	99.70	100.17	99.39	99.30	98.55	100.42	100.48	100.39	99.43	99.46	99.91
As	<15	30	35	<15	35	<15	<15	25	<15	<15	20	30	47	-	-	-	-	-	-	-	-	-	-	-	-
Ba	250	240	220	440	245	150	135	225	450	205	230	80	302	-	-	-	-	-	-	-	-	-	-	-	-
Be	10	6	7	10	5	4	5	4	4	4	4	18	6	-	-	-	-	-	-	-	-	-	-	-	-
Co	2	1	1	12	10	5	2	3	1	1	0	0	8	28	31	37	30	54	30	8	166	15	10	24	12
Cr	1	3	2	1	1	0	0	0	1	1	1	1	5	335	370	370	320	235	244	28	22	30	117	280	20
Cu	3	4	5	30	3	3	9	2	3	4	4	1	20	68	88	8	10	113	24	19	134	26	7	88	5
Li	141	107	120	148	18	32	18	28	14	20	24	1,650	74	36	47	40	15	103	56	20	9	16	28	44	52
Ni	1	3	3	1	2	6	5	2	2	1	14	1	1	155	165	160	250	134	94	32	70	110	44	64	8
Pb	10	3	9	18	19	44	4	16	15	11	12	25	23	17	19	18	20	50	17	15	22	14	16	21	17
Rb	590	460	660	560	500	550	530	690	770	690	720	660	518	-	-	-	-	-	-	-	-	-	-	-	-
Sn	30	30	<10	30	45	<10	<10	<10	<10	20	<10	30	50	<10	<10	<10	12	<10	12	650	975	55	60	20	1,120
Sr	105	90	95	90	80	85	30	85	90	80	85	70	78	-	-	-	-	-	-	-	-	-	-	-	-
Zn	63	60	34	29	12	24	267	26	29	17	25	26	21	62	55	55	30	455	162	242	434	220	100	1,210	530
Zr	175	160	190	180	35	10	25	25	15	20	< 10	30	32	-	-	-	-	-	-	-	-	-	-	-	-

TABLE 5

	Le29	30	31	32	33	34	35	36	37	38	39	40	41	42	43	44	50	51	52	53	54	55	56
SiO_2	48.0	52.4	50.1	49.6	43.6	60.4	47.8	58.3	53.7	52.8	64.4	36.4	34.1	37.6	37.4	34.8	36.1	36.0	35.6	47.6	39.5	29.8	32.5
TiO_2	0.87	0.99	0.69	0.72	1.11	0.59	1.06	0.66	0.60	1.03	0.34	2.53	1.83	2.87	1.38	2.53	0.70	2.38	1.97	1.97	2.95	2.81	2.67
Al_2O_3	15.99	15.77	11.61	11.86	26.71	17.52	24.35	19.00	15.31	20.86	18.00	13.07	9.17	15.36	11.66	14.23	12.20	14.58	13.07	15.73	23.52	18.11	15.09
Fe_2O_3	0.31	2.52	0.91	0.99	2.54	2.04	2.09	Total Fe Oxides as Fe_2O_3				2.79	31.91	3.13	2.68	1.45	1.60	13.26	6.62	9.74	6.66	15.28	11.42
								6.41	13.70	8.95	2.40												
FeO	7.49	4.27	6.04	8.54	6.13	5.67	5.77					23.59		17.88	24.33	24.26	39.41	16.22	29.60	7.06	3.77	2.23	9.73
MnO	0.19	0.18	0.45	0.47	0.06	0.04	0.03	0.19	0.22	0.24	0.11	0.23	0.24	0.21	0.31	0.30	0.91	0.40	0.15	0.21	0.69	0.49	0.45
MgO	8.34	5.23	6.76	3.94	3.55	4.12	4.28	1.75	3.16	3.92	0.84	5.74	4.43	5.32	6.15	6.54	1.70	4.34	2.48	3.22	2.20	6.67	6.83
CaO	10.61	9.65	20.78	19.50	5.89	1.20	4.66	0.30	0.22	1.22	1.20	2.56	3.23	3.35	3.98	2.77	0.81	0.88	1.00	1.44	11.63	11.73	13.14
Na_2O	0.45	1.09	0.47	0.84	1.18	2.43	0.96	6.77	0.20	4.02	8.65	0.63	0.38	0.93	0.19	0.15	0.11	0.11	0.14	0.22	0.16	0.08	0.66
K_2O	4.93	4.78	0.95	1.32	6.20	4.54	5.89	2.79	6.70	0.11	0.34	6.86	3.53	6.35	3.63	6.58	1.20	6.20	4.14	6.51	4.48	4.35	2.83
P_2O_5	0.38	0.36	0.13	0.42	0.19	0.13	0.22	0.17	0.38	0.41	0.13	0.89	0.45	1.00	0.67	0.89	0.22	0.35	0.51	0.64	0.12	1.10	1.24
H_2O^+	1.42	1.92	1.38	1.67	2.44	1.20	1.98	2.02	3.96	2.41	0.43	3.07	3.71	3.58	4.63	3.55	4.35	4.13	3.51	3.78	3.33	6.02	2.87
H_2O^-	0.25	0.31	0.26	0.39	0.28	0.35	0.22	0.36	0.18	1.84	0.16	0.36	0.80	0.68	0.98	0.40	1.18	1.20	1.53	2.21	0.30	0.75	0.12
Total	99.23	99.47	100.53	100.26	99.88	100.23	99.41	98.72	98.33	97.81	97.00	98.72	97.08*	98.26	97.99	98.45	100.49	100.05	100.32	100.33	100.31	99.42	99.55
Co	15	15	40	28	25	28	32					11	16	20	4	18	47	26	18	22	14	40	39
Cr	149	181	127	127	178	130	145					205	170	235	190	225	61	213	158	260	297	170	162
Cu	10	13	2	7	135	66	72					50	1.5%	40	125	10	205	83	29	82	61	23	5
Li	251	59	69	67	45	56	40					130	100	105	140	180	48	137	92	95	124	85	80
Ni	83	83	117	75	110	56	70					155	230	165	60	130	52	160	142	177	170	154	225
Pb	20	14	19	23	5	7	8					16	65	4	2	6	62	10	3	6	8	11	15
Sn	<10	<10	<10	<10	12	<10	<10					<10	2.6%	300	350	700	120	4,800	3,000	1,100	675	45	<10
Zn	149	116	128	194	75	58	64					340	1,130	145	500	385	300	325	230	335	348	920	168

* Total Includes SnO_2

TABLE 6

	Le 57	58	59	60	61	62	63	64	65	66	67	68	69	70	71	72	73	74	75	76
SiO_2	25.8	44.3	43.9	34.7	35.4	44.6	33.87	33.7	35.9	31.6	36.1	42.3	36.3	36.0	37.9	34.3	36.3	36.8	36.4	38.9
TiO_2	2.95	4.44	2.56	2.36	1.82	0.55	1.73	1.78	1.99	2.50	0.87	0.03	1.97	1.69	1.60	1.69	2.25	1.57	2.39	1.74
Al_2O_3	18.30	16.91	16.38	13.40	13.97	12.16	14.07	13.08	12.32	12.31	13.68	14.86	10.63	14.69	16.49	16.94	13.27	14.84	14.04	15.40
FeO	12.11	10.98	11.35	9.68	Total Fe Oxides as Fe_2O_3				6.35	6.05	10.11	1.78	4.78	8.57	4.19	4.81	2.33	2.95	5.81	5.86
Fe_2O_3	22.81	5.43	2.40	6.90	26.12	20.02	26.42	27.62	19.52	24.72	14.44	7.77	15.93	5.25	20.80	14 86	20. 6 5	16.87	18.74	13.17
MnO	0.77	0.37	0.36	0.35	0.40	0.30	0.31	0.37	1.23	0.52	0.32	2.50	0.70	1.20	0.32	0.55	0.74	1.38	0.27	0.48
MgO	6.44	4.06	4.53	4.18	8.87	3.46	8.85	7.96	2.67	3.11	8.65	2.34	4.69	1.75	3.97	5.95	6.31	4.59	4.69	2.48
CaO	1.59	5.61	10.18	23.78	1.64	6.67	3.27	2.93	7.15	5.76	1.36	18.40	12.28	26.22	4.12	12.51	5.66	9.28	3 98	14.42
Na_2O	0.01	1.77	1.61	0.72	0.06	0.13	0.33	0.24	0.20	0.16	0.18	0.17	0.28	0.15	0.04	0.50	0.08	0.09	0.07	0.14
K_2O	0.03	0.31	3.40	1.04	5.90	0.37	4.78	4.64	3.31	3.60	4.70	0.31	3.50	1.40	7.13	2.20	4.29	2.92	8.37	3.58
P_2O_5	1.00	1.00	0.79	0.68	0.61	3 81	0.55	0.36	0.64	0.65	0.14	0.40	0.34	0.39	0.16	0.63	0.46	0.23	0.31	0.86
B_2O_3	-	0.42	-	-	0.02	0.10	0.08	0.06	2.45	2.33	0.92	5.32	4.22	0.62	-	-	1.92	3.12	0 98	-
F	0.37	0.11	-	-	0.78	2.23	0 62	1.00	0.37	0.42	0.05	0.09	0.11	0.10	-	-	0.31	0.41	0.15	-
S	-	-	-	-	0.06	2.47	0.42	2.00	0.44	0.62	0.12	0.12	0.41	0.51	-	0.19	0.22	-	1.13	-
H_2O^+	7.24	3.52	1.67	1.36	4.47	3.60	4.33	1.11	3.80	4.60	6.11	1.77	2.43	0.90	2.69	3.59	3.85	3.85	2.12	2.61
H_2O^-	0.24	0.39	0.22	0.29	0.44	0.48	0.51	0.42	1.10	0.73	1.47	1.01	1.03	0.43	0.14	0.48	0.62	0.44	0.20	0.21
O≡F+S	0.16	0.05	-	-	0 35	1.87	0.42	1.17	0.36	0.41	0.05	0.06	0.20	0.23	-	0.07	0.21	0.17	0.48	-
Total	99.50	99.57	99.35	99.44	100.21	99.08	99.72	98.10*	99.08	99.27	99.17	99.11	99.40	99.64	99.55	99.13	100.38*	99.17	99.17	99 85
As	450	70	<15	40	150	40	8,900	6,700	540	470	<15	30	<15	<15	<15	400	< 15	<15	< 15	450
Be	4	21	13	16	24	110	28	23	100	33	8	760	20	4	15	14	190	450	47	15
Co	13	4	26	40	22	344	23	18	2	6	9	5	5	6	11	27	6	6	7	8
Cr	71	60	73	178	143	47	172	146	330	320	100	23	290	170	195	240	125	120	220	200
Cu	36	33	26	30	890	195	2,090	2,070	6,270	7,540	30	60	5,310	85	5	500	10	10	6,260	95
Li	238	95	46	34	348	215	318	285	115	140	165	20	90	60	205	160	170	110	165	85
Ni	15	10	18	95	39	48	64	37	10	14	190	6	17	36	17	515	55	46	35	25
Pb	11	1	1	20	20	555	20	25	12	2	4	5	1	10	8	13	9	7	8	11
Sn	2,100	5,200	<10	1,040	1,505	485	8,500	1.58%	6,500	1,400	6,000	4,800	600	800	<10	630	1.05	5,000	6,000	500
Zn	730	360	100	336	3,210	336	4,970	646	375	375	435	560	370	105	380	400	235	230	445	250

* Total includes SnO_2

Cr, Cu and Ni. Plots of niggli values (fig 9) do not show any definite trends but mg/c, mg/K and Ni and Cr/TiO_2 diagrams indicate that the rocks do fall within sedimentary fields rather than igneous (basaltic) fields. The close similarity in the composition of the positively identifiable calcareous sediments and the finely laminated Ca rich rocks of 6 level suggests that these rocks are also sedimentary in origin.

E1 Greenstones

Greenstone is a general field term used by the miners to describe a dark green coloured rock, which may be a basalt, a banded amphibolite of sedimentary or basaltic origin, a metasomatite, or a hydrothermally altered (chloritised or biotised) metasediment or metabasite. It is, however, a useful primary definition as it is not always apparent what the rock is.

Several distinct amphibolitic horizons intersect the mine workings (see maps 3 and 4). The main greenstone (of both metabasic and metasedimentary origin) horizons are as follows:

1. Adjacent to the Old Bal Lode, 1 level (massive banded amphibolite, probably basaltic in origin).
2. In the cross-cut for ~50 m north of the Unity Lode, 1 level (banded amphibolite, probably basaltic in origin).
3. In the area between the West Spar and Unity/Cockle veins, 4 level (banded amphibolites of calcareous

metasedimentary (?) and basaltic origin).

4. Bordering the South Lode, 4 level (several massive and banded amphibolite horizons of basaltic origin).
5. Several minor amphibolite horizons adjacent to the Foot-Wall Branch and Unity Veins, 6 level (of basaltic origin).
6. In the cross-cut immediately SE of the Unity Vein, 6 level (banded amphibolite of basaltic origin).
7. In the cross-cut between 420 - 820 m SE of the Old Bal Lode, 6 level (interbedded amphibolites of basaltic and calcareous metasedimentary origin and Ca-Fe-B metasomites).
8. In addition, several diamond drill holes (SJ3 and 5 and the UL series) revealed the presence of numerous amphibolitic and metasomatic horizons below the SW part of 601 cross-cut.

The greenstones can be subdivided into two groups:

a) banded or massive amphibolites of basaltic or calcareous sedimentary origin.
b) Ca, Fe, B and K metasomites.

In contrast with surface greenstone exposures, which are dominated by basaltic pillow flows, the subsurface greenstone sequence is dominated by banded amphibolites and metasomites. No pillow structures have been identified in the mine (with the possible exception of the hydrothermally altered greenstones adjacent to the Unity Lode, 1 level). All the amphibolite horizons

exposed in the mine workings are approximately concordant with the bedding in the adjacent metasediments, suggesting that these horizons were originally either interbedded coeval extrusive lavas, concordant pre-tectonic basaltic sheets or calcareous sediments.

E2 Banded amphibolites

Banded amphibolites occur on all three mine levels and are the dominant greenstone lithology in the diamond drill holes. The striped appearance of the amphibolite is the result of variation in both texture and composition. The bands range in width from 1 mm to 2 cm and they are usually parallel to the contacts of the individual units. Some of the bands have the appearance of basaltic flow structures and it is thought that this is the most likely controlling factor on the development of the striping. Individual bands may or may not be consistent along their dip and strike and occasionally the banding merges into massive amphibolite.

Texturally, the striped amphibolites are uneven grained and xenoblastic with a reticulate fibric of subparallel bands and clots of fibrous amphibole (pale green actinolite or hornblende), with accessory epidote and opaque ores, alternating with bands and lenses of granular plagioclase An_{40-60}, with accessory streams of sphene, calcite, opaque ores, epidote and rare quartz (plate 5). Immediately adjacent to the plutonic granite contact (diamond drill hole UL 42, 227 m), the banded amphibolites consist of alternating bands of

blue-green hornblende and granular diopside, with minor plagioclase, quartz and garnet.

Geochemistry - 6 samples of banded amphibolite were analysed (table 4). Compared to the surface basalts, the banded amphibolites are enriched in SiO_2, TiO_2, CaO, Na_2O, Cr, Cu, Ni, Pb and Zn, and depleted in Al_2O_3, Fe_2O_3, FeO, MgO, K_2O, P_2O_5, Co and Li.

Computed niggli values (fig 9) show that the major elements increase in al, alk, c and decrease in mg and fm as si increases. These trends are almost coincident with the trends displayed by the surface lavas, the Karroo dolerites (Walker and Poldervaart, 1949) and the Connemarra amphibolites (Evans and Leake, 1960).

Systematic decrease in mg with increase in si is probably the most reliable criterion of differentiation in basaltic magmas, especially if it can be correlated with increasing alkalis (particularly Na). A similar trend in the amphibolites, together with the trends already mentioned and plots on mg/k and mg/c variation diagrams, suggest that the banded amphibolites are igneous (basaltic) in origin.

Plots of silica/total alkalis (Kuno, 1966) indicate that the amphibolites could originally have been alkali basalts (although isochemical metamorphism is very unlikely).

Compared to the calcareous metasediments, which are broadly similar in composition, the banded amphibolites are enriched in TiO_2, Al_2O_3, MnO, Na_2O, Cr,

Cu, Ni and Pb, and depleted in SiO_2, FeO, MgO, CaO, K_2O, Li and Zn. Plots of Cr and Ni/wt. % TiO_2 clearly distinguish between the two groups of rocks.

It is, therefore, probable that the banded amphibolites are basaltic in origin and that they can be clearly distinguished from the calcareous metasediments.

Similarly striped amphibolites in Connemara (Evans and Leake, 1960) were considered to have formed as a result of tectonic and regional metamorphic processes. The banding in the amphibolites of Levant Mine is considered to be the result of metamorphic differentiation during thermal metamorphism, controlled by primary flow banding and secondary tectonic foliations, due to shearing parallel to primary flow banding.

E3 Metasomites

Rocks displaying metasomatic features i.e. replacement of the parental rock with material from elsewhere within the system (internal metasomatism) or with material introduced from outside the immediate system (external metasomatism), form approximately 40% of the total metabasite exposure in the mine.

In common with surface metasomites, there are several distinct metasomatic chemical trends which, if developed to completion, produce the following monomineralic assemblages:

chemical trend →	monomineralic assemblage	accessory phases
a) Enrichment in Ca - grossular garnet	garnet-magnetite±	calcite, epidote, clinozoisite actinolite, hornblende, sphene tremolite, chlorite, idocrase biotite, quartz, diopside
b) Enrichment in Fe - magnetite		
c) Enrichment in K - biotite±		magnetite, hematite, sphene calcite, actinolite chlorite, epidote, axinite, tourmaline, fluorite
d) Enrichment in B - tourmaline (Ca depleted) axinite (Ca enriched)		biotite, sphene, calcite magnetite, garnet, actinolite tremolite, diopside

The great variation in metasomatic trends, the degree of metasomatism and the overprinting of one metasomatism by another has led to the production of a great diversity of mineral assemblages in these rocks.

Ca-Fe metasomites - horizons containing an assemblage dominated by either garnet and/or magnetite occur in 601 cross-cut, between 480 and 650 m SW of the Old Bal Lode, and in several horizons within the greenstone lithologies recovered from boreholes below the SW part of 601 cross-cut. Those exposed in 601 cross-cut grade laterally into banded amphibolites in the NE part of the exposure and terminate abruptly against the Corpus Christi fault in the SW of the exposure. In general there is an increase in the proportion of magnetite towards the centre of the exposure (near 604 drive).

Texturally, these metasomites are uneven grained, banded or massive, xeno or hypidioblastic aggregates of anhedral or euhedral, isotropic or anisotropic garnet and

magnetite, intergrown with calcite, amphibole and epidote, and veined by later calcite, axinite, amphibole and chlorite.

The paragenetic sequence of many calciferous metasomites is as follows:

1. amphibole (hornhlende or actinolite-tremolite), plagioclase
2. epidote, calcite, magnetite
3. garnet, magnetite, epidote, clinozoisite, calcite, idocrase
4. calcite, epidote, axinite, tourmaline
5. calcite, chlorite

Geochemistry - samples of calciferous metasomite were analysed from 601 cross-cut (table 4). Compared to the parental banded amphibolites, the calciferous metasomites are enriched in CaO, total Fe oxides, MnO, P_2O_5, Pb, Li, Sn and Zn, and depleted in SiO_2, TiO_2, Al_2O_3, MgO, Na_2O, K_2O, Co, Cr, Ni and Pb. Fe rich metasomites are extremely depleted in SiO_2 and Al_2O_3.

Computed niggli values (fig 9) show that the major elements increase in al and c, and decrease in fm as si increases. Mg and alk do not show any systematic trends.

K metasomites - horizons containing an assemblage dominated by biotite ± orthoclase are usually spatially associated with mineralised horizons or fissure veins and often with boron rich assemblages (axinite or

tourmaline). They occur within the amphibolites of 601 cross-cut between 90 and 110 m NE of the Hen Vein, in 604 drive, and in the UL 14, 15 and 42 diamond drill holes.

The paragenetic sequence of several K metasomites is as follows:

1. amphibole (hornblende or actinolite), plagioclase
2. biotite, calcite, magnetite-ilmenite, quartz
3. orthoclase-quartz
4. axinite, tourmaline, calcite, quartz, ore-minerals

Geochemistry - most of the analysed K metasomites show evidence of other metasomatisms (mainly later boron metasomatism). Samples from 604 drive, collected from near the guide, contained an assemblage of biotite, orthoclase, opaque ores (hematite and magnetite) quartz, calcite and sphene. Compared to the banded amphibolites these rocks are enriched in K_2O, total iron oxides, P_2O_5, Cu, Li, Sn and Zn and depleted in SiO_2, TiO_2, Al_2O_3, MgO, CaO, Na_2O, Co, Cr, Ni and Pb.

B metasomites - the distribution of horizons containing boron rich minerals (axinite ± tourmaline) is very similar to that of the K metasomites. In addition, B metasomatism of Ca + Fe metasomites has produced axinite rich horizons on 4 and 6 levels and in the UL 14, 15 and 42, and SJ 3 and 5 diamond drill holes. Studies of mineral paragenesis indicate that B metasomatism post-dated the formation of Ca, Fe and K metasomites.

Geochemistry - as boron metasomatism commonly post-dates either Ca, Fe or K metasomatism, rocks containing boron rich minerals are extremely varied in chemistry. Compared to the banded amphibolites the boron - calciferous metasomites (axinite ± garnite, magnetite, calcite, amphibole) are enriched in B, CaO, total iron oxides MnO, P_2O_5, Sn, Zn and Be, and depleted in SiO_2, TiO_2, Al_2O_3, MgO, Na_2O, K_2O, Co, Cu, Cr, Li, Ni and Pb. The boron-potassium metasomites are enriched in B, total iron oxides, MnO, K_2O, P_2O_5, Cu, Li, Sn, Zn and Be, and depleted in SiO_2, Al_2O_3, MgO, CaO, Na_2O, Co, Cr, Ni and Pb.

F Structure

Folding - Fold structures are more difficult to distinguish in subsurface exposures, due to the lack of weathering and the obliteration of bedding strutures during hydrothermal alteration.

The structural style at outcrop is continued in the subsurface exposures, all four phases of deformation being represented. No F1 folds were observed in the mine, although the associated cleavage (S1) is frequently deformed by later tectonic events. F2 folds are less than 5 m in wavelength and have north plunging fold axes and moderate to steep dipping axial planes. Axial planar cleavage is usually absent, but the basaltic amphibolites are often sheared, parallel to the primary bedding foliation. The folds are similar in style and usually

assymetrical, with a short steep limb and a longer shallower limb. Apical thickening and limb attenuation are common in the pelites. The massive amphibolite horizons are characterised by a more open style of folding. A NW-SE geological cross-section through the mine (volume 2, map 6) along the Unity and Spar veins indicates that the structural style of folding is one of tight, assymetrical folds, alternating with more open upright flexures. F3 folding in pelites produced minor recumbent folds and warps on the steep dipping limbs of F2 folds. These folds occasionally display axial planar or shear cleavage. F4 folding in pelites and amphibolites produced minor NW trending, NW plunging open flexures and warps.

The orientation of fold axes and axial planes in the mine are displayed on two sterographic projections (Map 4). Fold axis maxima are at 010/10°N, 038/8°NE and 320/10°NW. Axial planes trend either NNE/NE and dip NW or SE at between 50 - 80°, or NW and dip steeply SW.

Fractures - Garnett (1962) considered that the joint systems in the granite had exerted a fundamental control on the distribution and orientation of late mineralised fissures. He defined four major sets of joint systems (page 228) and concluded that the primary and secondary joints were formed under a predominantly horizontal maximum stress, during the consolidation of the granite. These were later dislocated and enlarged by vertical stresses which accompanied mineralisation. The

structural continuation of many of the steep dipping, NW trending, fissure veins from granite into the aureole, suggests that the hornfelsed rocks of the aureole and the outer granite shell behaved similarly, during brittle deformation. It is possible, therefore, that the fracture systems in the aureole could have been produced simultaneously with, and within the same tectonic framework as the joint and tectonic fracture systems in the granite.

To test this hypothesis, a series of stereographic projections (Schmidt, lower hemisphere) were constructed, showing the distribution of poles to joints for specific geographical areas in the mine (map 4). No attempt was made to distinguish the joints genetically. Therefore, primary igneous cooling joints (in amphibolites), tectonic joints produced during orogenic activity and joints produced during and after thermal metamorphism, are included in the same diagrams. The contoured stereograms indicate that the main joint systems are as follows:

1. A dominant set trends between NNW and WNW and includes a prominant NW trending set. A majority of the joints dip SW at $70 - 85^{\circ}$.
2. A less well developed set trends between NE and ENE and dips predominantly SE at approximately $60 - 70^{\circ}$.
3. A minor set trends ENE or WNW and dips north or south at low angles ($\sim 40^{\circ}$).

The uniformity of the jointing throughout the aureole, both in surface and sub-surface exposures, suggests

that these joint sets were produced within a uniform stress field and the similarity in the orientation of joints in the aureole and granite (Garnett, 1962) suggests that they were formed contemporaneously.

Figure 10C shows the distribution of 1650 poles to joints in the aureole, combining the results of surface and sub-surface joint measurements. Two major joint maxima can be distinguished (>7.5%) trending 295/80° S, and 330/80° S. A minor maxima (>2.5%) trends 040/60° S. If it is assumed that the two NW trending joint maxima are an acute angled, conjugate shear pair, the orientation of the principal stress axes at the time of joint formation can be deduced (fig 10C). The distribution of the principal stress axes (based on this assumption) is as follows: P maximum is inclined ~6° towards the NW (312°), P intermediate is inclined ~84° NW and ~78° S, and P minimum is inclined ~12° towards the NE (042°).

Such a distribution of stress during joint formation (i.e. P max. ~ horizontal and P int. ~ vertical) might be expected in the deeper tectonic levels of the marginal zones of a pluton during, or soon after, emplacement (Moore, 1975). The distribution of the principal stress axes is similar to that deduced by Garnett (1962) for jointing in granite and the surface aureole rocks. The apparent conformity between the orientation of the dominant joint set (NW trending, SW dipping) and the mineralised fissure veins (fig 10C) suggests that, in common with the Geevor lodes, the Levant lodes and veins were produced by the enlargement

Fig 10

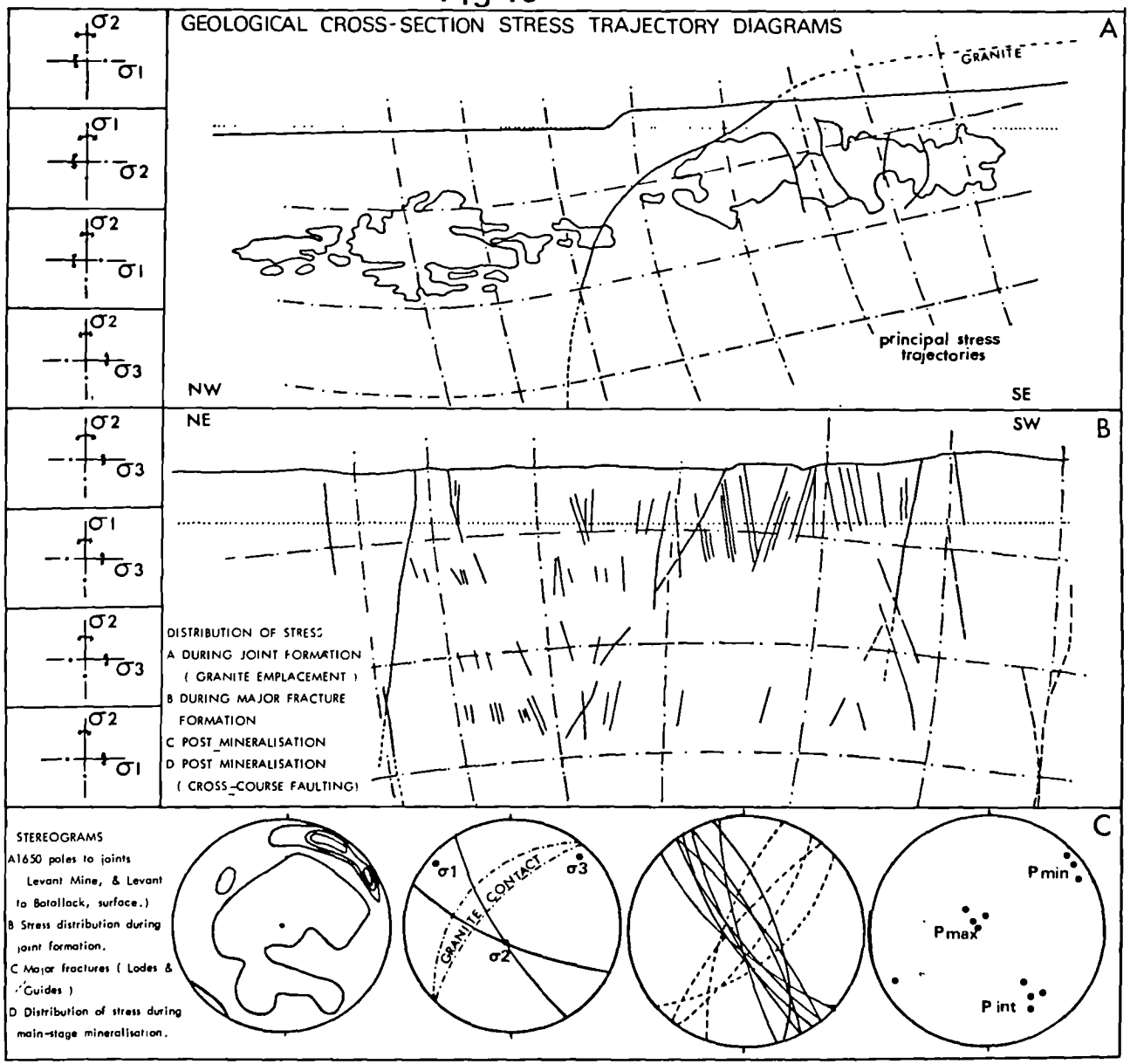
GEOLOGICAL CROSS-SECTION STRESS TRAJECTORY DIAGRAMS
A
GRANITE
principal stress trajectories
NW
SE
NE
SW
B
DISTRIBUTION OF STRESS
A DURING JOINT FORMATION (GRANITE EMPLACEMENT)
B DURING MAJOR FRACTURE FORMATION
C POST MINERALISATION
D POST MINERALISATION (CROSS COURSE FAULTING)
STEREOGRAMS
A1650 poles to joints Levant Mine, & Levant to Botallack, surface.)
B Stress distribution during joint formation.
C Major fractures (Lodes & Guides)
D Distribution of stress during main-stage mineralisation.
σ1
σ3
σ2
GRANITE CONTACT
C
Pmin
Pmax
P int

and dislocation of previous master joints.

The distribution and orientation of major, mineralised and barren fissure veins in the mine is illustrated in fig 11C . With reference to the stereographic projections, it can be seen that a majority of the mineralised (Sn, Cu, As) fissure veins trend between 300° & 350° and dip steeply (70 - 80°) SW. Major, barren cross-fractures trend between 020° & 050° and dip NW or SE at between 50 - 80°.

The distribution of stress during vein formation can be illustrated by constructing stress trajectory diagrams. Stress trajectories are lines which represent the orientations of the principal compressive or extensive stresses ($\sigma 1, \sigma 2$ and $\sigma 3$). Two of the principal stresses can be represented as trajectory lines on a geological plan or section corresponding to a principal plane. The variation in the distribution of stress, within the Levant-Geevor fissure vein system, must have been considerable, as is evident by the variation in the orientation of slickensides, in the veins and on the vein walls, the displacement of one vein by another and the displacement of marker horizons. The latter two features, however, indicate that the net displacement on most fissures was no more than a few metres and usually less than half a metre.

The fracture regime of this part of the St. Just fracture system is a complex combination of shear, oblique slip faults with a large component of either low angle

(strike slip) or high angle (normal or reverse) fault movement, interspersed with phases of dilatant extensional movement. Consequently, it is very difficult to construct a stress model which is applicable to the whole phase of vein formation. Fig 11 A & B illustrates two geological cross-sections through the fracture system. These sections approximately coincide with the principal stress planes during vein formation. The diagrams illustrate the probable orientation of the principal stress axes during four stages of fracture formation (constructed from the data of Garnett (1962) and this study).

1. The initial formation of the joint systems and formation of major fractures by the selective enlargement and disloaction of several joint sets. During this stage $\sigma 1$ was $\sim$horizontal, $\sigma 2$ was vertical ($\sigma 1 - \sigma 2$ principal plane was oriented NW/SE) and $\sigma 3$ was $\sim$ horizontal. This stress system produced strike-slip faults and was operative during the early stages of vein formation.
2. Later, during main stage mineralisation, the maximum compressive stress was oriented vertically, causing $\sigma 1$ and $\sigma 2$ to interchange. This stress system produced normal (and reverse) faults interspersed with dilatant extensional phases of movement.
3. Post-mineralisation (Sn, Cu, As) slickensides indicate that $\sigma 1$ and $\sigma 2$ returned to their initial orientation, so producing strike-slip faults ($\sigma 1 - \sigma 2$ principal plane was oriented NW/SE).

4. Post-mineralisation displacement of NW trending veins by NE trending veins (cross-fractures) indicates that the principal stress axes were oriented as follows: $\sigma 1 \sim$ horizontal, $\sigma 2 \sim$ vertical ($\sigma 1 - \sigma 2$ principal plane was oriented NE/SW and $\sigma 3 \sim$ horizontal.

It must be emphasised that this model is highly simplified, the principal stress axes probably being interchanged extensively, at least during the earlier stages of mineralisation.

Moore (1975) suggested that the fracture system, associated with the Land's End pluton, was produced when a hydraulic pressure, exerted from within the intrusion, exceeded the regional and local confining stresses. The distribution of stress around the north west periphery of the pluton during mineralisation was complex and involved repeated phases of horizontally and vertically directed maximum compressive stresses at the same tectonic level. This variation in the distribution of stress, in space and time, suggests that the pressure source, a hydraulic cell located in the core of the pluton, may have repeatedly changed its position in the pluton. When the pressure cell was at high tectonic levels the periphery of the pluton would be subjected to horizontally directed maximum compressive stresses. Such a stress distribution occurred during joint and early vein formation. As the pressure cell migrated to deeper tectonic levels, the maximum compressive stresses would be directed vertically through the margins of the pluton.

Periodic fluctuations in the level of the pressure cell could have led to the alternate production of strike-slip, normal fault and tensional extensional fractures in, and around, the periphery of the pluton.

G MINERALISATION

Two distinct types of mineralisation phenomenon can be distinguished in Levant Mine: 'high grade' vein cassiterite - sulphide deposits, and 'low to medium grade' cassiterite and cassiterite-sulphide replacements in granite, pelite and metabasite.

G1 FISSURE VEIN MINERALISATION

a) Main lodes

The Levant sett comprises three major lodes (the Old Bal Lode and the South & North Lodes) and several minor lodes (the North Vein, Treglown's Lode, Shop Lode, Prince of Wales Lode, Boscregan Lode and Guide Lode). The following details are based on the account given by Dines (1956). All measurements originally in fathoms have been converted to the nearest metre.

Old Bal Lode trends 330°, dips 80° NE and crosses the coast 80 m NE of Levant Zawn. Near Skip Shaft it splits into two parts, the southern branch being known as South Lode. Although rich Sn and Cu ore shoots are well developed in the upper levels, the metal content of the vein rapidly diminishes in depth and north west of its junction with the South Lode. It is developed for 403 m NW and 230 m SE of Skip Shaft to the 311 m level, for 366 m NW and 275 m SE between the 329 m and 421 m levels and for 92 m NW

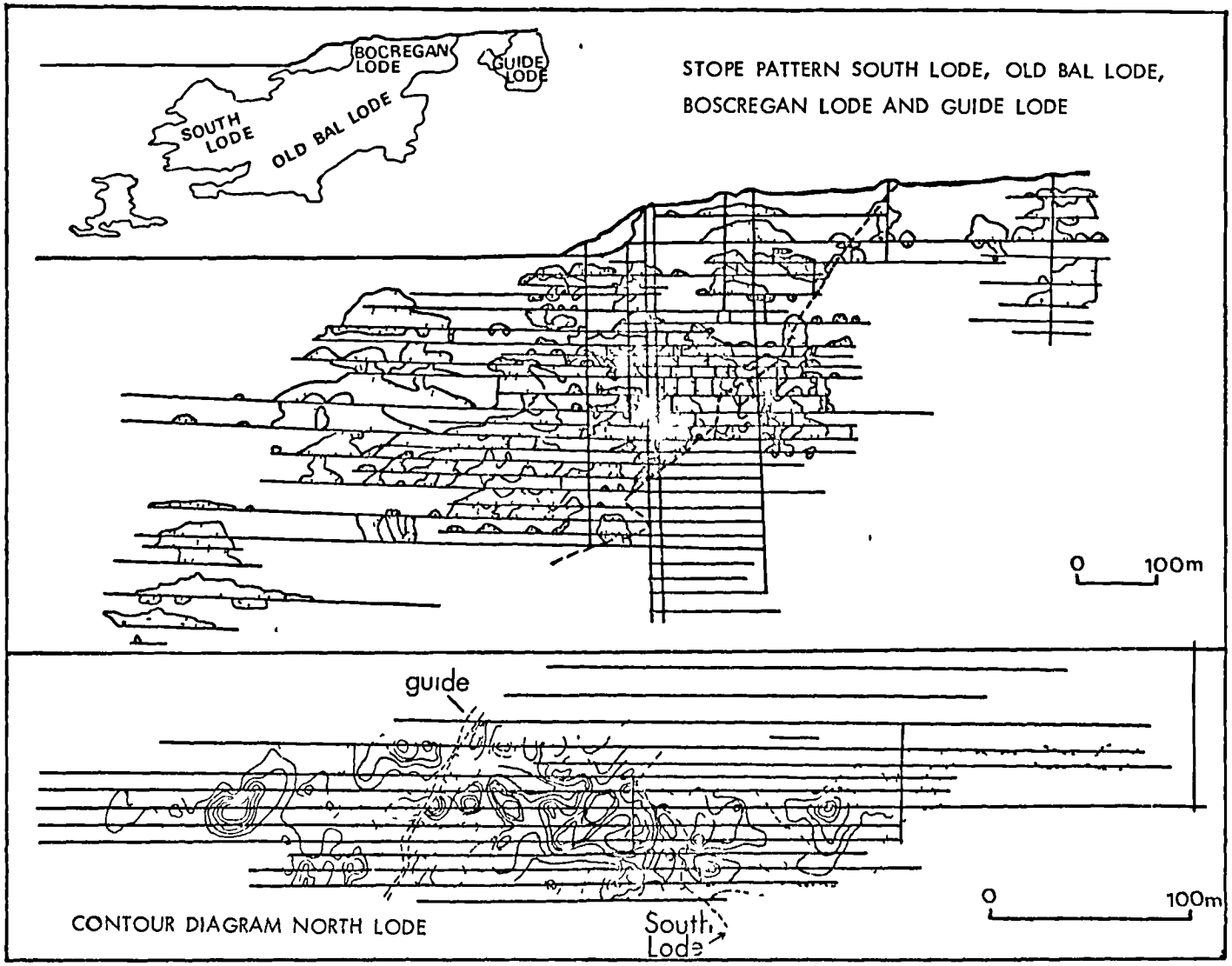
BOCREGAN LODE
GUIDE LODE
SOUTH LODE
OLD BAL LODE
STOPE PATTERN SOUTH LODE, OLD BAL LODE,
BOSCREGAN LODE AND GUIDE LODE
0 100m
guide
South Lode
CONTOUR DIAGRAM NORTH LODE
0 100m

fig 11

and 110 m SE (to the Man Engine Shaft) between the 384 m and 533 m levels.

South Lode trends 320°, dips steeply SW above, and NE below, the 421 m level. Stoping between the 101 m and 348 m levels commences 183 m NW of Skip Shaft and continues for about 275 m on all levels. Stoping between the 384 m and 509 m levels is extensive, but there is no longitudinal section of this part of the workings. It junctions with the North Lode near New Submarine Shaft where a rich shoot of Cu ore is said to occur.

North Lode trends 320° and dips SW at 70°. It is thought to be the structural continuation of the Number 2 Branch Lode of Geevor Mine. The mineralisation is reputed to be confined to a 0.5 m wide quartz leader, containing fluorite, cassiterite and copper sulphides. McAlister (1907) records that a cinnamon coloured garnet replaced the quartz on the 366 m level. Stoping is extensive between the 275 m and 641 m levels, and at its maximum lateral extent on the 509 m level where it extends for 1464 m. Below the 509 m level the stopes are confined to an area extending 275 m SE and 180 m NW of New Submarine Shaft.

Treglown's Lode branches from the north wall of North Lode about 128 m E of New Submarine Shaft. It trends 300° and is nearly vertical. It is developed for ~ 275 m from its junction with the

North Lode, between the 505 m and 597 m levels, but there are no sections.

Prince of Wales Lode trends 305°, dips north at 65° and lies ~ 220 m N of North Lode. Recent investigations in Geevor Mine suggest that it is the continuation of the Coronation Lode. The vein on the 275 m level is 0.5 - 0.8 m wide and contains an infill of vuggy quartz, brecciated quartz and wallrock fragments, chalcocite, arsenopyrite, pyrite, sphalerite, limonite and calcite. The lode is developed for short distances on the 275 m and 311 m levels, but it is not developed again until the 553 m level, where it junctions with South Lode.

North Vein lies 146 m N of the Prince of Wales Lode. It is only developed for short distances on the 275 m and 311 m levels.

Boscregan Lode trends 330°, dips steeply NE and lies S of South Lode. Worked from Boscregan Shaft the lode is developed for 165 m NW (to the coast) and 220 m SE down to adit level (73 m). Between the adit and the 69 m level, it is developed for 59 m NW and 128 m SE of the shaft. Stoping is patchy over the developed area, about 30% of the lode being removed.

Guide Lode trends 345° and dips steeply west. The lode is developed to the 146 m level, although stoping is mainly confined to an area

90 m N and 73 m S of Guide Shaft, between the surface and the 92 m level.

Longitudinal sections of the main lodes: North Lode, South Lode, Old Bal Lode and Guide Lode are reproduced in Fig 11 . The sections indicate that:

a) economic mineralisation is mainly localised outside the granite contact.

b) the ore shoot pitches NW at $\sim 20^{o}$.

c) metal values increase near the junction of two mineralised veins e.g. near the intersection of the North and South Lodes.

d) metal values decrease NW of major guides.

b) Minor veins

All the major fissure veins described in the previous section are situated in the old part of the mine and are mainly inaccessible at the present time. Development of the three cross-cuts exposed several new fissure veins, but further development for short distances along the strike of several of the veins proved that they were of little economic value. However, a study of the composition, structure and wallrock alteration has yielded valuable information concerning the evolution of the fissure system in this area. These data will be of value when exploration is resumed in the aureole, particularly along the strike continuations of many of the Geevor lodes.

The Foot-wall Branch vein systems

Several mineralised fissures split off the south wall of the Old Bal and South Lode fissure systems. Three of these fissures, collectively known as the Foot-wall Branch veins (FWB), have been developed for short strike lengths on levels 1, 4 and 6, but the structure and composition of the veins is different on each level.

FWB vein 6 level.

The vein system on 6 level consists of a group of three, subparallel veins, trending 320° and dipping ~ 75° SW. Only the most northern vein, lying 135 m south of the Old Bal Lode, is developed. NW of the corss-cut the vein is developed for a strike length of 90 m. SE of the cross-cut the vein intersects a granite sheet and is associated with extensive replacement mineralisation. This area will be described in a later section.

The main vein in the NW drive varies between 5 - 20 cm in width and is sporadically mineralised until it intersects a N-S trending quartz-hematite cross-fracture 70 m NW of the cross-cut. Slickensides in the FWB vein infill indicate 'normal fault' movement of ~0.5 m. The walls are locally fractured and inclusions of chloritised and hematised wallrock fragments are common within the vein. The composition of the vein varies considerably

along its strike length. Quartz, fluorite, arsenopyrite, pyrite, chalcopyrite and hematite are the dominant phases, with monir cassiterite, limonite and chalcocite (plate 6).

The probable vein paragenisis is:

1	2	3
quartz	chalcopyrite	quartz
arsenopyrite	quartz	limonite-hematite
cassiterite	chlorite	chalcocite
pyrite		
fluorite		
chalcopyrite?		
chlorite		

Wallrock alteration varies according to the host rock, either (1) pelite, (2) granite or (3) amphibolite. The main alteration assemblages for these three rock types are (1) quartz-albite-tourmaline ± chlorite, montmorillonite, hematite, sericite. (2) albite-tourmaline-quartz. (3) chlorite-tourmaline-axinite-ilmenite, sphene, quartz, calcite.

FWB vein 4 level.

A group of fissures trending 305° and lying 85 m south of South Lode, is mineralised for short strike lengths, between a NE trending quartz-limonite cross-course and an unknown distance to the SE. The main vein, which is developed for a strike length of 52 m, shows a distinct structural and textural variation along its strike length.

At the entrance to the drive there is a lenticular area ~ 0.5 m x 3 m of coarse vuggy vein material, consisting of well developed, crystal intergrowths of quartz (upto 8 cm), arsenopyrite (upto 5 cm), pink K feldspar, and green chlorite, with occasional cassiterite and sphalerite. Pegmatite-like pods in this area show a concentric, mineralogical structure consisting of an outer zone of 1) green chlorite ± arsenopyrite & cassiterite. which grades inwards into zones containing 2) pink alkali feldspar ± arsenopyrite & cassiterite and 3) quartz ± pyrite, chalcopyrite and sphalerite.

The vein itself consists of a 10 - 20 cm wide fissure, containing an assemblage of quartz, orthoclase, chlorite, arsenopyrite, cassiterite and hematite, with minor pyrite, chalcopyrite and sphalerite, within brecciated pelitic wallrocks (plate 6).

The probable vein paragenisis is:

1	2	3
quartz	chlorite	quartz
alkali feldspar	hematite	pyrite
arsenopyrite	cassiterite?	chalcopyrite
cassiterite		sphalerite

The pelitic wallrocks, adjacent to the vein in the brecciated zone contain minor veinlets of alkali feldspar. Pelitic clasts in the breccia are converted to an assemblage of alkali feldspar, quartz and tourmaline.

MINERALISATION

PLATE 6

A East Spar vein, 1 level

B Unity vein, 6 level

C Early cassiterite (zoned), arsenopyrite, orthoclase vein, Wheal Cock Mine dump

D Cross-section through the Foot-wall Branch vein, 4 level, showing brecciated silicified wallrock veined by pink alkali feldspar and a vein infill of arsenopyrite, alkali feldspar, chlorite, cassiterite, quartz, hematite and minor pyrite and chalcopyrite

E Cross-section through the main Foot-wall Branch vein, 6 level, showing a marginal vein infill of pyrite, arsenopyrite, cassiterite, chlorite and fluorite and a central vein infill of milky quartz

F Cross- section through the Hen Vein, 6 level, showing a central vein infill of pyrite, chalcopyrite and hematite, an older infill of arsenopyrite, quartz and cassiterite, and a younger peripheral infill of quartz, calcite, chlorite, fluorite, chalcocite and hematite

G Polished section, Hen vein, showing the junction between early arsenopyrite and later pyrite, chalcopyrite and hematite

H Cross-section through the Foot-wall Branch vein, 1 level, showing an outer quartz vein infill, containing minor chalcopyrite and pyrite, and an inner infill of massive pyrite, chalcopyrite and chalcocite

I Polished section Foot-wall Branch vein, 1 level, showing replacement of early pyrite-chalcopyrite by chalcocite

PLATE 7

A Crowns Guide, 604 drive, showing an outer vein infill of banded and vuggy quartz and a central infill of brecciated, hematised wallrock, cemented by quartz

B Polished section, Crowns Guide (surface), showing collomorphic texture (banded limonite surrounding a flake of hematite)

C Greenstone ore, disseminated pyrite and chalcopyrite (and cassiterite) in boron metasomatised amphibolite, 601 cross-cut

D Greenstone ore, thin section, showing disseminated cassiterite in a matrix of axinite, biotite and calcite

E Quartz, sphalerite, pyrite replacement 601 cross-cut

F Greenstone ore, stockwork, quartz, arsenopyrite, cassiterite, scheelite, fluorite and pyrite, Wheal Cock Mine dumps

G Quartz, pyrite, chalcopyrite, cassiterite replacement, 401 cross-cut

MINERALISATION

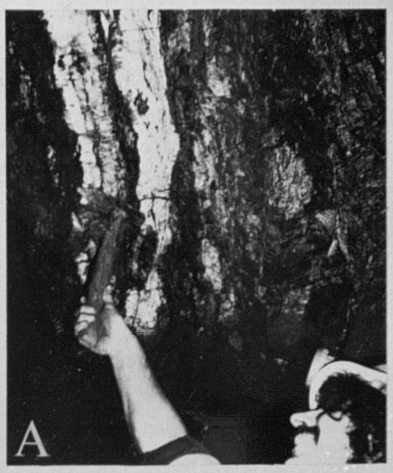

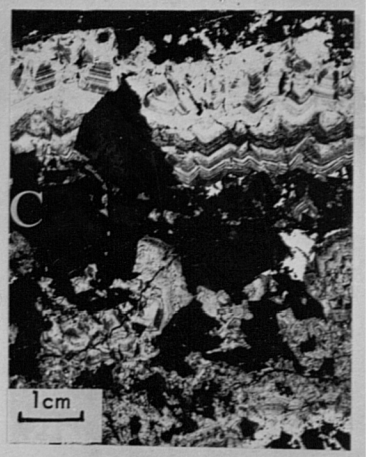

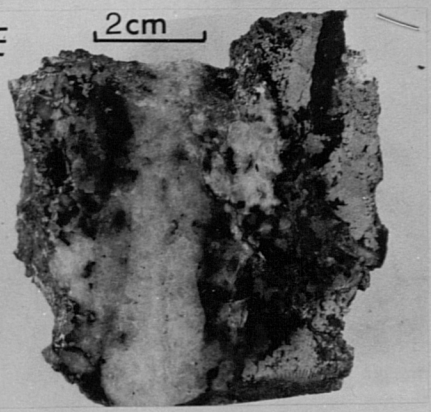

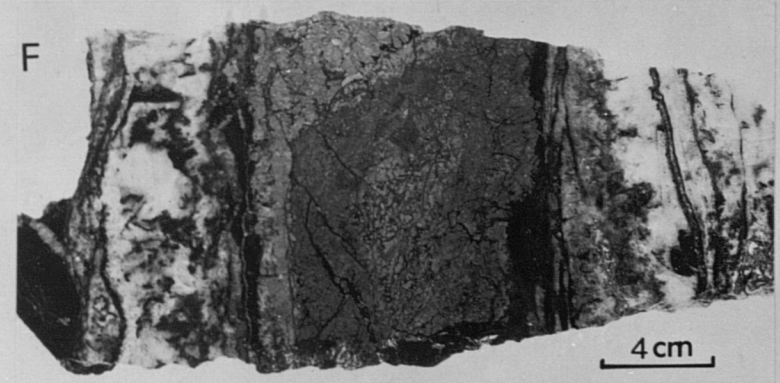

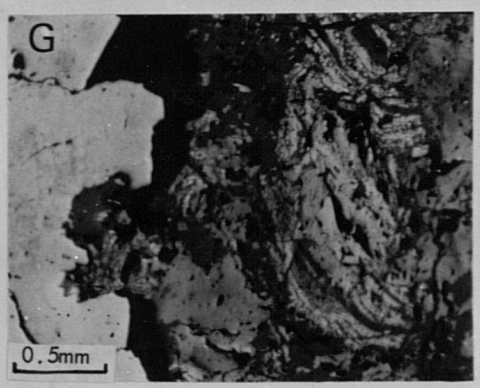

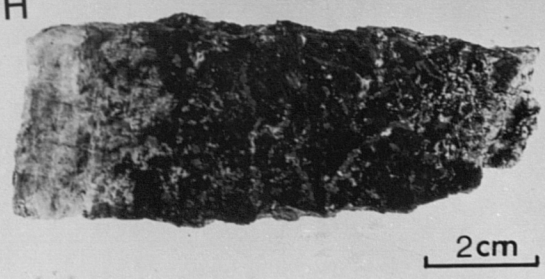

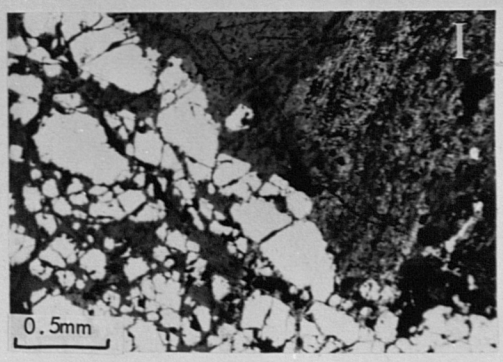

PLATE 6

MINERALISATION

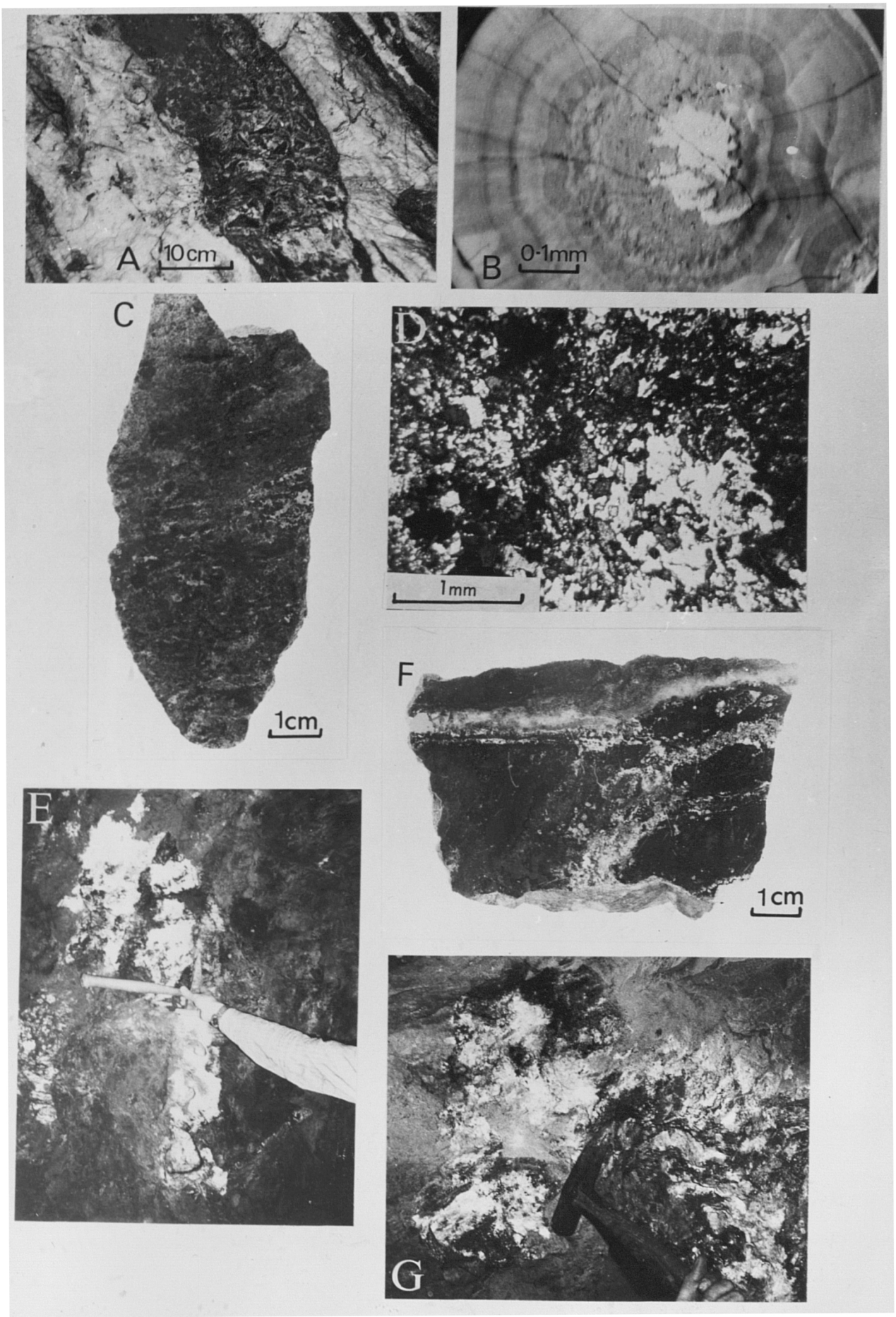

PLATE 7

The vein diminishes in size and mineral content NW of the cross-cut, until the structure is completely masked in the crush zone adjacent to the N-S trending, quartz-limonite cross-course.

FWB vein 1 level.

A fissure vein, trending 300°, dipping 75° SW and lying 30 m SW of the Old Bal Lode, is developed NW of the cross-cut for a distance of 127 m. The vein varies between 10 - 30 cm in width and contains an assemblage of quartz, chlorite, chalcopyrite, pyrite, cassiterite, arsenopyrite, chalcocite, hematite, limonite and kaolinite.

The probable paragenetic sequence is:

1	2	3	4
quartz	pyrite	quartz	botallackite
arsenopyrite	chalcopyrite	hematite-limonite	paratacamite
cassiterite		chalcocite	cuprite
chalcopyrite			
pyrite			

The most notable feature about this vein is the replacement of an early pyrite-chalcopyrite assemblage by chalcocite (plate 6).

The Moon vein fracture system.

The Moon vein fracture system is visible on all three levels and is probably the down-dip continuation of the Boscregan Lode, which was developed in the old part of the mine to a depth of

72 m. At surface the Boscregan Lode is 1.5 m wide and contains an infill of sheared quartz, hematite and limonite, with minor pyrite and chalcopyrite. The metabasite walls are chloritised and hematised. Subvertical slickensides in the vein and walls indicate normal fault movement.

On 1 level the Moon vein is 1.5 m wide, trends 320° and dips south at 65°. It consists of a fractured zone containing a vein infill of brecciated and sheared quartz, hematite and limonite.

On 4 level the Moon vein structure has been utilized for cross-cutting and is developed in the old workings for a strike length of at least 60 m. The structure is ~ 1 m wide, trends 330° and dips 70° S. The vein infill consists of banded quartz, hematite and limonite.

On 6 level the Moon vein structure is not so clearly defined and appears to have splayed into several fractures (although the exposure is confused by the intersection of the East Spar and Moon vein fracture systems). The fracture zone occupies a strike normal distance of ~ 5 m and contains several minor quartz-hematite-limonite veins.

The Spar vein complex.

Several minor quartz veins, which could be the surface expressions of the Spar vein system, outcrop around Carn Du.

On 1 level the two fracture systems which form the Spar vein complex intersect ~ 225 m SW of the Old Bal Lode. East Spar, trends 330° and dips 80° NE. It consists of a 1 m wide, banded and sheared quartz-hematite-limonite vein with included pelitic wallrock fragments. West Spar, trending 325° and dipping 70° SW is also 1 m wide and is structurally and compositionally similar to the East Spar vein. The junction zone, which is ~ 10 m SE of the cross-cut, is ~ 8 m wide and consists of several interlaced quartz-hematite-limonite veins. Both veins contain sporadic, pyrite and chalcopyrite. The pelitic wallrocks are chloritised and hematised.

On 4 level East Spar vein is not developed. It consists of a 0.8 m wide zone of sheared quartz, hematite and limonite, trending 325° and dipping 70° NE. West Spar vein is developed for 90 m NW and 50 m SE of the cross-cut. It consists of a fractured zone containing several quartz-hematite veins, trending 350° and dipping 75° SW. Most of the vein is barren but a 10 cm wide vein NW of the cross-cut contains disseminated pyrite, chalcopyrite, arsenopyrite and cassiterite. The fracture system becomes splayed in the NW of the drive and extensive wallrock alteration has caused the roof of the drive to collapse. The dominant alteration assemblage is montmorillonite, chlorite, quartz and limonite.

On 6 level the East Spar vein intersects

the Moon vein fracture system 200 m SW of the Old Bal Lode. The vein is 0.5 m wide, trends 320°, dips 75° NE and contains an infill of quartz and limonite.

West Spar junctions with the Cockel vein (?) 270 m SW of the Old Bal Lode. This fracture system was misidentified as the Unity fissure system, but it is probably a combination of the Cockle, West Spar and Unity vein systems. Although the compound fracture system was developed for ~390 m NW of the cross-cut, there is no evidence of extensive mineralisation in any part of it. Individual fissures contain banded, crustified and brecciated quartz, hematite and limonite veins, with rare pyrite and chalcopyrite. Only very minor tin values were recovered from the vein system. Chlorite and limonite are the dominant wallrock alteration phases.

The Cockle vein.

This vein outcrops in the cliffs 85 m south of the Unity Shaft, where it consists of a 0.5 m wide infill of crustified and brecciated quartz, hematite and limonite, with minor chalcopyrite and pyrite. It trends 335° and dips 60° N.

The vein is not exposed on 1 level, although it was probably intersected in the UL 18 diamond drill hole, ~ 25 m SW of the Unity Lode.

On 4 level the Cockel vein (misidentified as the Unity vein) trends 325° and dips 70° N. The

vein is 0.5 m wide and contains a crustified and brecciated infill of quartz, hematite and limonite.

On 6 level the cockle vein junctions with the West Spar vein in the cross-cut.

The Unity vein system.

At outcrop the Unity vein trends 330° and dips steeply north. The fissure contains a 0.3 m wide, crustified quartz, hematite-limonite, chlorite infill, with sporadic pyrite and chalcopyrite. The Unity Lode was worked in the later half of the last century when it was stoped to a depth of 110 m.

On 1 level the lode trends 335° and dips 80° N. The vein is 0.3 m wide and consists of crustified and brecciated quartz, hematite and limonite, with included wallrock fragments. Mineralisation is sporadic but appears to have occurred in two distinct phases. The first phase consisted of cassiterite impregnations and veinlets in brecciated wallrock. The cassiterite occurs in two generations, early dumpy tetragonal crystals (upto 5 mm in size) and later acicular needles growing on the earlier crystals. The second phase of mineralisation was confined to the vein and consists of quartz, hematite-limonite and chalcocite.

It is probable that the Unity fissure system is either merged with the Cockle vein system below 1 level or that it has been displaced to the SW by

the Cockle vein fracture system. Although drives on 4 and 6 levels have been named after the Unity fracture system, it seems probable that these drives are on several different fissure veins.

The Hen vein.

This vein is exposed near the end of 601 cross-cut. It is developed for a strike length of 30 m NW and 42 m SE of the cross-cut. The vein is 0.2 m wide, trends 340° and dips 80°S. It is thought to be the down-dip continuation of the Hen Lode which is developed in the Wheal Cock Mine. Mineralisation consists of early quartz, arsenopyrite and cassiterite, followed by pyrite and chalcopyrite and, finally, by pyrite, sphalerite, chalcopyrite, chalcocite, hematite, limonite, calcite, chlorite and quartz (plate 6).

The sphalerite veins.

Two unnamed quartz, calcite, sphalerite, pyrite veins, trending 350° and 030° and dipping 60° NE and NW respectively, intersect 601 cross-cut between 290 - 300 m south west of the Old Bal Lode.

Cross-fractures.

In addition to the NW trending mineralised fissure veins, there are numerous barren cross-veins. These veins are either minor quartz or calcite

stringers, localised in master joints, or major quartz, calcite, hematite, jasper, limonite veins, localised in normal, reverse and oblique-slip faults. The veins are characterised by vuggy, crustification, breccia and cockade structures. Incremental growth zoning in quartz and collomorphic texture (plate 7) are also common.

The main cross-fractures occur:

a) On 4 level, 450 m NW of Skip Shaft on South Lode. The cross-fracture trends 040° and dips 75° SE. The same structure intersects the Unity drive on 6 level 290 m NW of the cross-cut.
b) In 401 cross-cut, 150 m SW of South Lode. The structure trends 020° and dips 70° NW.
c) In 604 drive, 915 m SW of the Old Bal Lode. The structure trends 280° and dips 55° N.

Numerous smaller cross-fractures occur throughout the mine.

c) Distribution of vein mineralisation

The formation of metal bearing veins was dependent on two factors:

1) The availability of suitably oriented fractures which acted as open channelways to allow the movement of metal bearing fluids and offer potential sites for metal deposition.
2) The availability of metal bearing fluids.

The well developed joint systems in and around the perphery of the pluton offered a potential for the development of open channels during later periods of stress. During mineralisation the stress distribution was such as to cause the preferential tectonic reactivation of the NW trending joint systems in the aureole. However, although the distribution of major fractures is fairly uniform throughout the project area, vein cassiterite and cassiterite-sulphide mineralisation is confined to two zones, in the extreme north west (North, South, Old Bal and Foot-wall Branch veins) and in the south west (the vein systems of Wheal Cock and Botallack Mine). This suggests that the movement of metal bearing fluids was not uniform throughout the area, but was mainly confined to two narrow linear belts. Both these belts are fed by major steep dipping fractures which extend for considerable distances into the pluton and, presumably, tapped a metal bearing fluid reservoir.

d) Wallrock alteration

Metabasites - four traverses were made in the hydrothermally altered basaltic amphibolite wallrocks, adjacent to four different fissure veins. The main textural change, as the vein is approached, is the obliteration of coarse, compositional banding and the formation of an uneven grained, structureless

fabric. The visible alteration envelope is usually between 10 - 30 cm wide, although the envelope surrounding the quartz-hematite vein in 604 drive is over 5 m wide.

The main mineralogical changes produced during hydrothermal alteration are the conversion of the amphibole and plagioclase in the amphibolite to an assemblage of either a) chlorite, hematite ± sulphides, quartz, epidote, montmorillonite, ilmenite, sphene, apatite, tourmaline and calcite (traverse 2, 3 & 4) or b) biotite, hematite, chlorite ± orthoclase, quartz and sphene.

The wt. % chemical variations in the four traverses are illustrated in figure 12 . Major component and trace element distributions are extremely variable but, in general, the following conclusions, regarding their distributions, can be made. SiO_2, Al_2O_3, TiO_2, CaO, Na_2O and K_2O are depleted from the wallrock, immediately adjacent to the vein, and total Fe oxides (Fe_2O_3 and sometimes FeO), K_2O, P_2O_5, MnO, Sn, Cu, As and Zn are enriched. MgO shows no definite trend and K_2O may be depleted or enriched. Compared to the relatively unaltered amphibolite, outside the visible alteration envelope, the hydrothermally altered rocks have lost Si, Ca, Na and K and gained Fe, K, P, Mn, Sn, Cu, As and Zn.

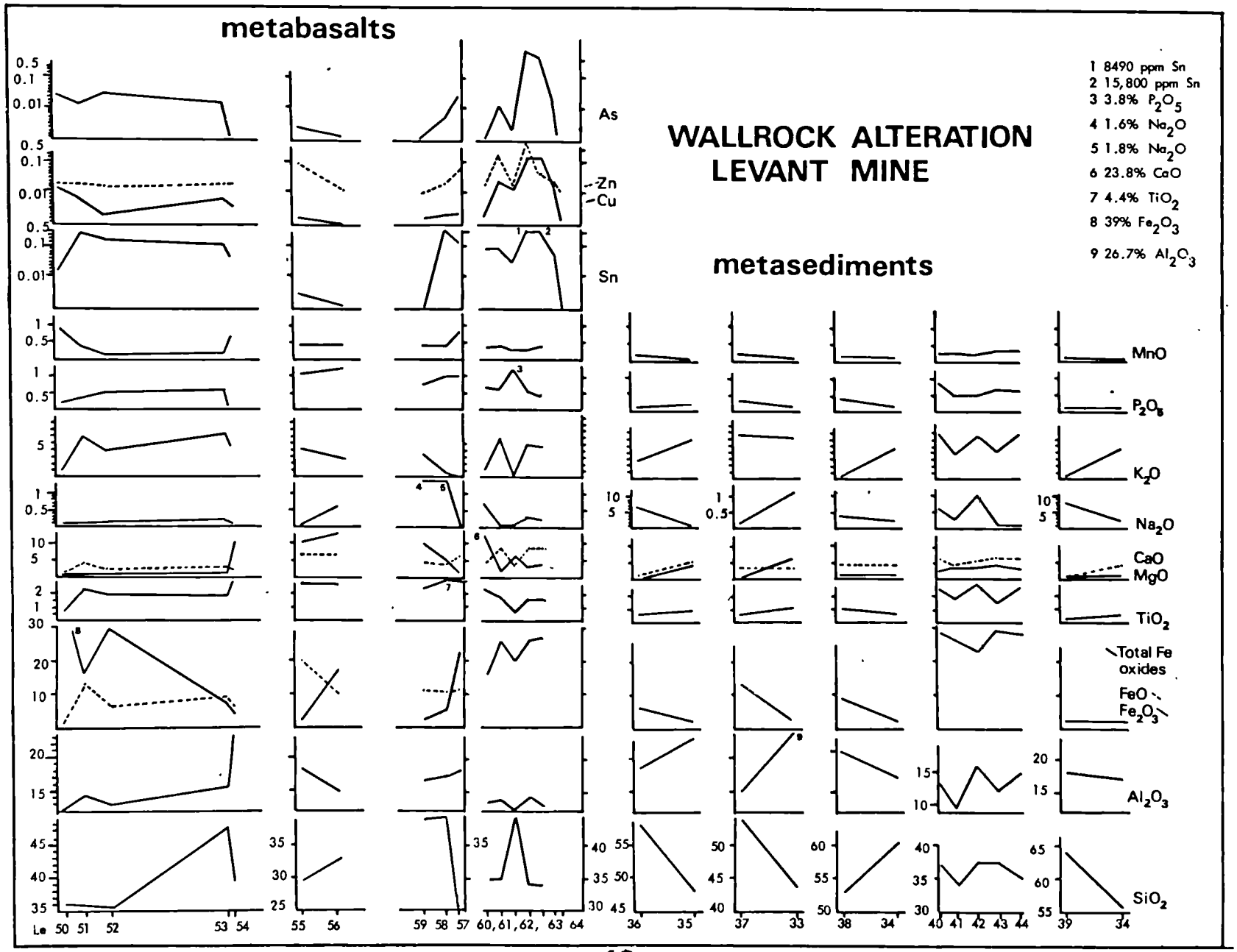
metabasalts
metasediments
WALLROCK ALTERATION
LEVANT MINE
1 8490 ppm Sn
2 15,800 ppm Sn
3 3.8% P_2O_5
4 1.6% Na_2O
5 1.8% Na_2O
6 23.8% CaO
7 4.4% TiO_2
8 39% Fe_2O_3
9 26.7% Al_2O_3
As
Zn
Cu
Sn
MnO
P_2O_5
K_2O
Na_2O
CaO
MgO
TiO_2
Total Fe oxides
FeO
Fe_2O_3
Al_2O_3
SiO_2
Le 50 51 52 53 54
55 56
59 58 57 60,61,62, 63 64
36 35
37 33
38 34
40 41 42 43 44
39 34

Fig12

Pelites - the main textural change during the hydrothermal alteration of pelites is the obliteration of sedimentary laminae and the formation of an equigranular structureless fabric. The visible alteration envelope is usually between 10 - 30 cm wide, although envelopes of upto 1 m in width are developed adjacent to some of the larger fissure veins.

The main mineralogical changes produced during hydrothermal alteration are the conversion of the original quartz-muscovite-biotite (brown) assemblage to an assemblage of either a) albite-quartz-tourmaline b) quartz-albite-orthoclase c) chlorite ± orthoclase or biotite d) quartz-montmorillonite-chlorite-tourmaline e) chlorite-biotite (green) f) chlorite-hematite g) quartz tourmaline or h) quartz-sericite.

Comparisons of the major chemical components of hydrothermally altered and unaltered pelites are illustrated in figure 12 . The main chemical changes (on a wt. % comparison) of the main alteration assemblages are as follows:

a) albite-quartz-tourmaline - TiO_2, CaO, K_2O decrease, SiO_2, Al_2O_3, Na_2O increase and MnO, P_2O_5, MgO and total Fe oxides show little variation.

b) quartz-albite-orthoclase - Al_2O_3, TiO_2, CaO, MgO, K_2O, P_2O_5 decrease and SiO_2 total Fe oxides, Na_2O and MnO increase.

c) chlorite-orthoclase - Al_2O_3, TiO_2, CaO, Na_2O decrease, SiO_2, total iron oxides, K_2O, P_2O_5, MnO increase and MgO shows little variation.

d) quartz-montmorillonite-chlorite-tourmaline - SiO_2, K_2O decrease, Al_2O_3, total Fe oxides, TiO_2, Na_2O, P_2O_5, MnO increase and MgO and CaO show little variation.

e) chlorite-biotite. Compared to the unaltered pelites, the hydrothermally altered pelites are depleted in SiO_2, Al_2O_3 and Na_2O and enriched in FeO, K_2O, TiO_2, MgO, CaO, MnO and P_2O_5.

In general, the altered pelites have lost Si, Al, Ti, Ca, Mg, K, Mn and P, and gained Fe, Mg, Na (sometimes K and Al).

Although only a limited number of hydrothermally altered samples were subjected to mineralogical and chemical analysis, these data, together with the field investigations, suggest that hydrothermal alteration at Levant Mine has produced chlorite, biotite and hematite rich assemblages in the metabasites, and quartz, chlorite, biotite, alkali feldspar, tourmaline, montmorillonite and sericite rich assemblages in the pelites.

Other studies of the hydrothermal alteration of pelites at Wheal Jane and Mount Wellington Mines (Cotton, 1973 and Rayment et. al. 1971), suggest that sericitisation, involving a depletion of Fe, Mn, Mg and Li and enrichment in K, Ba and Rb, is the

dominant type of alteration. Sericitisation does not appear to be developed to the same extent at Levant Mine, although this does not preclude the possibility that sericitisation is developed along the strike continuations of the Levant fissure veins.

e) The fluid inclusion study

The object of this study was to attempt to characterise the hydrothermal fluids responsible for the various stages of ore-mineral deposition. Several samples were carefully selected, primarily for their paragenetic significance. The five general stages of ore deposition and the samples selected to represent them are outlined below:

1. quartz- K feldspar-arsenopyrite ± cassiterite (samples C1, C2 & L1).
2. cassiterite without sulphides (sample 5a).
3. cassiterite with sulphides (samples L3 & carbona samples).
4. sulphides (samples L2 & L4).
5. hypogene sulphide alteration (sample L5b)

A description of the samples studied, their location and fluid inclusion characteristics are presented in table 7 .

Types of inclusions

In any single sample there is usually a variety of morphological, compositional and genetic

(P, PS and S) types of inclusion. Some of the main types of inclusion are reproduced in plate 10. (Although these inclusions are from samples collected in Geevor Mine, they are very similar to those found in Levant Mine.) The main types of inclusion in quartz, fluorite and cassiterite are as follows:

1. Well shaped, or irregular shaped, 2 phase (L + V) inclusions, with a variable sized gas bubble (~10 - 60% vol.), occurring in random, non-planar groups (P and PS), in planar groups parallel to primary growth zones (P) and in cross-cutting planar arrays (PS and S). They usually constitute the dominant proportion of the inclusion population in any sample.
2. Well shaped, or irregularly shaped, 3 phase (L + V + S) inclusions, containing either 1 or 2 colourless, isotropic phases and/or 1 or 2 prismatic or irregularly shaped, birefringent solids. The two cubic phases are halite and sylvite(?) but the birefringent phases were not identified (possibly sulphates?). The other solid phases observed were: a small, non-magnetitic, opaque phase, a mass of birefringent fibres and a hexagonal plate-like phase (mica or clay mineral?). This type of inclusion is particularly common in fluorite formed during the cassiterite-sulphide stage of mineralisation.
3. Rare monophase (V) inclusions occurring in

TABLE 7

Fluid inclusion samples, location, paragenesis and inclusion characteristics

Sample	Location	Paragenisis	Type of inclusion	Probable P,PS or S	Total T_h range	Salinity eq.wt.% NaCl	Probable ore-stage
C1	Wheal Cock	qtz-scheelite ars-flu	L + V	P, PS	400-430	-	pre-cass?
	Mine Dumps		L + V	S	260-330	-	sulphides?
C2	Wheal Cock	qtz-K feld-cass	L + V	P, PS	370-420	-	early K feld-ars ± cass
	Mine Dumps		L + V	S	290-340	-	sulphides?
			LEVANT MINE				
L1	Foot-wall Branch vein,	qtz-K feld-ars-cass	L + V	P, PS	350-380	-	early K feld-ars ± cass
	Level 4		L + V	S	220-270	-	sulphides
L2	small stringer near Old Bal Lode, Level 6	flu-K feld-cass-ars-cp	L + V	P, PS	340-360	17-19	post cass
			L + V + S	S	230-280	14-15 & 30-32	sulphides
			L	S	70		?
L3	Hen Lode	qtz-py.cp. ar. sphal	L + V	P, PS	350-390	-	?
	Level 6		L + V + S	S	270-340	-	cass+ sulphides?
			L + V	S	210-230	-	
			L	S	70	-	sulphides
L4	Vein	qtz-sphal-py.	L + V	P, PS	280-320	-	
	Level 6		L + V	S	140-190	-	sphal-py
L5	Unity Lode	qtz-cass-chalc-hem	L + V	P, PS	330-360	-	cass
	Level 1		L + V	S	180-250	-	chalcocite?
			L + V	S	100-150	-	?
			L	S	70	1 - 1.5%	

CB1 For details of the Carbona fluid inclusion samples see page

qtz mineral studied

cross-cutting planar arrays (S).

4. Well shaped, or irregularly shaped, monophase (L) inclusions, occurring in cross-cutting planar arrays and forming upto 10% of the total inclusion population.

Discussion of results

The results of thermometric and salinity studies of selected ore-gangue mineral associations are presented in figure 16b & 35 . As might be expected, individual samples of vein material showed evidence of repeated penetration by fluids with different temperatures and salinity characteristics. These variations however, are not continuous (i.e. secondary inclusion populations displaying continuously changing temperature and salinity values), instead, the total inclusion population, displays three or four, well defined, T_h and salinity ranges. Similar population characteristics not only occurred in adjacent samples, but were found to occur in samples from different veins in widely separated parts of the mine.

This observation suggests that at least parts of the Levant-Cock fissure system, were subjected to periodic pulses of hydrothermal fluid of fairly restricted composition (temperature & salinity) rather than there being a continuous spectrum of hydrothermal activity in any single fissure.

The thermometric results indicate that the fissure system was utilised by fluids, which had a total homogenisation temperature range of between $<70^{o}C$ - $430^{o}C$, with most of the mineralisation occurring in the T_h range $200-400^{o}C$. This latter T_h range, can be subdivided into an upper (T_h $300-400^{o}C$) range, when most of the cassiterite was deposited, and a lower (T_h $200-300^{o}C$) range, when most of the sulphides were deposited. The T_h range $280-320^{o}C$ appears to be characterised by simultaneous cassiterite and sulphide deposition.

The salinity data (tables 7 & 10), must be interpreted with great care, as it was often impossible to measure the same inclusions as were utilised in the heating stage experiments. For this reason only very tentative conclusions regarding the changes in fluid salinity, will be attempted.

No salinity data were obtained for the cassiterite stage of deposition, but P & PS inclusions in fluorite, post-dating cassiterite and pre-dating sulphides yielded salinities in the range 17 - 19 eq. wt. % NaCl. P & PS inclusions in quartz and fluorite intergrown with sulphides, yielded salinities in the range 14 - 32 eq. wt. % NaCl. The sulphide without cassiterite stage of mineralisation is characterised by lower salinity fluids in the range 2 - 10 eq. wt. % NaCl. The lowest temperature fluids in the system ($<70^{o}C$), are predominantly of low salinity, 1 - 7 eq. wt. % NaCl.

Conclusions

1. The highest temperature fluid inclusions homogenised in the T_h range 400 - 430°C (Wheal Cock Mine) and 350 - 390°C (Levant Mine). These fluids deposited quartz-K-feldspar-arsenopyrite-cassiterite and scheelite. No salinity data were obtained for these fluids.
2. Quartz, coeval with K-feldspar, arsenopyrite and cassiterite (L1) was formed in the T_h range 350 - 380°C. Fluorite, post-K-feldspar and cassiterite (L2) was formed in the T_h range 340 - 360°C, from moderately saline fluids (17 - 19 eq. wt. % NaCl).
3. Cassiterite, without sulphides (Unity Lode 1 level), was formed in the T_h range 330 - 360°C.
4. Fluorite, coeval with sulphide, chalcopyrite, pyrite and arsenopyrite, and cassiterite (CB2), was formed in the T_h range 280 - 320°C, from fluids of variable salinity (16 - 30 eq. wt.% NaCl).
5. Planes of secondary inclusions, thought to be coeval with sulphide (pyrite, chalcopyrite) deposition, homogenised in the T_h range 220 - 270°C (L1) and 230 - 280°C (L2). These later fluids were of variable salinity (14.5 - 32 eq.wt.% NaCl). Quartz, coeval with minor chalcopyrite and pyrite (CB 8), was formed in the T_h range 200 - 260°C, from fluids of low salinity (5 - 7 eq. wt. % NaCl).

6. Planes of secondary inclusions, associated with altered sulphides (L5), yielded homogenisation temperatures in the range 180 - 250°C.
7. Fluid inclusions, formed in the T_h range 110 - 170°C, were of variable salinity.
8. Low temperature (<70°C) fluid inclusions were of low salinity (<10 eq. wt. % NaCl).

G2 REPLACEMENT MINERALISATION

In addition to the fissure vein mineralisation, replacement mineralisation is extensively developed throughout the mine. This section is divided into two parts: The first part describes an unusual replacement cassiterite-sulphide ore-body within a granite sheet and the second part describes a variety of mineralisation phenomenon (including replacement mineralisation) which are confined to metabasite and pelitic horizons and are known locally as 'greenstone ore'.

G3 THE CARBONA

a) Introduction

During the exploration programme a mineralised granite sheet was intersected on the 601 cross-cut, approximately 120 m SW of Skip shaft. Further development and a subsequent diamond drill programme revealed that the mineralisation was extensive and locally intensive, but extremely irregular in distribution and value. The mineralisation is characterised by disseminated and massive cassiterite-arsenopyrite-chalcopyrite-pyrite replacement and fissure veins, associated with intense hydrothermal wallrock alteration. The ore-body is localised within, and adjacent to, a granite sheet complex, near its junction with the mineralised Foot-wall Branch vein system.

b) The granite

The granite sheet is between ~5-8 m wide and dips south-east at ~20° (fig 13). It is intruded into a sequence of fine-grained dark pelites (quartz-biotite-muscovite), which have been metamorphosed to equigranular biotite rich hornfelses. A spotted rock, possibly of basic volcanic parentage also occurs in the vicinity of the sheet. This horizon has been converted to a hornfels containing quartz, plagioclase, sphene, tourmaline, cassiterite, sulphides and chlorite. The granite sheet is almost coincident with the local bedding foliation, although local discordancy, as a result of surface irregularities and variations in the dip of the sheet, is common. Contacts are sharp and generally finer-grained than the interior. The sheet also displays internal banding, a feature typical of many of the sheets in the contact zone. The banding is defined by alternating bands of quartz and alkali feldspar, alkali feldspar and tourmaline rich horizons on a centimetre scale.

The granite is a white, moderately coarse (0.5 cm), aphyric, leucocratic rock composed of microperthitic orthoclase, with well-developed patch and band exsolutions, primary quartz, with undulose extinction and sutured grain boundaries, plagioclase An_{10-15}, which is sericitised, biotite and muscovite. Accessory minerals include apatite, fluorite, tourmaline and opaque ores. The average modal %

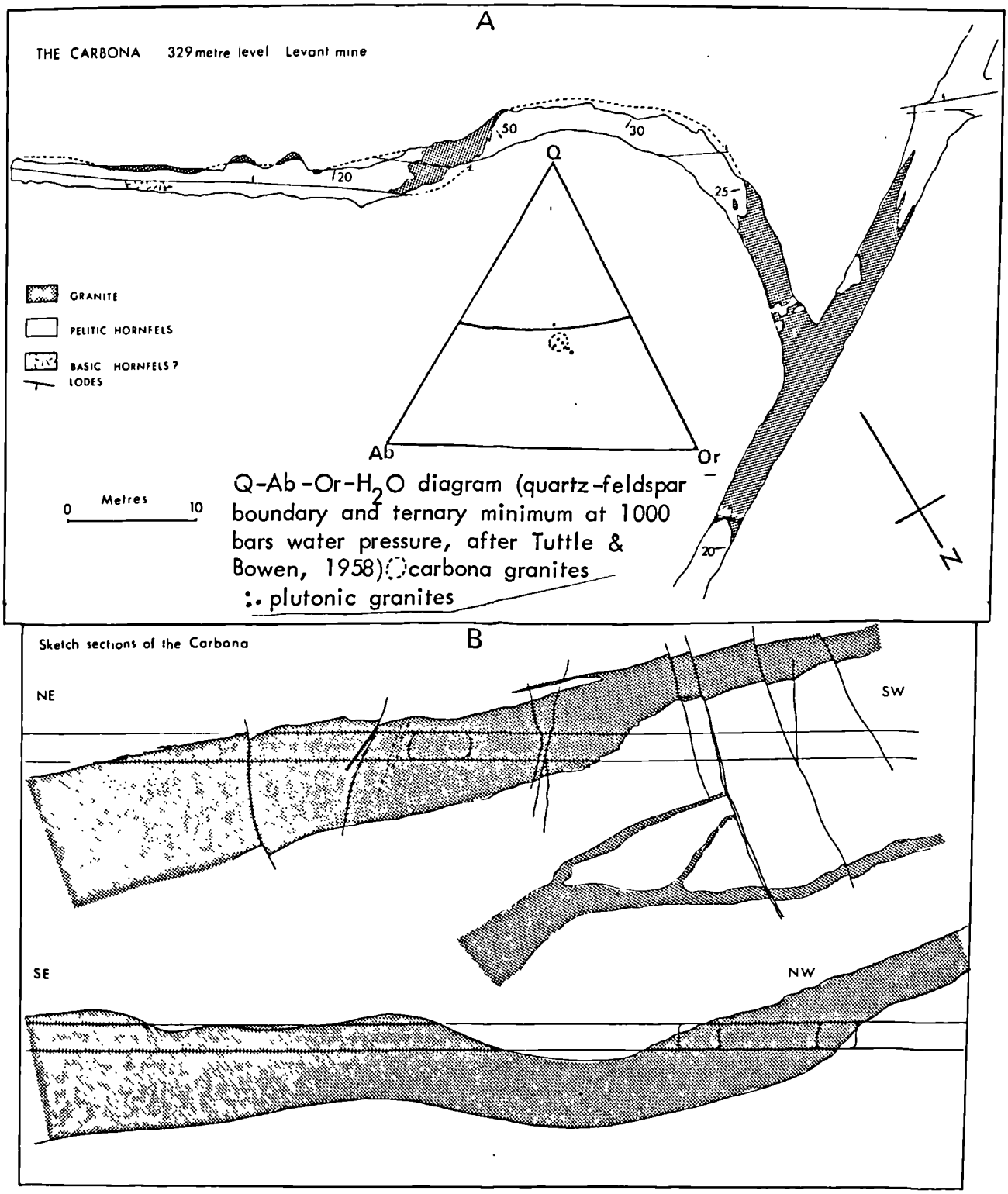
A
THE CARBONA 329 metre level Levant mine
50
30
20
25
GRANITE
PELITIC HORNFELS
BASIC HORNFELS ?
LODES
Q
Ab
Or
Metres
0
10
20
N
Q-Ab-Or-H2O diagram (quartz-feldspar boundary and ternary minimum at 1000 bars water pressure, after Tuttle & Bowen, 1958) ○ carbona granites
∴ plutonic granites
B
Sketch sections of the Carbona
NE
SW
SE
NW

Fig 13

of six unaltered granites is quartz 35.5, orthoclase (microperthite) 32.5, plagioclase 27.0, muscovite 2.0, biotite 2.5, tourmaline 0.5. With reference to the system Q-Or-Ab-H_2O, figure 13 (Tuttle and Bowen, 1958), the unaltered granites plot close to the ternary minimum for a water pressure of 1 Kb. The granite is enriched in B, Li, Rb, F, Sn, Cu and As, and depleted in Ba, Sr and Zr, compared to a published average for low-calcium granites (Turekian and Wedepohl, 1961). These geochemical features suggest that the sheet was derived from a well fractionated magmatic source.

c) The traverse

The cross-cut intersection of the granite shows that the unaltered leucogranite in the north-east passes south westwards into a mineralised and hydrothermally altered zone. A sample traverse along the cross-cut revealed the nature of the mineralogical and chemical changes involved in this transition.

The main mineralogical changes are displayed graphically in figure 15b. All the major changes appear to occur abruptly, approximately 10 m north-east of the south contact, although there is no apparent structural feature controlling this boundary. Macroscopically the recrystalised altered granite is pink or white in colour and rapidly decomposes on exposure.

The most obvious mineralogical change in the mineralised zone is the inverse relationship of quartz and orthoclase with albite. Modal analysis figure 15 indicates that the secondary production of albite has occurred mainly at the expense of quartz and orthoclase. The other mineralogical changes are:

1. The sericitisation of orthoclase and plagioclase, particularly in the outer alteration envelope.
2. The development of secondary, unstrained quartz, in both the outer and inner alteration zones.
3. The chloritisation of biotite and muscovite, in the outer envelope.
4. The chloritisation of albite, in the inner alteration zone.
5. The development of fluorite and secondary tourmaline, in the inner alteration zone.
6. The late formation of kaolinite in the inner alteration zone.

The variation in the main chemical components in the traverse, are displayed graphically in figure 15a. The main wt. % chemical changes, compared to the unaltered granite, are as follows:

1. Components which decrease in the inner alteration zone: SiO_2, K_2O, Rb and Ba.
2. Components which increase in the inner alteration zone: Na_2O, MgO, total Fe, Al_2O_3, MnO, TiO_2, H_2O, B, S, F, Sn, Cu, As, Pb, Zn, Be and Sr.

PLATE 8, THE CARBONA

A Unaltered granite, quartz, perthitic orthoclase, oligoclase, muscovite and tourmaline

B Sericitised granite, outer alteration zone(both feldspars seicitised)

C Partial replacement of orthoclase by albite

D Complete replacement of original granite assemblage by albite

E Disseminated pyrite-chalcopyrite rimmed by chlorite in albitised granite

F Disseminated arsenopyrite in tourmalinised and albitised granite

G Disseminated cassiterite in albitised granite

H Disseminated pyrite-chalcopyrite in albitised granite (reflected light)

I Massive pyrite-chalcopyrite-arsenopyrite replacing tourmaline

A, B, C, D, E, F- photographed in transmitted light

PLATE 8

d) Hydrothermal alteration

The data obtained from the cross-cut traverse together with other samples from within the ore-body revealed the general alteration pattern displayed in fig 14b . The mineralised zone is characterised by a 10-15 m wide, NW trending belt of intense alteration, dominated by semi-pervasive albitisation with associated tourmalinisation, chloritisation, fluoritisation and local silicification, hematisation and orthoclasation. Within this zone, fissure controlled alteration, in the form of tourmalinisation, chloritisation and silicification, is well developed. Although these assemblages are mainly confined to the granite, they also occur in pelites, within the mineralised zone. The outer envelope is characterised by weak silicification and sericitisation.

The observed macroscopic and microscopic alteration pattern appears to have been produced by one main phase of pervasive alteration followed by several phases of vein controlled alteration. Three phases of hypogene alteration can be distinguished:

1. The main phase of pervasive alteration is characterised by albite, tourmaline, fluorite (colourless and green) and minor quartz.
2. The main phase of mineralisation is characterised by vein controlled alteration assemblages containing tourmaline, quartz, fluorite (green), chlorite, albite, orthoclase and rare

dumortierite. Quartz, epidote sericite and calcite are alteration products typical of the end of this stage of mineralisation.

3. Later, less intense, hydrothermal activity produced minor quartz veining, caused the local oxidation of sulphides and, locally, partially converted albite to montmorillonite and kaolinite. This alteration is mainly confined to the wallrocks of late fissure veins, although the kaolinite may be the product of more pervasive 'low temperature' hydrothermal alteration. Partial analysis (by microprobe microanalyser) of primary oligoclase and secondary albite are presented in table 8 . The albites contain between 97.4 - 98.8 mol. % Ab, 0.6 - 0.7 mol. % An and 0.6 - 1.9 mol. % Or, whereas the primary plagioclase crystals contain between 73.7 - 91.5 mol. % Ab, 6.7 - 21.2 mol. % An and 1.6 - 5.1 mol. % Or.

e) Chemical changes during alteration

Rock analyses of the unaltered and altered granites are presented in table 8 . The main chemical changes on a wt. % comparison have already been described. However, there are other methods of portraying and quantifying the bulk chemical changes of the altered rocks.

The AKF-ANF, molecular proportion triangular variation diagrams contain most of the main chemical components of the granite system. Plots of

rock analyses on these diagrams (fig 14c) graphically indicate the main chemical changes which have taken place within the system. The two obvious trends are K depletion and F component enrichment. Unfortunately, the Na enrichment is masked by the relatively greater F component enrichment.

Further information concerning the nature of the chemical changes involved during alteration can be obtained by comparing the gram equivalents of elements in altered and unaltered rock. The gram equivalent of an element is the weight in grams which combines with or displaces 8 grams of oxygen, 1 gram of hydrogen or its equivalent. If a constant total volume is assumed these results can be modified by multiplying the wt. % by the density of the rock.

A comparison of the gram equivalents for the main components in altered and unaltered granite/ 1000 cc rock (table 8) indicates that there is an overall net loss of material in the altered zone. The consistently largest losses are shown by Si (-29.6 to -17.2 gm. equivs.). There are also compensatory gains in Al (+2.69 to + 10.12 gm equivs.), Fe (+1.84 to 6.28 gm. equivs.) and H (+0.49 to +5.33 gm. equivs.), and a net gain (+0.75 to 2.84 gm. equivs) in bases (Ca+Mg+Na+K). K is consistently lost.

The apparently large overall net loss to the system could be counter balanced by material not accounted for in these crude calculations, such as B, S, F, Sn, Cu and As, which form considerable wt. %

TABLE 8 THE CARBONA

	CB 1	2	3	103	105	107	109	111	114	116	118	119	120	123	125	128	34	35	36	37
SiO_2	74.00	76.11	74.17	75.62	76.14	75.16	74.60	76.15	74.19	74.77	57.88	56.91	57.67	61.81	64.26	62.38	59.91	63.95	63.60	60.10
TiO_2	0.01	0.02	0.01	0.01	0.01	0.01	0.02	0.01	0.01	0.01	0.09	0.12	0.18	0.09	0.07	0.08	0.13	0.00	0.00	0.02
Al_2O_3	13.48	13.00	13.35	12.89	12.77	13.22	13.20	12.69	13.53	13.25	14.13	15.98	15.66	17.20	17.20	19.18	17.91	17.90	16.88	19.06
Fe_2O_3	0.05	0.04	0.05	0.07	0.10	0.12	0.14	0.16	0.12	0.18	Total iron oxides as FeO						4.15	0.58	2.59	2.43
FeO	0.80	0.99	0.85	0.95	0.70	0.47	0.42	0.70	0.76	0.94	5.55	8.36	7.96	4.42	2.47	3.14	3.41	2.01	1.81	2.00
MnO	0.01	0.02	0.01	0.01	0.01	0.01	0.01	0.01	0.01	0.01	0.09	0.12	0.18	0.09	0.07	0.08	0.04	0.06	0.09	0.11
MgO	0.12	0.17	0.09	0.09	0.06	0.14	0.11	0.11	0.12	0.12	0.61	0.67	0.72	0.61	0.55	0.56	0.38	0.27	0.74	0.69
CaO	0.54	0.39	0.54	0.58	0.56	0.54	0.56	0.79	0.28	0.50	0.74	0.77	0.68	0.55	0.59	0.55	0.73	0.12	1.23	1.32
Na_2O	2.93	3.86	3.47	3.31	2.48	3.75	3.25	3.36	2.70	3.10	6.55	7.35	7.38	9.24	8.68	7.38	5.34	9.82	7.35	8.74
K_2O	6.64	4.30	5.64	5.53	6.11	5.18	6.14	4.69	6.82	5.57	0.20	0.22	0.17	0.21	1.34	3.37	6.28	0.46	0.76	1.00
P_2O_5	0.13	0.09	0.33	0.03	0.03	0.03	0.21	0.02	0.51	0.03	0.29	0.05	0.07	0.66	0.06	0.08	0.11	0.24	0.05	0.09
B_2O_3	0.14	0.04	0.12	0.00	0.22	0.14	0.12	0.12	0.12	0.06	0.08	0.10	0.06	0.36	0.30	0.14	0.21	0.35	0.35	0.36
F	0.56	0.41	0.62	0.71	0.40	0.56	0.62	0.60	0.45	0.84	0.67	0.90	0.45	0.51	0.67	0.10	0.24	0.40	0.56	0.51
S	-	0.00	-	-	0.01	-	0.00	0.01	0.02	0.03	1.27	4.32	2.27	0.68	0.69	0.22	-	0.42	0.25	0.24
H_2O^+	0.30	0.54	0.26	0.06	0.15	0.14	0.02	0.02	0.01	0.31	2.10	1.15	1.02	0.83	0.58	0.53	0.16	1.20	1.26	1.22
H_2O^-	0.11	0.23	0.17	0.10	0.10	0.18	0.26	0.23	0.12	0.20	1.83	1.85	1.34	0.50	1.28	1.02	0.77	1.17	1.47	1.48
O F&S	0.24	0.17	0.26	0.30	0.17	0.24	0.26	0.25	0.19	0.35	0.76	1.90	1.05	0.47	0.54	0.08	0.11	0.32	0.33	0.30
Total	99.58	100.04	99.42	99.66	99.68	99.41	99.42	99.42	99.58	99.57	97.06*	98.09*	95.98*	98.46*	98.27*	98.73*	99.66	98.63	98.66	99.07
As	50	40	50	20	85	45	30	40	50	55	15,550	4,500	20,000	480	470	2,100				
Ba	220	225	190	200	210	200	190	210	180	85	30	35	30	80	165	170				
Be	5	8	4	5	7	5	5	6	6	5	10	25	1,900	50	25	20				
Co	8	9	8	7	7	8	6	6	5	6	25	20	35	20	10	3				
Cr	4	6	4	5	4	6	5	4	5	6	6	7	10	6	4	11				
Cu	20	20	20	35	35	35	55	120	20	30	5,420	5,650	8,500	6,350	9,100	2,050				
Li	75	55	92	76	81	93	86	75	58	75	60	52	97	65	51	85				
Ni	1	2	1	2	2	1	2	2	2	2	7	7	7	10	7	7				
Pb	40	14	14	14	16	16	14	16	18	22	42	47	105	22	8	26				
Rb	485	540	530	480	475	480	505	515	510	490	<10	<10	<10	<10	<10	125				
Sn	40	60	50	60	15	70	15	70	35	50	45,200	9,550	9,460	9,250	1,450	1,330				
Sr	85	80	70	75	70	80	75	75	70	70	85	70	75	80	80	75				
Zn	25	22	15	41	22	16	12	25	40	20	610	320	240	40	15	120				
Zr	40	25	30	20	35	20	25	20	45	<10	<10	<10	20	25	15	20				

* Total includes SnO_2

	Feldspars 1	2	3	4	5
SiO_2	64.98	64.69	66.86	65.14	63.40
Al_2O_3	20.29	21.43	21.41	20.22	22.98
CaO	0.13	0.13	0.13	1.46	4.51
Na_2O	11.53	10.73	11.43	10.57	8.65
K_2O	0.35	0.11	0.11	0.27	0.91
Total	97.28	97.09	99.94	97.66	100.45
Si+Al	3.79	3.81	4.03	3.81	4.03
Na+K+Ca	0.98	0.89	0.98	0.96	1.01
Ab	97.40	98.60	98.80	91.50	73.70
Mol% An	0.60	0.70	0.60	6.70	21.20
Or	1.90	0.70	0.60	1.60	5.10

partial analysis of feldspars (microprobe)
1-3 albites from albitised zone
4-5 oligoclase, unaltered granite

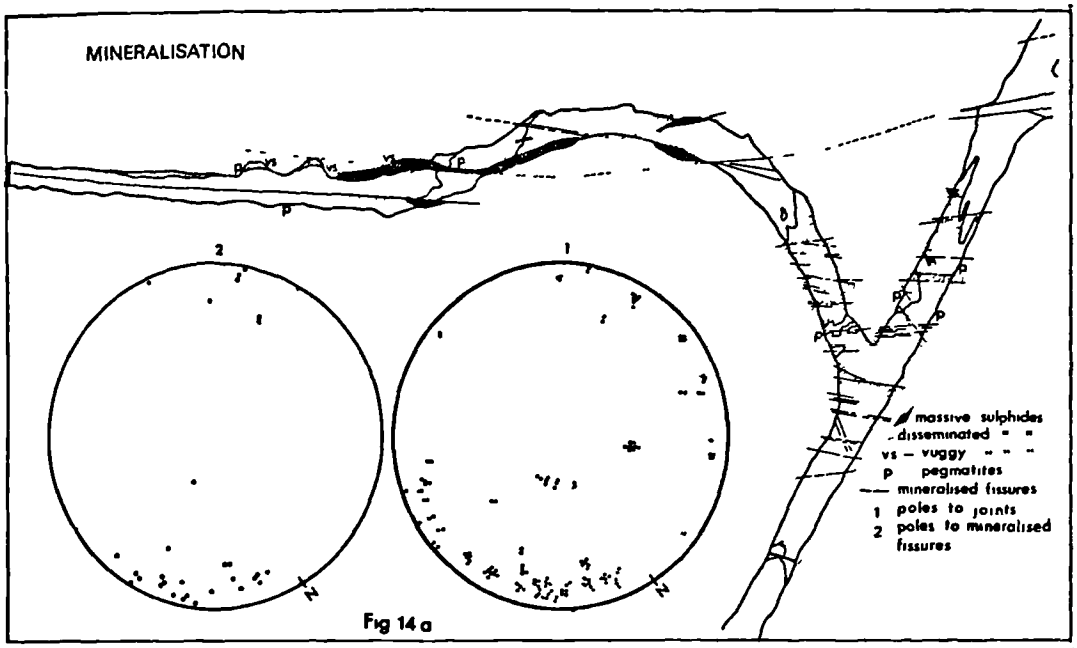

Fig 14 a

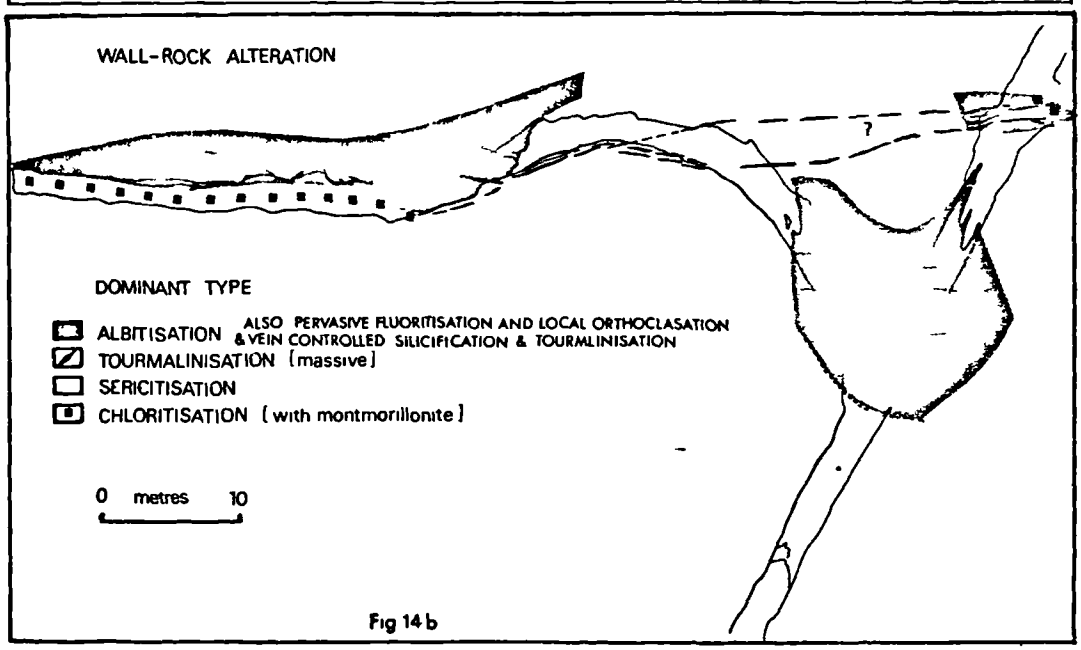

Fig 14 b

Mol. prop. triangular variation diagram

A- Al_2O_3 - (Na_2O+K_2O)

F- total iron oxides as FeO, +MgO+MnO

N- Na_2O

K- K_2O

○ unaltered granites

• albitised granites

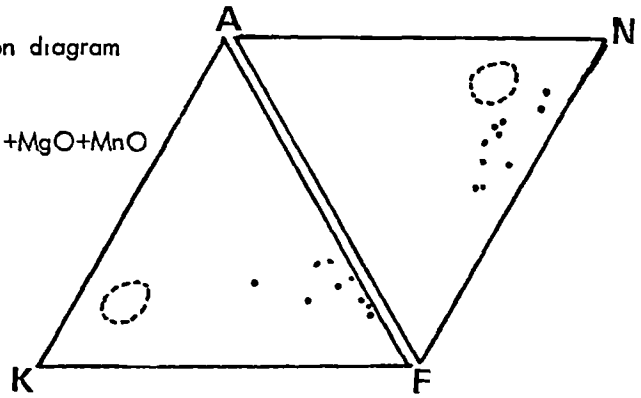

FIG 14C

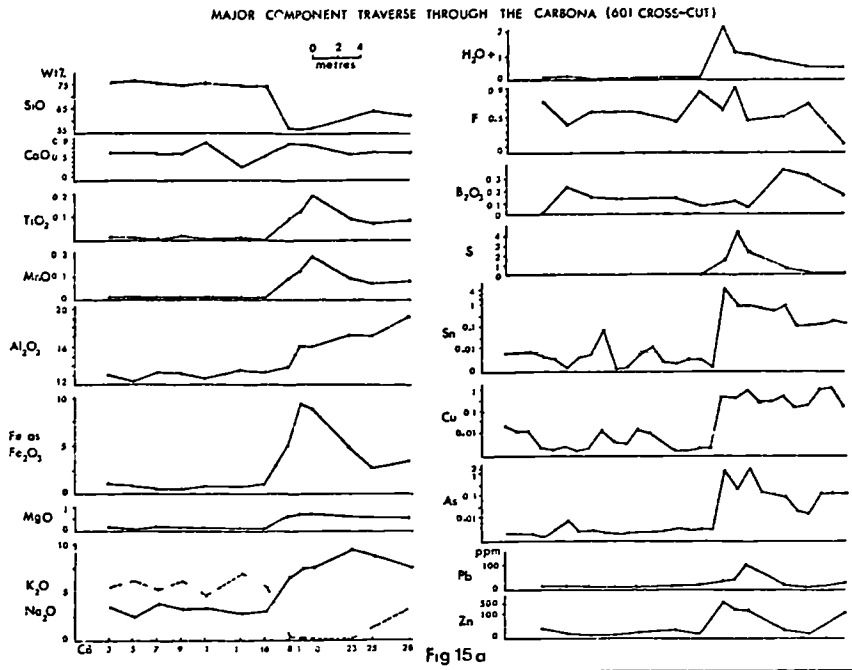

Fig 15a

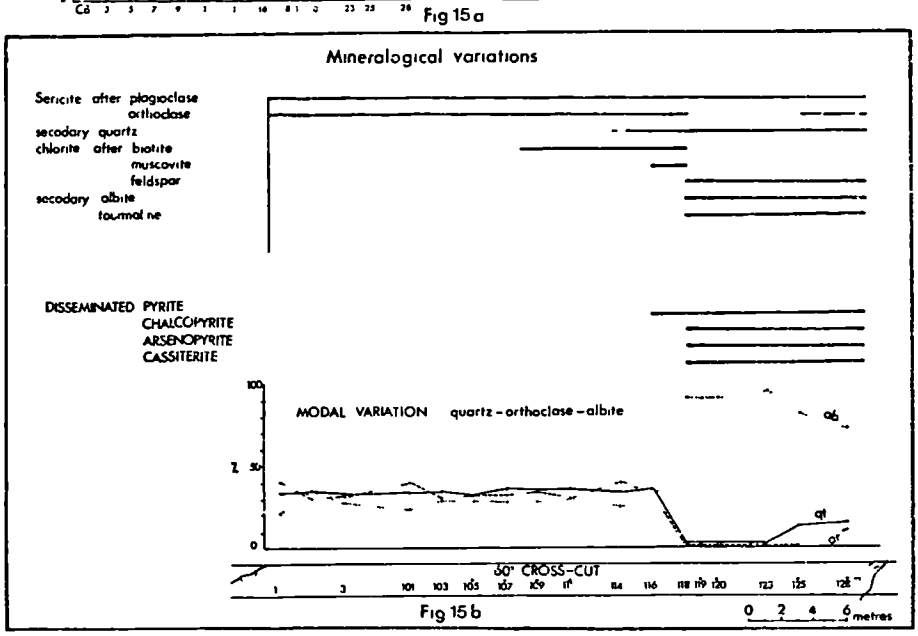

Fig 15b

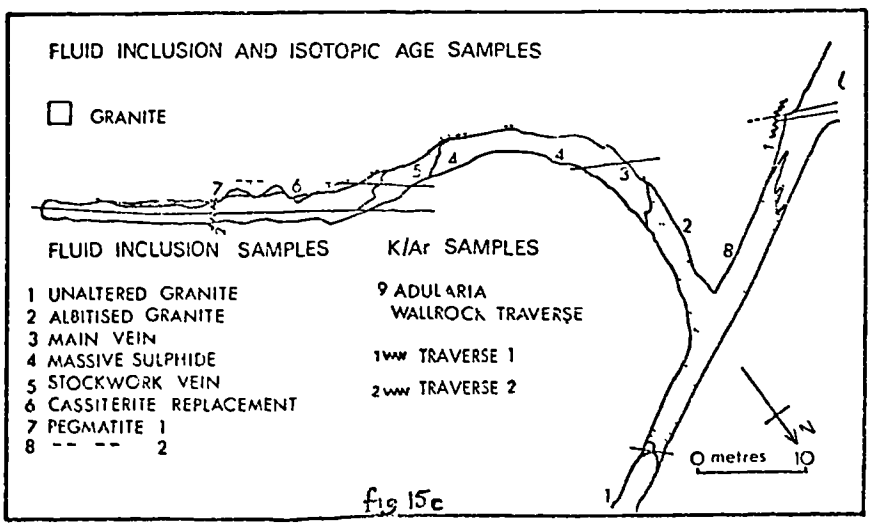

fig 15c

proportions of the rock in the mineralised zone. That net losses did occur locally is indicated by non-tectonic, quartz filled cavities in the contact and roof zones, suggesting local volume changes in these areas.

f) Mineralisation

Morphologically several distinct types of mineralisation can be distinguished, although compositionally, the ore phases which comprise the various types are similar. For descriptive purposes the mineralisation will be divided into the following types:

1. fissure veins
2. minor disseminations
3. stockwork
4. massive replacement

The distribution and type of mineralisation is shown in figure 14a.

1. fissure veins

The Foot-wall Branch vein system on the 329 m level is composed of several minor, rather than one major, fissure veins, and many of the veins intersect the granite sheet.

Vein 1 is located 12 m east of the south drive, trends N-S, is subvertical and downthrows the granite on the west by about ½ m. The vein consists of a 10-20 cm wide crush zone of sheared

pink granite, containing secondary massive vuggy quartz, tourmaline chlorite and minor pyrite and chalcopyrite.

Vein 2, 10 m west of the first vein, trends 316° and dips 80° SW. The vein consists of altered granite, quartz, orthoclase, a green clay mineral possibly montmorillonite, chlorite, hematite and disseminated pyrite.

Vein 3, the main Foot-wall Branch vein, lies 18 m west of the south drive. In the cross-cut the vein consists of two separate, north-west trending, subvertical structures, surrounded by a 2 m wide alteration envelope, in which the pelites have been converted to an assemblage of tourmaline, albite, chlorite, hematite, quartz, sericite and montmorillonite. Both veins contain a similar infill of quartz, hematite, arsenopyrite, pyrite, chalcopyrite and fluorite. The veins unite and the single structure exposed in the south drive consists of a central barren quartz zone (8 cm wide), bordered by mineralised margins, containing arsenopyrite, pyrite, cassiterite, chalcopyrite, fluorite and chlorite. Several other small veins containing quartz, hematite, pyrite and chalcopyrite occur in the cross-cut immediately west of vein 3.

A possible strike continuation of vein 2 intersects the southern drive 35 m from the drive entrance, and continues in the roof of the drive until the drive is terminated. For most of its

length the vein consists of a narrow (5-15 cm wide), sheared quartz-hematite fissure infill containing cassiterite, arsenopyrite, pyrite, chalcopyrite and chalcocite, and bordered by chloritised and hematised pelitic wallrocks. However, where the fissure intersects the granite a zone of intense replacement mineralisation is developed and both the granite and the adjacent pelites have been albitised and tourmalinised in addition to the chlorite-hematite wallrock assemblage. Mineralisation consists of massive replacement and disseminations of cassiterite, pyrite, arsenopyrite and chalcopyrite, with associated fluorite and orthoclase.

A synopsis of the paragenisis of all the veins is given in table 9 . The proposed tectonic and mineral paragenetic history of the fissure system is as follows:

i) early shearing, brecciation and faulting of the granite, production of NW trending fissures.

ii) deposition of quartz ± tourmaline and minor cassiterite.

iii) deposition of quartz, fluorite, chlorite, arsenopyrite, pyrite, cassiterite and late chalcopyrite. (Depositional phases 2 and 3 were emplaced in dilatant, tensional extensional fissures.)

iv) deposition of quartz-hematite and chalcocite.

MINERAL PARAGENESIS

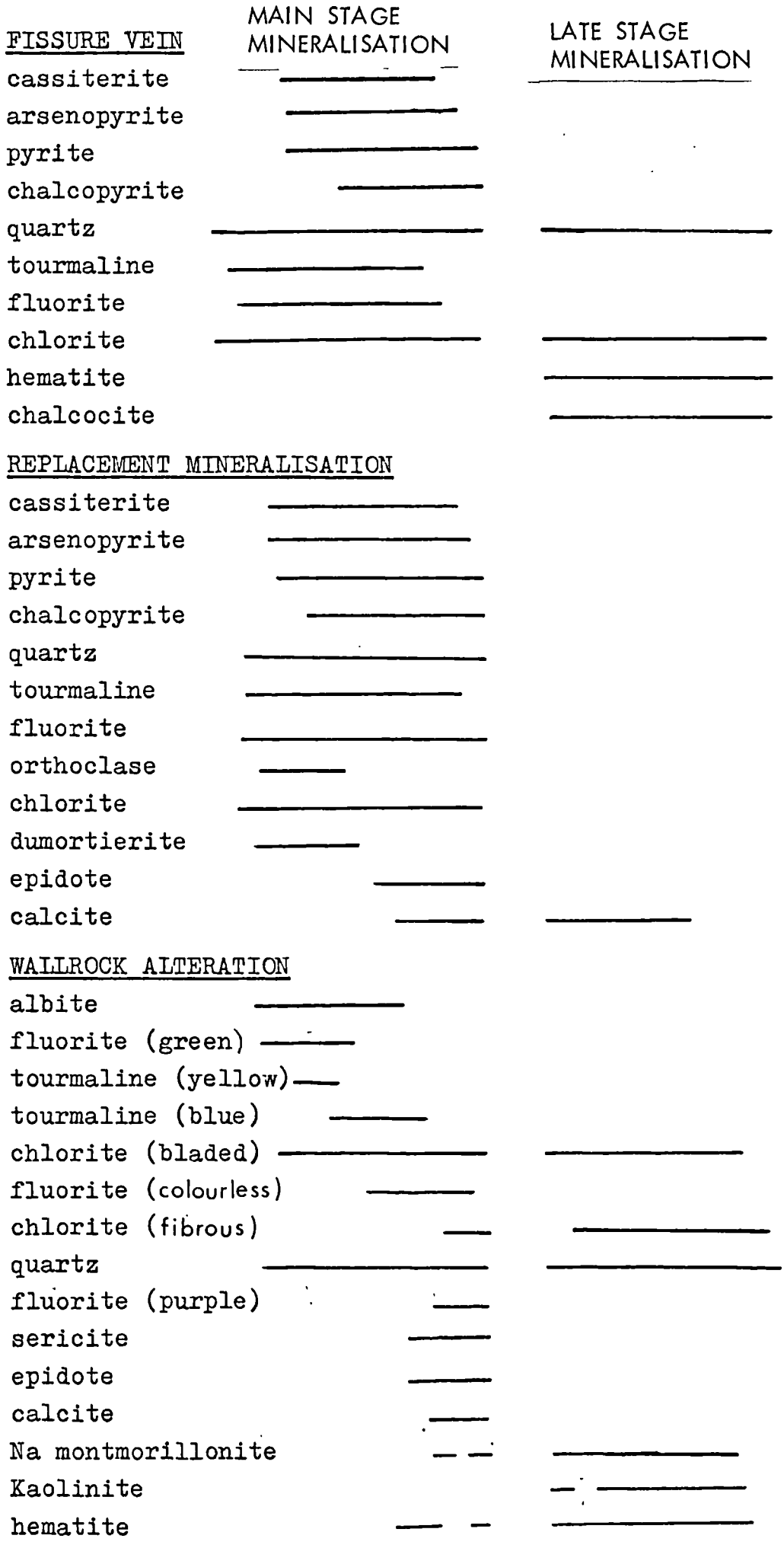

TABLE 9

This stage of mineralisation was accompanied by shearing and brecciation of the walls and the earlier vein infill.

2. minor disseminations

Minor disseminations of sulphides and cassiterite occur in the irregular alteration envelope surrounding the main mineralised zone. The ore-minerals, cassiterite, arsenopyrite, pyrite and chalcopyrite form between 0.1 and 5% of the rock, and occur in all lithologies (granite, pelite and metabasite) in the replacement zone. Average tin and copper values for this type of mineralisation are between approximately 1000-3000 p.p.m. for both metals.

In granite the ore-phases usually occur as small 0.1-0.4 mm anhedral grains, initially located on the silicate grain boundaries but at higher densities the ore-phases replace the silicates. The ore phases are often intergrown with chlorite and fluorite.

In altered pelites, sulphides and cassiterite occur in disseminations parallel to the bedding foliation and cleavage, and in irregular clots of tourmaline and alkali feldspar.

Thin and polished section studies of this type of mineralisation suggests that the ore-mineral paragenetic sequence is cassiterite-arsenopyrite and pyrite-chalcopyrite.

3. the stockwork

A zone of anastomosing veinlets occurs in a NW trending belt about 10 m wide in the most intensely mineralised part of the ore-body. The stockwork consists of an irregular network of quartz-tourmaline stringers and clots in altered granite and pelite. Individual veinlets contain pyrite, arsenopyrite or chalcopyrite. Although cassiterite was not observed, it might be expected to be part of the vein assemblage.

4. massive replacement

Massive replacement mineralisation occurs in the central part of the southern drive near the contact of the main Foot-wall Branch vein with the upper contact of the granite sheet. Mineralisation occurs in granite and pelite and is particularly well developed near the junction of both lithogies. Characteristically, the replacement is massive and structureless, but occasionally vuggy, cavity infill structures occur. Massive cassiterite and sulphide replacement in pelites is usually associated with, but post-dates, intense tourmalin isation.

The ore-phases in common with the other types of mineralisation are pyrite, arsenopyrite, chalcopyrite and cassiterite. Gangue minerals contemporaneous with ore deposition are quartz, chlorite, orthoclase and fluorite (green and

colourless). Calcite and hematite post-date ore deposition.

Vugs occurring within the zone of massive sulphides show the depositional sequence: orthoclase-cassiterite, arsenopyrite, pyrite, chalcopyrite-green fluorite, purple fluorite.

Massive replacement in granite is associated with the extensive development of tourmaline, chlorite, quartz, orthoclase, fluorite (green) and rare dumortierite. The ore is characteristically massive and often occurs in bands, lenses and vugs. The first type of structure is particularly well developed in the south east wall and roof of the southern drive $\sim$ 35 m from the drive entrance. The structure consists of lenses and bands of orthoclase, cassiterite, sulphides and fluorite, in a matrix of chloritised and tourmalinised granite, containing minor ore-phases. Vuggy structures also occur in the same area and are usually composed of cassiterite, sulphides, quartz and tourmaline. The general depositional sequence in such vugs is tourmaline, cassiterite, quartz, arsenopyrite, pyrite $\rightarrow$ chalcopyrite, quartz $\rightarrow$ quartz, calcite.

Tin and copper values for this type of ore are less than 3% and 4% respectively.

'Pegmatites'

Irregular and regular shaped cavities containing coarse euhedral crystals of quartz are common throughout the main zone of mineralisation and particularly near the contact. Two types can be distinguished, inwardly zoned, regularly shaped bodies upto 20 cm in diameter, and larger, upto 1 m, irregularly shaped bodies, associated with intensely tourmalinised hostrock. The first type consists of an outer chloritised envelope, bordered by inward terminating pink orthoclase and finally quartz. Cassiterite is often associated with the chlorite and orthoclase, and pyrite, arsenopyrite and chalcopyrite with the quartz. The second type consists of quartz and sometimes tourmaline, and late fluorite (colourless and purple). The quartz contains numerous euhedral inclusions of pyrite-arsenopyrite and chalcopyrite but the fluorite is barren.

A summary of the vein, replacement and wallrock mineral paragenisis is presented in table 9 . Both the replacement and vein mineralisation display similar ore-mineral paragenisis, i.e. cassiterite-arsenopyrite + pyrite→chalcopyrite + pyrite, probably indicating the coeval nature of the two types of mineralisation.

In general albitisation pre-dates mineralisation. Early alteration is characterised

by assemblages indicative of strong cation metasomatism, i.e. albite (locally K feldspar), chlorite and tourmaline. Mineralisation is characterised by fluorite. Post-mineralisation changes in the wallrock assemblages are minor, mainly the development of white mica (sericite) and local Na montmorillonite and kaolinite. These assemblages are indicative of feldspar hydrolysis reactions.

A more detailed discussion of the formation of the feldspar constructive alteration is presented on page 245.

g) The fluid inclusion study

The object of this study was to distinguish, if possible, the hydrothermal fluids which were responsible for the vein and replacement mineralisation and hydrothermal alteration. The following samples were carefully selected for study:

CB1 the main mineralised vein in the area of the ore body.

2 fluorite coeval with sulphides (zone of massive replacement).

3 quartz coeval with sulphides (zone of massive replacement).

4 quartz coeval with cassiterite (zone of massive replacement).

5 unaltered granite.

6 albitised granite (fluorite).

7 albitised granite (quartz).

8a, b & c quartz, colourless fluorite and purple fluorite from a zoned quartz-fluorite pegmatitic pod.

9 quartz containing sulphide inclusions (pegmatitic pod 601 cross-cut).

The location of the samples is shown in figure 14 c .

Most of the material was unsuitable for distinguishing the exact genetic relationship (P, PS or S) of the fluid inclusions. Therefore, this study only attempts to define in general terms the different phases of hydrothermal activity.

Inclusion types present

Each sample contained a variety of morphological, compositional and genetic (P, PS & S) inclusion types. The main types of inclusion in all the minerals studied, quartz, fluorite and cassiterite, are as follows:

1. Well shaped or irregular, 2 phase (L + V) inclusions with a variable sized gas bubble (~ 5-50% vol.) occur in random, non-planar groups (P and PS), in planar groups parallel to primary growth zones (P) and in cross-cutting planar arrays (PS and S). They usually constitute the dominant proportion of the inclusion population in any sample.

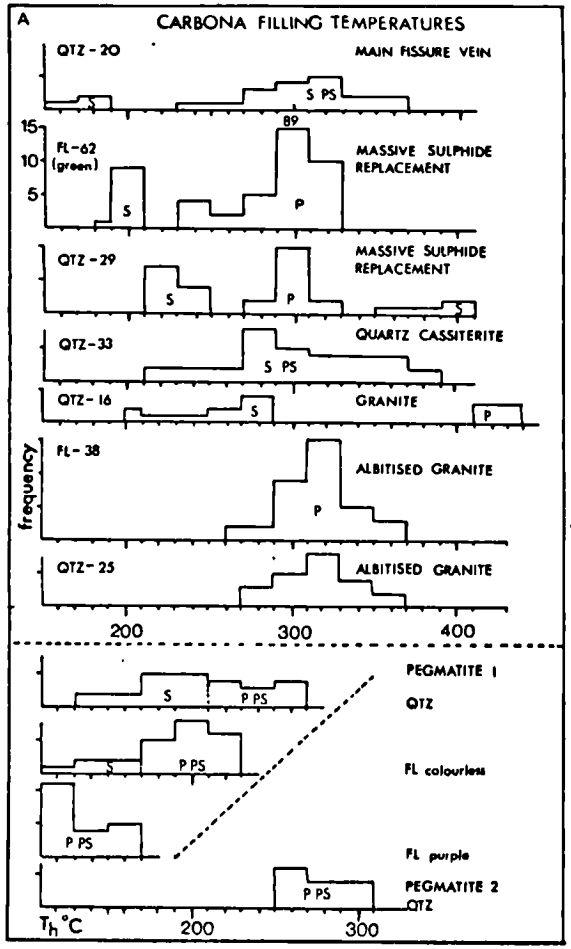

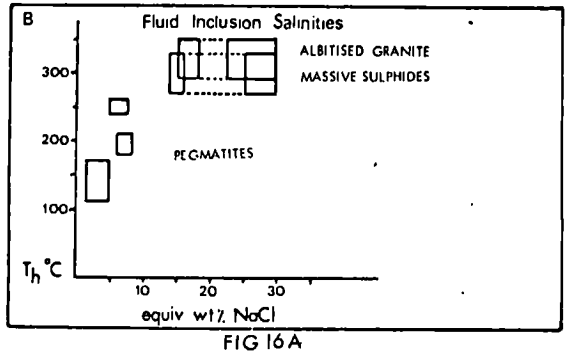

FIG 16A

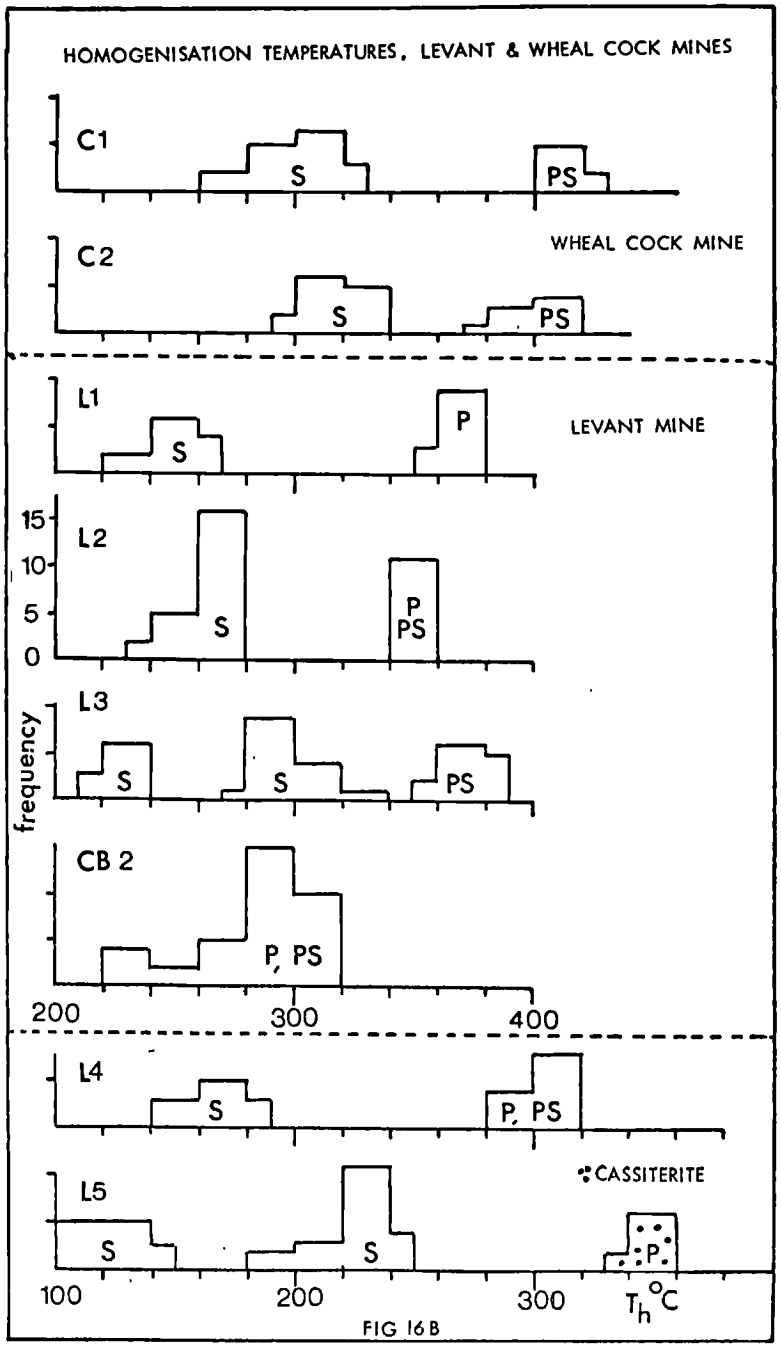

FIG 16B

2. Well shaped or irregularly shaped, 3 phase (L + V + S) inclusions containing either a single colourless isotropic phase (halite) and/or 1 or 2 unidentified prismatic or irregularly shaped birefringent solids. The other solid phases observed are:
   a) a small opaque phase.
   b) colourless fibrous birefringent masses.
   This type of inclusion occurs in random non-planar groups (P and PS) and cross-cutting planar arrays (S).
3. Rare monophase gas inclusions occur in cross-cutting planar arrays (S) or rare isolated inclusions (P?)
4. Well shaped or irregularly shaped monophase (liquid) inclusions occur in cross-cutting planar arrays.

Results

The results of the thermometric and salinity studies are presented in table 10 and figure 16 . All the quoted temperatures are minimum formation temperatures, uncorrected for the effects of pressure.

The homogenisation temperature data indicate that:

1. the main phase of alteration (albitisation) was developed in the T_h range 270-370°C (probably mainly between 290-330°C).

2. Quartz and fluorite associated with vein and massive sulphide mineralisation contain many generations of inclusions, which show a large homogenisation temperature range. The main phase of ore deposition (cassiterite, arsenopyrite, chalcopyrite and pyrite) occurred in the T_h range 270-330°C (probably mainly between 290-320°C). Although no homogenisation temperatures were obtained for cassiterite, because of the very small size of individual crystals, the early formation of this phase in the paragenetic sequence suggests that it may have formed in the upper part of this temperature range. Early deposition of vein quartz occurred in the T_h range 350-400°C.
3. Quartz pegmatites containing inclusions of arsenopyrite, pyrite and chalcopyrite formed in the T_h range 250-310°C. A zoned quartz-fluorite pegmatite displays a continuous temperature decrease from quartz (T_h 270°C) to purple fluorite (T_h 114°C).

The salinity data indicate that:

1. The fluids responsible for albitisation were of moderate but highly variable salinity mainly between 15.5 - 18 and 22 - 33 equiv. wt. % NaCl.
2. Fluorite coeval with massive sulphide replacement contained P and PS inclusions with salinities mainly in the range 14 - 16 equiv. wt. % NaCl.

TABLE 10

SUMMARY OF INCLUSION DATA FOR THE CARBONA ORE BODY

CB	SAMPLE DESCRIPTION	INCLUSION TYPE	TH.RANGE	NUMBER MEASURED	SALINITY EQ.WT.% NaCl	NUMBER MEASURED
	Main Fissure Vein,	S	230-370	17		
1	quartz		150-190	3		
	Massive Sulphide	P + PS ?	270-330	106	14-15.5	25
	Replacement,	S	230-270	6	also 24.5-29	6
2	fluorite	S	180-210	10	6-8	7
	Massive Sulphide	S	350-410	4		
	Replacement,	P + PS ?	270-330	14		
3	quartz	S	210-250	11		
	Cassiterite Replacement,	P + PS ?	270-390	33		
4	quartz	S	210-270	6		
	'Unaltered' Granite,	P + PS ?	410-440	6		
5	quartz	S	200-290	10		
	Albitised Granite,	P	260-370	38		
6	fluorite	PS				
	Albitised Granite,	P	270-370	25	15.5-18	23
7	quartz	PS			22-30	6
	Pegmatite 1,	P + PS	210-270	11	5-7.5	7
	quartz	S	130-210	14		
	colourless Fluorite	P + PS	170-230	19		
8		S	110-170	5		
	pale green Fluorite	P + PS	110-170	20	1-5	6
	Pegmatite 2,					
9	quartz	P + PS	250-310	14		

Planes of S inclusions were of higher 25-30 equiv. wt.% NaCl or lower 6-8 equiv. wt.% NaCl, salinity.

3. Inclusion fluids associated with the zoned quartz-fluorite pegmatite varied in salinity between 5-7.5 equiv. wt.% NaCl in quartz and 1 to 5 equiv. wt.% NaCl in fluorite.
4. There was a general decrease in the salinity of the fluids with decreasing temperature.

h) K/Ar dating

A recent K/Ar dating study (A Halliday, written communication) concerned with dating hydrothermal alteration assemblages and gangue phases associated with mineralisation has revealed some interesting results regarding the hydrothermal history of the ore-body.

Two veins were studied (fig 14c). Traverse (a) is located in the south wall of 601 cross-cut through the main Footwall Branch vein and traverse (b) is located adjacent to the SE extension of vein 2. In addition, a sample of adularia, paragenetically associated with massive sulphides (Cu, As, Fe), was collected from the most intensely mineralised area. The results indicate the probability of several phases of hydrothermal activity at approximately 270, 210, 160, 100 M.a. The earliest phase of activity is undoubtedly connected with the main phase of alteration and mineralisation, although it is not

clear to what extent the other individual phases of activity have affected the ore body. The main phase sulphides and hypogene alteration in the core of the ore-body do not appear to have suffered extensive alteration (except on a small scale) and it is, therefore, unlikely that the main portion of the ore-body was penetrated by large volumes of later fluid. However, oxidation of sulphides in traverse (a), the late formation of chalcocite hematite and montmorillonite in vein 2 (b) and the occurrence of kaolinite in the albitised alteration zone, suggest that some 'late, low-temperature fluids' did penetrate the ore-body.

i) Summary

This study has considered four aspects of the ore body: the distribution, nature and paragenisis of mineralisation, the associated hypogene alteration, the character of the mineralising fluids (as indicated by fluid inclusions) and the temporal relationship of the hydrothermal events.

The mineralising fluids, which entered the granite sheet through the Footwall Branch vein system, caused intense metasomatism and deposited cassiterite, pyrite, arsenopyrite and chalcopyrite, during the cassiterite-sulphide stage of mineralisation. The replacement mineralisation was probably due to an increase in the mineral and fracture porosity in the granite sheet, due to local metasomatic and tectonic activity.

The wallrock alteration assemblage (dominated by albite) indicate that the fluids initially had high cation/H^+ ratios and high Na/K ratios. These fluids reacted with the granite and probably, by a cation exchange reaction, formed the observed assemblage. Local K feldspar was produced when Na/K ratios decreased. Later fluids probably had low cation/H^+ ratios and caused the degradation of Na feldspar to kaolinite and locally montmorillonite.

The fluid inclusion studies indicate that there was a continuum of hydrothermal activity in T_h range < 70-400^oC. The main phase of hypogene alteration was produced in the T_h range 270-370^oC and the main phase of cassiterite and sulphide deposition was in the T_h range 270-330^oC.

K/Ar dating studies indicate the possibility of several distinct phases of hydrothermal activity ($\sim$ 270, 200, 160, 100 M.a.). The replacement cassiterite and sulphide mineralisation is associated with the first age (270 M.a.) and vein quartz-hematite-chalcocite and wallrock montmorillonite (and kaolinite?) are associated with the 160 M.a. age. The effects of the $\sim$ 200 M.a. event and the youngest event are not known.

G3 'GREENSTONE ORE'

a) Introduction

Greenstone ore is a useful field term which describes non-fissure vein cassiterite mineralisation, occurring within hydrothermally altered basaltic and pelitic rocks. Although described as ore, most of the investigated deposits are of localised occurrence and low grade (less than 0.2% SnO_2). However, some of the deposits, notably those at Wheal Cock and Grylls Bunny mines, have been exploited and have yielded moderately large tonnages of between 1 - 2% SnO_2.

The following types can be distinguished (fig 19):

1. Disseminations in the highly altered wallrock, bordering mineralised and unmineralised fissure veins.

2a. High density stockworks and replacements at the fractured junction of two intersecting fissure veins.

2b. Low density stockworks located in fracture zones and fold closures.

3. Lenticular or irregularly shaped replacements associated with boron metasomatised host rocks.

b) Tin distribution

In view of the widespread development of disseminated and replacement cassiterite, within the basaltic aureole rocks, a study was made to evaluate

the distribution of Sn in the various hornfelses and metasomites. These data were compiled from this study, Floyd (1968), Cotton (1973), Khan (1972) and Levant Mine SJ 3 and SJ 5 diamond drill reports. Obviously there are difficulties in correlating information from many sources, whose petrographic and analytical reliability is extremely variable. These data, however, show some general trends which are in reasonable agreement.

The data are divided into 4 groups, and summarised in table 11 :

1) hornblende and/or actinolite, plagioclase hornfelses.
2) cordierite, cummingtonite, anthophyllite, plagioclase hornfelses.
3) massive calc-silicate metasomites.
4) discordant vein calc-silicate and boron rich metasomites.

The distribution of Sn within the different metabasite hornfels groups indicates a progressive enrichment in Sn from the cordierite, anthophyllite ± cummingtonite, biotite assemblages (average <10 ppm), through hornblende, plagioclase and actinolite, plagioclase assemblages (average 12.3 ppm) to garnet metasomites (average 267 ppm) and garnet, axinite, tourmaline metasomites (average 849 ppm). A similar study (Floyd, 1968) also shows the same general trend.

Tin distribution in the metabasite hornfelses (ppm)

Hornfels type	source	this study	Floyd (1968)	Cotton (1973)	Khan (1972)	Geevor Mine SJ3 + SJ5 reports	All sources except Geevor
cordierite	minimum	<10	<5	-	1	-	1
anthophyllite ±	maximum	45	<5	-	72	-	72
plagioclase	mean	<10	<5	-	11.3	-	9.6
cummingtonite biotite	number of samples	67	14	-	20	-	101
hornblende	minimum	<10	<5	-	0	< 25	<5
plagioclase	maximum	16	33	-	999	200	33
+	mean	11	14	-	24	85	12.3
actinolite plagioclase	number of samples	23	15	-	?	155	36
massive	minimum	<10	41	170	18	< 25	10
garnet	maximum	1450	59	270	440	5000	1450
metasomites	mean	267	50	215	168	536	228
	number of sample	33	2	6	14	108	55
garnet	minimum	160	-	510	43	-	43
axinite	maximum	2000	-	740	999	-	2000
tourmaline	mean	849	-	600	520	-	687
metasomatic veins	number of samples	13	-	3	11	-	27

Table 11

Since the hornblende/actinolite, plagioclase hornfelses are probably most representative of the least altered basaltic material, a value of 12 ppm can be considered as an approximate primary Sn value for these rocks. An average Sn value of 17 ppm for similar assemblages elsewhere in the aureole can be derived from the data of Floyd (1968), and an average Sn value of 14 ppm was obtained by Khan (1972) for dolerites which had been subjected to low grade metamorphism.

If the cordierite-anthophyllite assemblages are considered to be the submarine degraded and isochemically metamorphosed equivalents of the hornblende hornfelses, it is probable that the low tin contents of these rocks is the result of its loss during submarine alteration. The concentration of Sn in the calcium rich metasomites suggests that Sn was locally mobilised at this time i.e. during contact metamorphism, and concentrated in these horizons. Floyd (1968) suggested that the Sn^{2+} ion may have substituted for the Ca^{2+} ion, thus offering an explanation for the positive correlation of the two elements. The much larger concentration of Sn in the Ca and Ca + B metasomatic veins probably heralds the start of hydrothermal vein mineralisation in the aureole.

c) Types of greenstone ore

1) Wallrock replacements.

One of the commonest types of greenstone ore occurs in the hydrothermally altered (usually basaltic) wallrocks, bordering mineralised or unmineralised fissure veins, such as the Hen and Foot-wall Branch veins and the Crowns Guide, all 6 level.

The extensive alteration envelope bordering the Crowns Guide, which is exposed in 604 drive, was studied in detail and the results of the distribution of Sn, Cu and Zn are presented in fig 10 . Although the guide contains only hematite and limonite, the wallrock contains Sn values (120 - 4800 ppm) for distances of several metres away from the vein. Vanning assay recovered SnO_2 values of between 0.1 - 0.3% and one value of 1% immediately adjacent to the fissure.

The ore-phases, cassiterite ± pyrite, arsenopyrite and chalcopyrite, occur as small, less than 0.1 mm, isolated grains, within a matrix of biotite, chlorite, hematite and variable amounts of K-feldspar, axinite, tourmaline, fluorite, quartz, sphene and calcite.

Although such deposits are of extremely low and variable grade, wide alteration envelopes, particularly those bordering major guides which

were tectonically active during mineralisation, offer a potential for high tonnage.

2a) High density stockworks near fissure vein intersections.

Although only one example of this type of ore-body has been recorded, the potential exists for other similar deposits. This type of mineralisation was briefly recorded in the Botallack Mine reports, at the beginning of this century. The ore-body is said to have occurred at the brecciated junction of two fissure veins, in the Wheal Cock section of the mine. The deposit was found, and subsequently exploited, during the sinking of Skip Shaft. The overall grade of the deposit was between 1 - 2% SnO_2, and the stopes were reputed to have been upto 30 m wide. Although there are no descriptions of the ore, numerous dumps around the shaft suggest that the ore consisted of a cassiterite rich stockwork, or replacements in amphibolites. The replacement ore consists of relatively coarse (0.3 mm) intergrowths of cassiterite and green chlorite, in a matrix of chloritised amphibolite. The stockwork (plate 7) consists of anastomosing veinlets, usually < 1 cm wide, containing quartz, fluorite, orthoclase, scheelite, cassiterite and arsenopyrite in chloritised and biotised amphibolite. More rarely, single veinlets (upto 3 cm wide) occur,

containing coarse (1 cm) crystals of strongly zoned, brown cassiterite, pink orthoclase and rare arsenopyrite, in a chloritised and biotised amphibolite matrix. It was not possible to determine the relationship of these veinlets to the stockwork and massive replacement samples.

2b) Low density stockwork.

This type of deposit is probably quite common, although it is very difficult to define and evaluate. No examples of this type of mineralisation have been exposed and this description is based on the drill core recovered from the UL 15 diamond drill hole.

The mineralisation consists of a system of subvertical microfractures and veinlets between <1 mm - 3 cm wide, occurring over a strike-normal distance of several metres and a strike length of unknown, but probably limited, extent.

An example of this type of mineralisation occurs below the end of 601 cross-cut. Diamond drill hole UL 15 intersected a mineralised stockwork between 176 and 206 m from its collar. The development of the cross-cut to the point of intersection proved a mineralised fissure vein (the Hen vein), but no stockwork. Figures 17 & 18 illustrate the main geological features of this area. The stockwork is, apparently, spatially

related to the intersection of the Hen vein with an anticlinal closure in the interbedded pelites and metabasites. The area above the stockwork in the cross-cut is composed of massive, banded amphibolite which contains a few mineralised joints (calcite, quartz, pyrite).

A section of drill core between 191.5 and 194.5 m was examined in detail. The stockwork is developed in finely foliated, dark hornfelses, probably of pelitic parentage, and consisting of green biotite, chlorite, quartz, opaque phases and calcite. The microveinlets, which traverse the hornfels, contain a varied assemblage of quartz, calcite, fluorite, green and brown chlorite, cassiterite, pyrite, arsenopyrite and chalcopyrite. Several fractures contain quartz, chlorite, biotite, rutile, ilmenite, topaz and an unidentified phase, possibly a zeolite. The vein paragenesis is:

1. cassiterite-arsenopyrite-pyrite-chalcopyrite (or topaz & biotite).
2. fluorite-calcite-quartz-(zeolite?).
3. chlorite.

Locally, within the stockwork zone, the host rock is converted to an assemblage of chlorite, biotite, quartz, fluorite, calcite and sphene, with small amounts of fine grained cassiterite, pyrite and chalcopyrite.

Analysis of five samples from the stockwork zone (table 6) indicate that the hornfelses are depleted in SiO_2, Al_2O_3 and Na_2O, and enriched in FeO, K_2O, TiO_2, MgO and CaO, compared to the analysed unaltered pelites. Anomalously high Cu, Zn, Sn and As values are confined to the areas of highest fracture density and there is very little lateral dispersion.

3) Metasomatic replacements.

This type of mineralisation consists of disseminated cassiterite or cassiterite-sulphide concentrations within a limited horizon and is usually associated with boron and potassium rich alteration assemblages (tourmaline, axinite and biotite). For completion, areas of anomalously high Sn values, but not containing cassiterite, have also been included in this section. The following types of mineralisation can be recognised:

a) Disseminated cassiterite and sulphides, associated with biotite-axinite host. This type of mineralisation is exposed in 601 cross-cut.

b) 'High' Sn, Cu and Zn values, associated with massive and vein, garnet-axinite (magnetite) metasomites. Examples of this type occur in metasomatic horizons and veins of Botallack

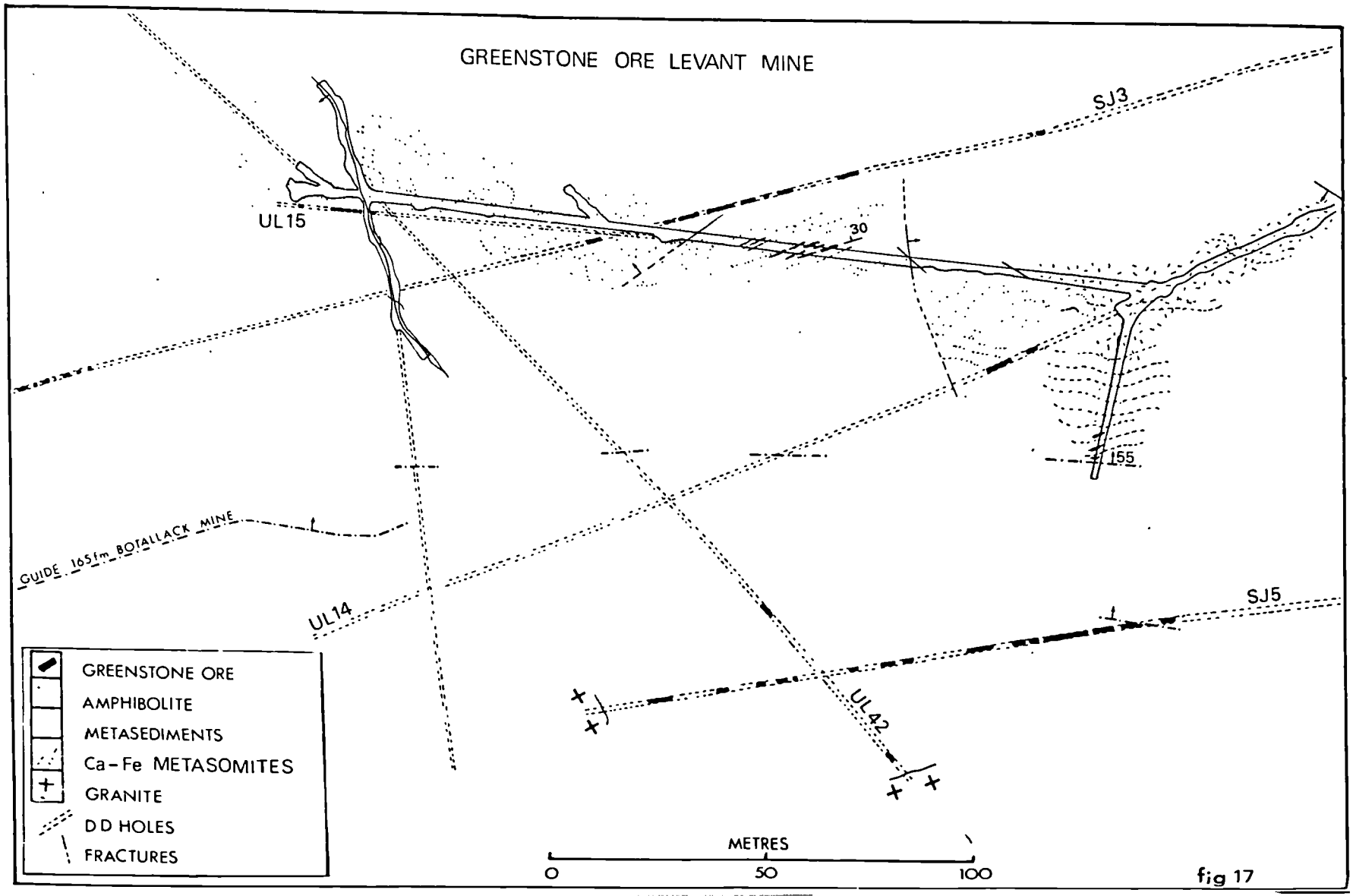
GREENSTONE ORE LEVANT MINE
SJ3
UL15
30
155
GUIDE 165fm BOTALLACK MINE
UL14
SJ5
UL42
GREENSTONE ORE
AMPHIBOLITE
METASEDIMENTS
Ca-Fe METASOMITES
GRANITE
D D HOLES
FRACTURES
METRES
0
50
100

fig 17

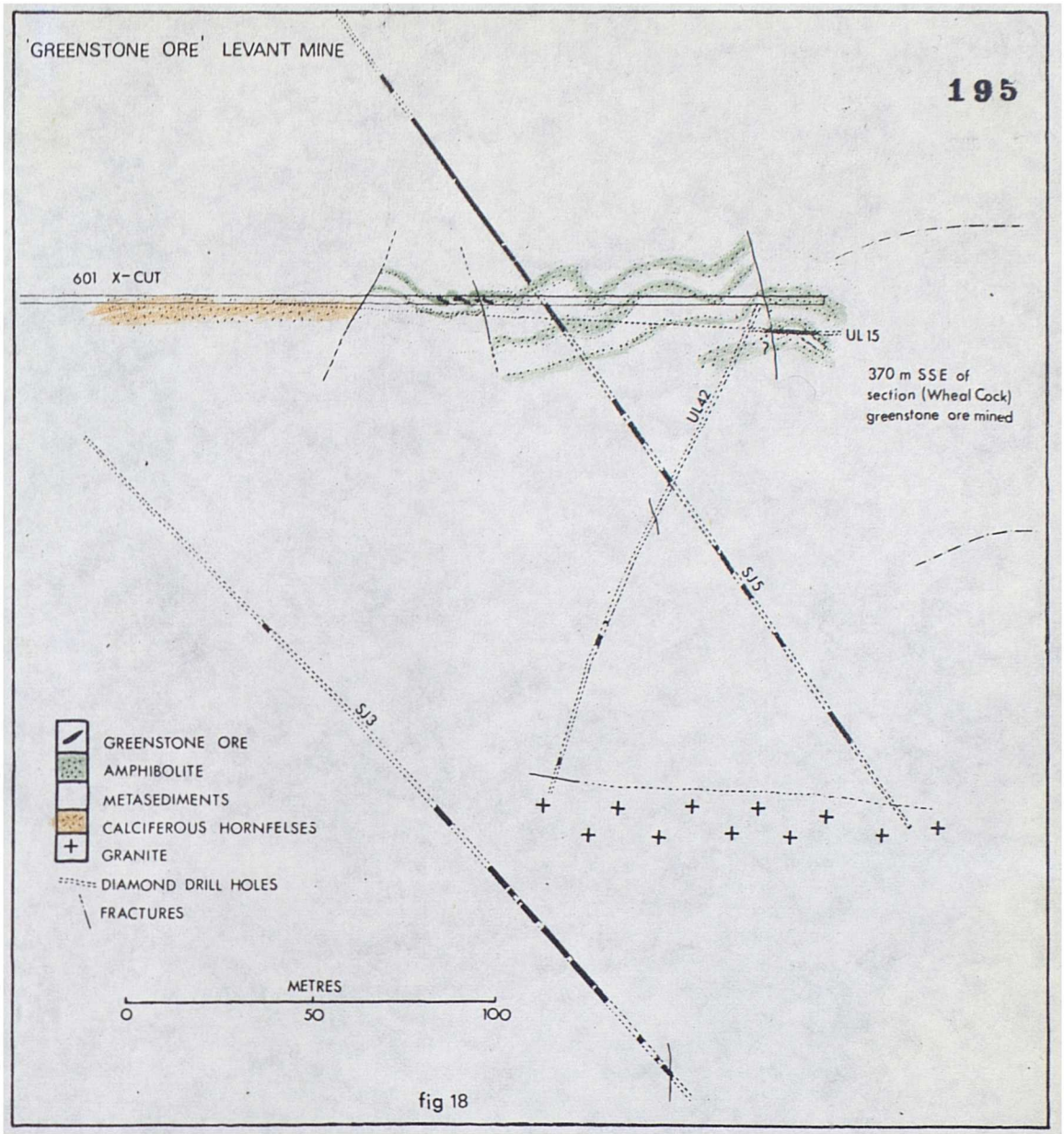
'GREENSTONE ORE' LEVANT MINE
601 X-CUT
UL15
370 m SSE of section (Wheal Cock) greenstone ore mined
UL42
SJ5
SJ3
GREENSTONE ORE
AMPHIBOLITE
METASEDIMENTS
CALCIFEROUS HORNFELSES
GRANITE
DIAMOND DRILL HOLES
FRACTURES
METRES
0
50
100

fig 18

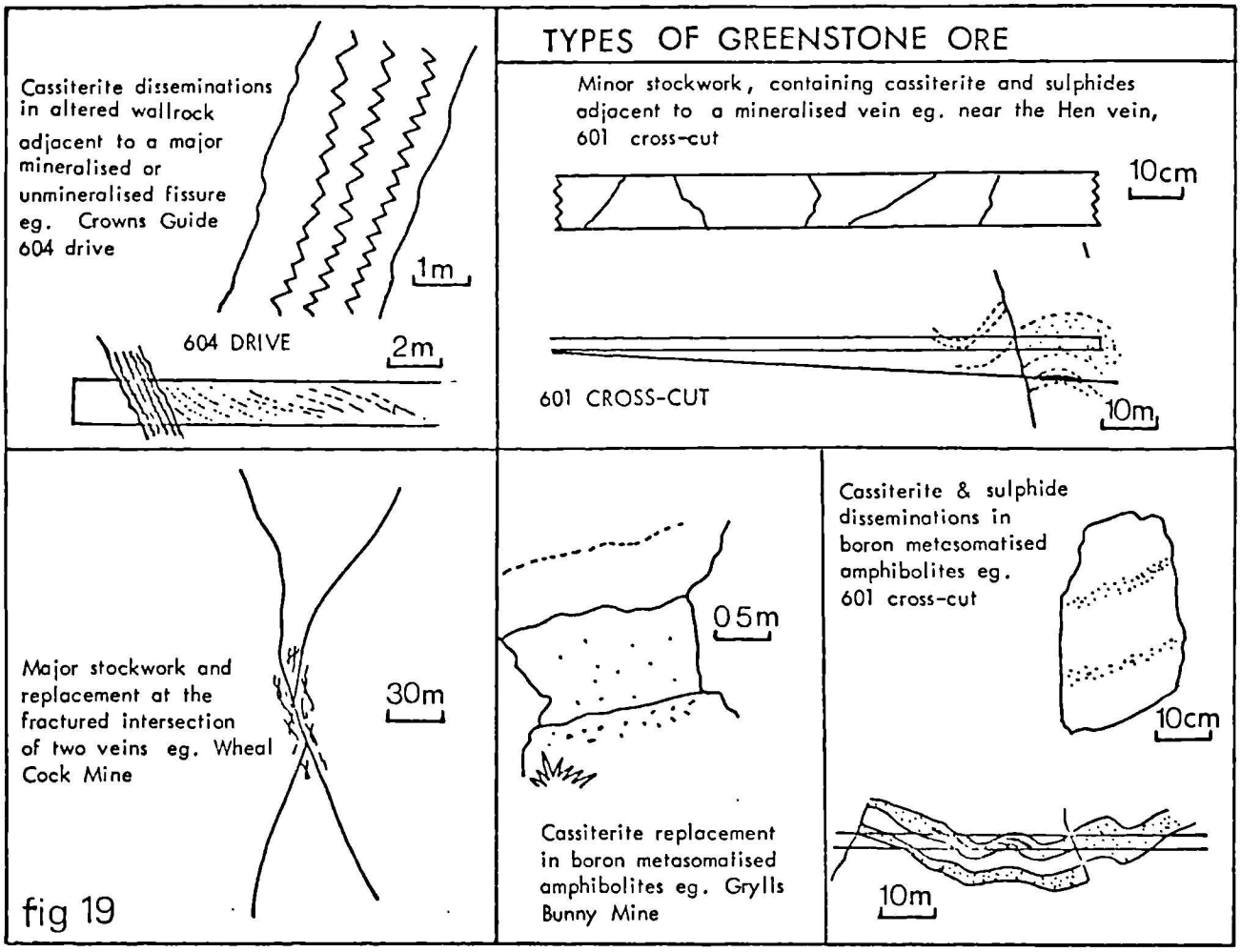
Cassiterite disseminations in altered wallrock adjacent to a major mineralised or unmineralised fissure eg. Crowns Guide 604 drive
1m
604 DRIVE
2m
TYPES OF GREENSTONE ORE
Minor stockwork, containing cassiterite and sulphides adjacent to a mineralised vein eg. near the Hen vein, 601 cross-cut
10cm
601 CROSS-CUT
10m
Major stockwork and replacement at the fractured intersection of two veins eg. Wheal Cock Mine
30m
0.5m
Cassiterite replacement in boron metasomatised amphibolites eg. Grylls Bunny Mine
Cassiterite & sulphide disseminations in boron metasomatised amphibolites eg. 601 cross-cut
10cm
10m

fig 19

and in Levant Mine in several diamond drill hole intersections.

c) Miscellaneous replacements (a) K-feldspar, chlorite, cassiterite, sulphides (401 cross-cut) (b) Sphalerite, pyrite, chlorite (601 cross-cut).

d) Disseminated cassiterite, associated with a biotite-tourmaline host. This type is exposed at outcrop in the Grylls Bunny Mine at Botallack.

3a) Two, approximately 3 cm thick, metabasite horizons, containing disseminated cassiterite and sulphides are exposed in 601 cross-cut (figs 17 & 18), ~100 m NE of the Hen vein. The two basic horizons are interbedded with pelites and banded calcareous sediments and the mineralised horizon dips at a low angel (~ 20^{o} NW). The original metamorphic assemblage (actinolite, plagioclase) in the amphibolite horizons has been converted to an assemblage of biotite, axinite, calcite, sphene, chlorite and fluorite, with microveinlets of quartz, alkali feldspar and hematite. Similar horizons occur in 604 drive and the UL 14 diamond drill hole.

The ore-minerals, cassiterite (0.1 - 0.2%) and sulphides (chalcopyrite and pyrite) are sporadically distributed through the horizon, but always occur in disseminations, parallel to the

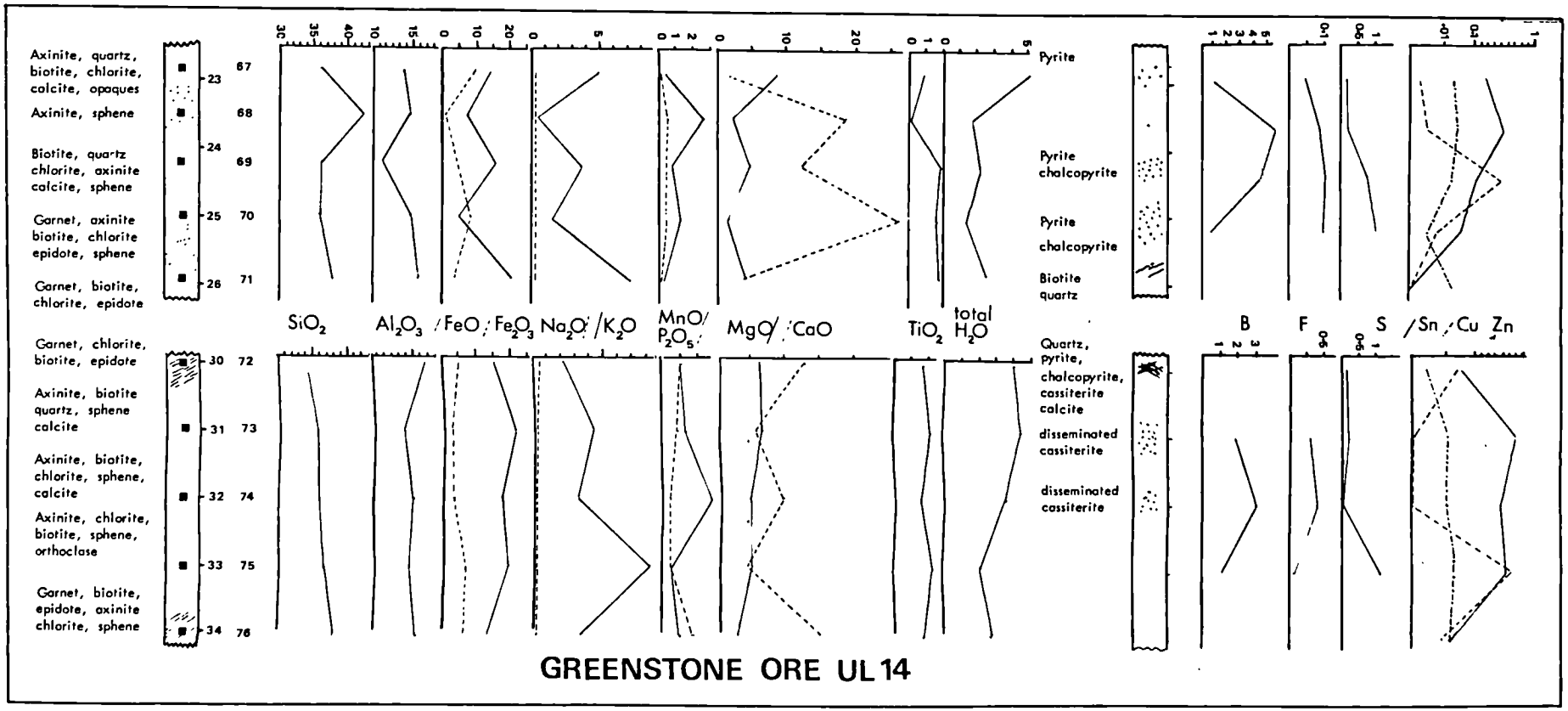
Axinite, quartz, biotite, chlorite, calcite, opaques
Axinite, sphene
Biotite, quartz chlorite, axinite calcite, sphene
Garnet, axinite biotite, chlorite epidote, sphene
Garnet, biotite, chlorite, epidote
Garnet, chlorite, biotite, epidote
Axinite, biotite quartz, sphene calcite
Axinite, biotite, chlorite, sphene, calcite
Axinite, chlorite, biotite, sphene, orthoclase
Garnet, biotite, epidote, axinite chlorite, sphene
23
24
25
26
30
31
32
33
34
67
68
69
70
71
72
73
74
75
76
SiO2
Al2O3
FeO
Fe2O3
Na2O
K2O
MnO
P2O5
MgO
CaO
TiO2
total H2O
Pyrite
Pyrite chalcopyrite
Pyrite chalcopyrite
Biotite quartz
Quartz, pyrite, chalcopyrite, cassiterite calcite
disseminated cassiterite
disseminated cassiterite
B
F
S
Sn
Cu
Zn
GREENSTONE ORE UL14

Fig 20

metasomatic foliation, which in this area dips approximately 20° NW. Cassiterite occurs as small (0.1 mm) crystals, usually associated with axinite. Pyrite and chalcopyrite occur as irregularly shaped grains and clots, upto 4 mm in size, in narrow bands, parallel to the metasomatic foliation. Examples of this type of mineralisation are shown in plate 7.

Two samples of biotite-axinite metasomite were analysed (Le 65 & 66). Compared to the banded basaltic amphibolites, the mineralised metasomites are enriched in B, FeO, Fe_2O_3, MnO, K_2O, P_2O_5, Cr, Cu, Li, Sn and Zn, and depleted in SiO_2, TiO_2, Al_2O_3, MgO, CaO, Na_2O, Co, Ni and Pb.

Although the two samples yielded 6500 and 2500 ppm Sn respectively, recovery of cassiterite was no more than 0.2 wt. %, suggesting that some of the Sn may be localised within the silicate phases (biotite, sphene or axinite).

Similar metasomatic lithologies to those exposed in 601 cross-cut were recovered from UL 14 diamond drill hole, between 25 and 30m from the collar. A sample traverse was made through the metasomatised horizon and the results of a mineralogical and geochemical study are presented in figure 20 and table 6 .

The horizon consists of structureless

and banded amphibolites, and calciferous metasomites (amphibole-plagioclase, garnet-magnetite), which have been partially or completely converted to an assemblage of axinite, biotite, chlorite, quartz, orthoclase, opaque ores, calcite and sphene. Locally axinite forms upto 95% of the rock.

Compared to the analysed banded amphibolites the metasomatised zone is enriched in B, Fe_2O_3, FeO, MnO, K, P_2O_5, Sn, Cu, Li, Zn and, occasionally, Be, and depleted in SiO_2, TiO_2, Al_2O_3, Na_2O, Co, Cr, Ni and Pb. The highest Sn values, upto 7500 ppm Sn, coincide with the axinite rich horizons, demonstrating a positive correlation between B and Sn. Visible cassiterite is rare and vanning assay did not reproduce the same 'high' Sn values. It might, therefore, be expected that some of the Sn is localised within silicates, particularly axinite, biotite and sphene.

3b) It was stated earlier that the calciferous metasomites contain higher Sn values (average Sn 228 ppm) than the amphibolites (average Sn 12 ppm). These lithologies constitute a concentration of Sn (and sometimes Cu & Zn) and must, therefore, be considered as a type of mineralisation. These horizons, however, rarely contain ore-mineral phases and it is probable that the majority of

the Sn (Cu and Zn) enters the structure of silicate phases and is, consequently economically non-recoverable.

Within the Ca metasomatites, there is a general sequence of Sn enrichment from the massive garnetiferous hornfelses (average 267 ppm) through discordant garnet rich veins (average 830 ppm) to garnet, axinite and tourmaline metasomites (average 849 ppm). A study of some of the individual calc-silicate phases from several Ca metasomatic veins (Jackson & Alderton, 1974) indicates that the later B rich phases contain the highest Sn (and Be) values. The positive correlation between high Sn and B values probably indicates simultaneous transport and deposition of these elements.

None of these occurrences offer a potential for tin metal extraction, as tin values are subeconomic and the tin is in a non-recoverable form i.e. either as microscopic cassiterite particles or located within a silicate structure. The tin enrichment is important as it indicates that tin was available, although only in small amounts, during contact metamorphism and metasomatism, so, providing a link with the economically sterile, thermal metamorphic environment and the metalliferous, hydrothermal environment.

3c) Miscellaneous replacements.

A 2 cm wide, NW trending, irregularly shaped zone of replacement mineralisation occurs on 4 level ~ 125 m SW of South Lode (plate 7). The mineralisation is spatially related to several, narrow (1 - 2 cm), subvertical veins, containing orthoclase, quartz, chlorite, pyrite, chalcopyrite and cassiterite. The irregularly shaped zone of replacement containing disseminated cassiterite and massive chalcopyrite, pyrite and sphalerite, is developed adjacent to the veinlets, in chloritised pelites. Several quartz filled, vuggy cavities are also associated with the mineralisation. Individual cavities are approximately spherical in shape, upto 20 cm in diameter and, typically, display a concentric mineralogical structure, which is similar to some of the pods on the Foot-wall Branch Vein (4 level). The inwardly zoned sequence is as follows:

a) The original biotite rich pelites are converted to an assemblage of quartz, chlorite and orthoclase, with minor disseminated pyrite and chalcopyrite, and local massive pyrite and chalcopyrite.

b) Adjacent to the vug, there is often a discontinuous zone, < 1 cm wide, containing cassiterite, minor pyrite and chalcopyrite.

c) The rim of the vug contains pink, inward terminating orthoclase crystals which are often overgrown with chlorite, quartz and minor pyrite, chalcopyrite and sphalerite.

d) The vugs, themselves, contain large (5 cm long) euhedral, quartz crystals with minor interstitial pyrite, chalcopyrite and sphalerite.

In addition to the mineralisation developed around, and within, the vugs, there are irregularly shaped areas of massive replacement pyrite-chalcopyrite-sphalerite.

The miner paragenesis in this area is as follows:

1) cassiterite-orthoclase.
2) quartz-pyrite-chalcopyrite.
3) pyrite replaced by chalcopyrite.
4) quartz-sphalerite-pyrite-chalcopyrite.

A similar, irregularly shaped zone of replacement occurs in 601 cross-cut ~275 m SW of the Old Bal Lode. This zone of replacement is spatially related to a NE trending, subvertical, vuggy fissure vein which contains quartz, sphalerite and pyrite. The banded amphibolites which host the replacement are intensely chloritised and contain irregularly shaped masses of vuggy quartz. Within the chloritised

amphibolite, irregular zones of massive sphalerite (and minor pyrite) occur. The paragenesis is unique to the project area and it might represent a relatively late stage of mineralisation.